



GRADUATE SCHOOL  
EAST TENNESSEE STATE UNIVERSITY

East Tennessee State University  
Digital Commons @ East  
Tennessee State University

---

Electronic Theses and Dissertations

Student Works


---

12-2021

## Distinguishing *Mustela* From *Neogale* (Mustelidae) Through Both a Qualitative and Quantitative Analysis of Skull and Tooth Morphology

Ronald W. Peery  
*East Tennessee State University*

Follow this and additional works at: <https://dc.etsu.edu/etd>

 Part of the [Ecology and Evolutionary Biology Commons](#), [Paleobiology Commons](#), and the [Paleontology Commons](#)

---

### Recommended Citation

Peery, Ronald W., "Distinguishing *Mustela* From *Neogale* (Mustelidae) Through Both a Qualitative and Quantitative Analysis of Skull and Tooth Morphology" (2021). *Electronic Theses and Dissertations*. Paper 4010. <https://dc.etsu.edu/etd/4010>

This Thesis - unrestricted is brought to you for free and open access by the Student Works at Digital Commons @ East Tennessee State University. It has been accepted for inclusion in Electronic Theses and Dissertations by an authorized administrator of Digital Commons @ East Tennessee State University. For more information, please contact [digilib@etsu.edu](mailto:digilib@etsu.edu).

Distinguishing *Mustela* From *Neogale* (Mustelidae) Through Both a Qualitative and  
Quantitative Analysis of Skull and Tooth Morphology

---

A thesis

presented to

the faculty of the Department of Geosciences

East Tennessee State University

In partial fulfillment

of the requirements for the degree

Master of Science in Geosciences, Paleontology

---

by

Ronald W. Peery

December 2021

---

Joshua X. Samuels, Chair

Blaine W. Schubert

Steven C. Wallace

Keywords: *Mustela*, *Neogale*, mustelines, weasels, distinguishing characters, morphology

## ABSTRACT

### Distinguishing *Mustela* From *Neogale* (Mustelidae) Through Both a Qualitative and Quantitative Analysis of Skull and Tooth Morphology

by

Ronald W. Peery

Weasels and mink (*Mustela* and *Neogale*) can be difficult to distinguish osteologically due to similarities in morphology, thus suggesting the need for an accurate tool in distinguishing among taxa. This study utilized a combination of character state and stepwise discriminant function (DFA) analyses to examine potential distinguishing features of skull and tooth morphology. Measurements and ratios were collected from all 18 extant musteline species, as well as the extinct *Neovison macrodon*, *Mustela rexroadensis*, *Mustela meltoni*, *Mustela gazini*, and *Mustela jacksoni*. Unidentified musteline specimens from the Gray Fossil Site were also included. Results of the character state analysis and DFA proved fairly reliable in distinguishing both extant and fossil taxa. The character state analysis revealed six useful morphological characters to aid in distinguishing between genera while the DFA demonstrated reliable separation of genus, species, and clade. For both analyses, morphology of the carnassials (P4, m1) and M1 contributed most to distinction.

Copyright 2021 by Ronald W. Peery

All Rights Reserved

## ACKNOWLEDGEMENTS

I would like to sincerely thank my committee members, Dr. Joshua Samuels, Dr. Blaine Schubert, and Dr. Steven Wallace for their assistance and feedback. I would also like to thank the remaining faculty and staff of East Tennessee State University's Department of Geosciences for their assistance and support. Thanks to the Smithsonian Natural History Museum and the East Tennessee State University Museum of Natural History for allowing me to collect data for this study. Many thanks to April Season Nye and Brian Compton for their assistance with collections. I would like to give a special thanks to my family, friends, and fellow graduate students. I couldn't have done this without your phenomenal encouragement and support. Lastly, to Cheyenne – thank you so much for your unparalleled love and support. You have been my source of solace throughout this remarkable journey.

## TABLE OF CONTENTS

|   |    |
|---|----|
| ABSTRACT.....   | 2  |
| ACKNOWLEDGEMENTS.....                                   | 4  |
| LIST OF TABLES.....                                     | 8  |
| LIST OF FIGURES.....                                    | 11 |
| CHAPTER 1. INTRODUCTION.....                            | 13 |
| Research Questions.....                                 | 14 |
| CHAPTER 2. PHYLOGENY AND SYSTEMATICS OF MUSTELINES..... | 15 |
| CHAPTER 3. EVOLUTIONARY HISTORY OF MUSTELINES.....      | 22 |
| Origin of Mustelidae.....                               | 22 |
| Origin of Mustelinae.....                               | 22 |
| Origin of <i>Mustela</i> and <i>Neogale</i> .....       | 23 |
| CHAPTER 4. CHARACTERISTICS OF MUSTELINES.....           | 26 |
| Skull and Dental Characters of Mustelidae.....          | 26 |
| Skull and Dental Characters of Mustelinae.....          | 27 |
| Skull and Dental Characters of <i>Mustela</i> .....     | 27 |
| Skull and Dental Characters of <i>Neogale</i> .....     | 30 |
| CHAPTER 5. ECOLOGY OF MUSTELINES.....                   | 33 |
| Habitat and Distribution.....                           | 33 |
| Dietary Ecology.....                                    | 35 |
| Sexual Dimorphism.....                                  | 36 |
| Geographic Variation.....                               | 38 |
| CHAPTER 6. METHODOLOGY.....                             | 42 |
| Measurements and Statistical Analyses.....              | 42 |
| Character State Analysis.....                           | 47 |
| CHAPTER 7. RESULTS.....                                 | 53 |
| Character State Analysis.....                           | 53 |
| Extant Taxa Analysis.....                               | 57 |
| Genus Classification.....                               | 57 |
| Species Classification.....                             | 61 |

|   |     |
|---|-----|
| Clade Classification .....                        | 68  |
| ' <i>Neovison</i> ' <i>macrodon</i> Analysis..... | 73  |
| Genus Classification .....                        | 73  |
| Clade Classification.....                         | 75  |
| <i>Mustela rexroadensis</i> Analysis .....        | 77  |
| Genus Classification .....                        | 78  |
| Clade Classification.....                         | 79  |
| <i>Mustela meltoni</i> Analysis.....              | 81  |
| Genus Classification .....                        | 82  |
| Clade Classification.....                         | 83  |
| GFS musteline Analysis.....                       | 85  |
| Genus Classification .....                        | 86  |
| Clade Classification.....                         | 87  |
| Extinct Pleistocene Taxa Analysis.....            | 89  |
| Genus Classification .....                        | 90  |
| Species Classification.....                       | 91  |
| Clade Classification.....                         | 93  |
| <i>Mustela</i> sp. Analysis .....                 | 96  |
| Genus Classification .....                        | 97  |
| Species Classification.....                       | 98  |
| Clade Classification.....                         | 100 |
| CHAPTER 8. DISCUSSION.....                        | 104 |
| Character State Analysis .....                    | 104 |
| Extant Taxa Analysis .....                        | 106 |
| Genus Classification .....                        | 106 |
| Species Classification.....                       | 107 |
| Clade Classification.....                         | 108 |
| Extant Pleistocene Taxa Classification .....      | 108 |
| ' <i>Neovison</i> ' <i>macrodon</i> Analysis..... | 109 |
| <i>Mustela rexroadensis</i> Analysis .....        | 111 |
| <i>Mustela meltoni</i> Analysis.....              | 112 |

|  |     |
|--|-----|
| GFS musteline Analysis.....  | 113 |
| Extinct Pleistocene Taxa Analysis.....   | 116 |
| <i>Mustela</i> sp. Analysis .....  | 118 |
| CHAPTER 9. CONCLUSIONS .....   | 119 |
| REFERENCES .....   | 121 |
| APPENDIX: Examined Specimens of <i>Mustela</i> and <i>Neogale</i> Utilized in the Analyses ..... | 138 |
| VITA.....  | 147 |



## LIST OF TABLES

|   |    |
|---|----|
| Table 1. Definitions of Osteological Measurements Used in the Analysis<br>and Their Abbreviations .....   | 43 |
| Table 2. Definitions of Ratios Used in the Analysis and Their Abbreviations.....  | 46 |
| Table 3. Evolutionary Clades of Mustelines .....  | 47 |
| Table 4. Definitions of Skull and Tooth Characters Used in the Analysis .....   | 48 |
| Table 5. Character State Distribution Among <i>Mustela</i> , <i>Neogale</i> , and <i>Neogale vison</i> With<br>Distinguishing Characters Highlighted.....           | 54 |
| Table 6. Percentages of Distinguishing Characters Between <i>Mustela</i> and <i>Neogale</i> .....   | 55 |
| Table 7. Percentages of Distinguishing Characters Among Holocene Musteline Taxa .....   | 56 |
| Table 8. Extant Genus Analysis Structure Matrix, Eigenvalue, Percent Variance Explained,<br>and Wilks' $\lambda$ for Discriminant Function 1 .....                  | 58 |
| Table 9. Extant Genus Analysis Classification Matrix.....   | 60 |
| Table 10. Extant Species Analysis Structure Matrix, Eigenvalue, Percent Variance Explained,<br>and Wilks' $\lambda$ for Discriminant Functions 1, 2, 3, and 4 ..... | 62 |
| Table 11. Extant Species Analysis Classification Matrix.....  | 63 |
| Table 12. Extant Clade Structure Matrix, Eigenvalue, Percent Variance Explained,<br>and Wilks' $\lambda$ for Discriminant Functions 1, 2, and 3 .....               | 68 |
| Table 13. Extant Clade Analysis Classification Matrix.....  | 69 |
| Table 14. Summary of Pleistocene Specimens of Extant Species Classification Matrix .....  | 72 |
| Table 15. ' <i>Neovison</i> ' Genus Analysis Structure Matrix, Eigenvalue,<br>Percent Variance Explained, and Wilks' $\lambda$ for Discriminant Function 1 .....    | 74 |
| Table 16. ' <i>Neovison</i> ' <i>macrodon</i> Genus Analysis Classification Matrix.....   | 74 |

|   |    |
|---|----|
| Table 17. ‘ <i>Neovison</i> ’ <i>macrodon</i> Clade Analysis Structure Matrix, Eigenvalue, Percent<br>Variance Explained, and Wilks’ $\lambda$ for Discriminant Functions 1 and 2 ..... | 76 |
| Table 18. ‘ <i>Neovison</i> ’ <i>macrodon</i> Clade Analysis Classification Matrix .....  | 76 |
| Table 19. <i>Mustela rexroadensis</i> Genus Structure Matrix, Eigenvalue,<br>Percent Variance Explained, and Wilks’ $\lambda$ for Discriminant Function 1 .....                         | 78 |
| Table 20. <i>Mustela rexroadensis</i> Genus Analysis Classification Matrix.....   | 79 |
| Table 21. <i>Mustela rexroadensis</i> Clade Analysis Structure Matrix, Eigenvalue, Percent<br>Variance Explained, and Wilks’ $\lambda$ for Discriminant Functions 1 and 2 .....         | 80 |
| Table 22. <i>Mustela rexroadensis</i> Clade Analysis Classification Matrix.....   | 80 |
| Table 23. <i>Mustela meltoni</i> Genus Analysis Structure Matrix, Eigenvalue, Percent Variance<br>Explained, and Wilks’ $\lambda$ for Discriminant Function 1 .....                     | 82 |
| Table 24. <i>Mustela meltoni</i> Genus Analysis Classification Matrix .....   | 82 |
| Table 25. <i>Mustela meltoni</i> Clade Analysis Structure Matrix, Eigenvalue, Percent Variance<br>Explained, and Wilks’ $\lambda$ for Discriminant Functions 1 and 2 .....              | 83 |
| Table 26. <i>Mustela meltoni</i> Clade Analysis Classification Matrix .....   | 84 |
| Table 27. GFS Musteline Genus Analysis Structure Matrix, Eigenvalue,<br>Percent Variance Explained, and Wilks’ $\lambda$ for Discriminant Function 1 .....                              | 86 |
| Table 28. GFS Musteline Genus Analysis Classification Matrix.....   | 87 |
| Table 29. GFS Musteline Clade Analysis Structure Matrix, Eigenvalue,<br>Percent Variance Explained, and Wilks’ $\lambda$ for Discriminant Function 1 .....                              | 88 |
| Table 30. GFS Musteline Clade Analysis Classification Matrix.....   | 88 |
| Table 31. Extinct Pleistocene Genus Analysis Structure Matrix, Eigenvalue,<br>Percent Variance Explained, and Wilks’ $\lambda$ for Discriminant Function 1 .....                        | 90 |

|   |     |
|---|-----|
| Table 32. Extinct Pleistocene Genus Analysis Classification Matrix.....   | 91  |
| Table 33. Extinct Pleistocene Species Analysis Structure Matrix, Eigenvalue, Percent Variance<br>Explained, and Wilks' $\lambda$ for Discriminant Functions 1 and 2 ..... | 92  |
| Table 34. Extinct Pleistocene Clade Analysis Structure Matrix, Eigenvalue, Percent Variance<br>Explained, and Wilks' $\lambda$ for Discriminant Functions 1 and 2 .....   | 94  |
| Table 35. Extinct Pleistocene Clade Analysis Classification Matrix .....  | 95  |
| Table 36. <i>Mustela</i> sp. Genus Analysis Structure Matrix, Eigenvalue,<br>Percent Variance Explained, and Wilks' $\lambda$ for Discriminant Function 1 .....           | 97  |
| Table 37. <i>Mustela</i> sp. Genus Analysis Classification Matrix.....  | 98  |
| Table 38. <i>Mustela</i> sp. Species Analysis Structure Matrix, Eigenvalue,<br>Percent Variance Explained, and Wilks' $\lambda$ for Discriminant Functions 1 and 2 .....  | 99  |
| Table 39. <i>Mustela</i> sp. Clade Analysis Structure Matrix, Eigenvalue,<br>Percent Variance Explained, and Wilks' $\lambda$ for Discriminant Functions 1 and 2 .....    | 101 |
| Table 40. <i>Mustela</i> sp. Clade Analysis Classification Matrix.....  | 102 |

## LIST OF FIGURES

|  |    |
|--|----|
| Figure 1. Phylogenetic tree of superfamily Musteloidea with red box outlining subfamily Mustelinae .....           | 17 |
| Figure 2. Phylogenetic tree of subfamily Mustelinae and their clade designations used throughout the analysis..... | 18 |
| Figure 3. <i>Mustela erminea</i> skull in dorsal (top), ventral (center), and right lateral (bottom) views .....   | 29 |
| Figure 4. <i>Neogale vison</i> skull in dorsal (top), ventral (center), and right lateral (bottom) views .....     | 32 |
| Figure 5. Current world range of Mustelinae.....   | 34 |
| Figure 6a. Linear measurements of skull used in the analysis.....  | 44 |
| Figure 6b. Linear measurements of mandible used in the analysis .....  | 45 |
| Figure 7. Discriminant scores from DF1 for extant genus analysis.....  | 58 |
| Figure 8. Bivariate plots comparing P4PastW/ProW and CBL and P4PastW/ProW and m1TriL/TalL.....                     | 59 |
| Figure 9. Extant species analysis scatterplot comparing DF1 vs. DF2.....   | 64 |
| Figure 10. Pleistocene specimens of extant species analysis scatterplot comparing DF1 vs. DF2.....                 | 65 |
| Figure 11. Extant clade analysis scatterplot comparing DF1 vs. DF2.....  | 70 |
| Figure 12. Pleistocene specimens of extant species clade analysis scatterplot comparing DF1 vs. DF2.....           | 71 |
| Figure 13. ‘ <i>Neovison</i> ’ <i>macrodon</i> clade analysis scatterplot comparing DF1 vs. DF2 .....              | 77 |
| Figure 14. <i>Mustela rexroadensis</i> clade analysis scatterplot comparing DF1 vs. DF2.....                       | 81 |

|  |     |
|--|-----|
| Figure 15. <i>Mustela meltoni</i> clade analysis scatterplot comparing DF1 vs. DF2 ..... | 85  |
| Figure 16. GFS musteline clade analysis scatterplot comparing DF1 vs. DF2 .....          | 89  |
| Figure 17. Extinct Pleistocene species analysis scatterplot comparing DF1 vs. DF2 .....  | 93  |
| Figure 18. Extinct Pleistocene clade analysis scatterplot comparing DF1 vs. DF2 .....    | 96  |
| Figure 19. <i>Mustela</i> sp. species analysis scatterplot comparing DF1 vs. DF2.....    | 100 |
| Figure 20. <i>Mustela</i> sp. clade analysis scatterplot comparing DF1 vs. DF2.....      | 103 |
| Figure 21. GFS musteline left M1 and left P4 in occlusal view .....                      | 114 |

## CHAPTER 1. INTRODUCTION

The mustelid subfamily Mustelinae (weasels, stoats, ferrets, minks, and polecats) (Oliveira do Nascimento 2014) are the most species-rich group of carnivorans in the world today (King 1989) with a total of 18 extant species between two separate genera (*Mustela* and *Neogale*) (Wozencraft 2005; Patterson et al. 2021); however, the taxonomic status of taxa within the group has long been a subject of debate. *Mustela* and *Neogale* can be very difficult to distinguish morphologically due to similar skeletal and dental features (Abramov 2000; Patterson et al. 2021). Moreover, high degrees of sexual dimorphism and geographic variation, which are commonly evident throughout mustelines (King and Powell 2007) may pose further challenges for distinguishing these taxa at both the genus- and species-level. Although a considerable number of studies have analyzed both phylogenetic and morphological relationships among mustelines (e.g., Anderson 1989; Abramov 2000; Heptner et al. 2001; Marmi et al. 2004; Sato et al. 2003; Harding and Smith 2009; Law et al. 2017), further analysis is necessary in order to understand how readily skull and dental characters could be used to determine their taxonomic status. No previous studies have combined both a quantitative and qualitative approach to this topic, using both qualitative characters and a wide variety of linear measurements across a large dataset including all extant musteline taxa. When considering the fossil record of mustelines, this degree of difficulty distinguishing taxa is drastically increased due to their scarce and often fragmentary skeletal remains. These challenges call for better tools for distinguishing both genera and species of mustelines. The purpose of this study is to compare *Mustela* and *Neogale* using a combination of linear measurements of the skull and teeth, as well as a qualitative assessment of the variability of diagnostic characters, including examination of all 18 extant

species and fossil material from five extinct taxa, five extant Pleistocene-aged North American taxa, and two unidentified specimens from the Gray Fossil Site.

*Research Questions*

- Can *Mustela* and *Neogale* be distinguished based on differences in skull and tooth morphology alone?
- If *Mustela* and *Neogale* are morphologically distinct, does each species accurately correspond with its current generic taxonomic status?
- If extant taxa within Mustelinae can be distinguished based on skull and tooth morphology, can these features be used to identify their fossil remains?

## CHAPTER 2. PHYLOGENY AND SYSTEMATICS OF MUSTELINES

Within Mustelidae, five subfamilies were originally supported by Simpson (1945) and included Mustelinae (weasels, stoats, ferrets, mink, martens, and wolverines), Lutrinae (otters), Mellivorinae (honey badgers), Melinae (badgers), and Mephitinae (skunks). However, recent molecular and phylogenetic studies (Koepfli et al. 2008; Sato et al. 2012; Law et al. 2017) have supported a total of eight subfamilies consisting of Mustelinae (weasels, stoats, ferrets, mink), Lutrinae (otters), Guloninae (martens, fishers, tayra, and wolverines), Ictonychinae (grisons, African polecats), Helictinidinae (ferret-badgers), Melinae (Eurasian badgers), Mellivorinae (honey badgers), and Taxidiinae (American badgers) (Figure 1). It is now supported that Mephitidae diverged prior to the origin of Mustelidae, forming a discrete family (Koepfli et al. 2008; Sato et al. 2012; Law et al. 2017). Extant members of Mustelidae are considered to be a monophyletic group based on the loss of the carnassial notch on the P4, absence of the M1 postprotocrista, absence of the M2, absence of alisphenoid canal, and ventral closure of the suprameatal fossa (Bryant et al. 1993; Baskin 1998; Marmi et al. 2004; Paterson et al. 2019).

As traditionally treated, subfamily Mustelinae is widely considered to be polyphyletic (Bryant et al. 1993; Koepfli and Wayne 1998; Hosoda et al. 2000; Koepfli et al. 2003; Sato et al. 2003; Koepfli et al. 2008), as it has been used as a catchall for many of the early, poorly differentiated taxa as well as divergent genera of doubtful affinity, so that determining the earliest true members of the subfamily has been nearly impossible (Anderson 1989). Mustelines have retained several plesiomorphic characters (Anderson 1989); however, identified synapomorphies for the group include an anteroposteriorly reduced M1 with the metacone close to the paracone, an anteroposteriorly expanded internal lobe on the M1, a reduced to absent m1



metaconid, a single rooted m2, and inflated auditory bullae (Bryant et al. 1993; Wolsan 1993; Baskin 1998; Paterson et al. 2019).

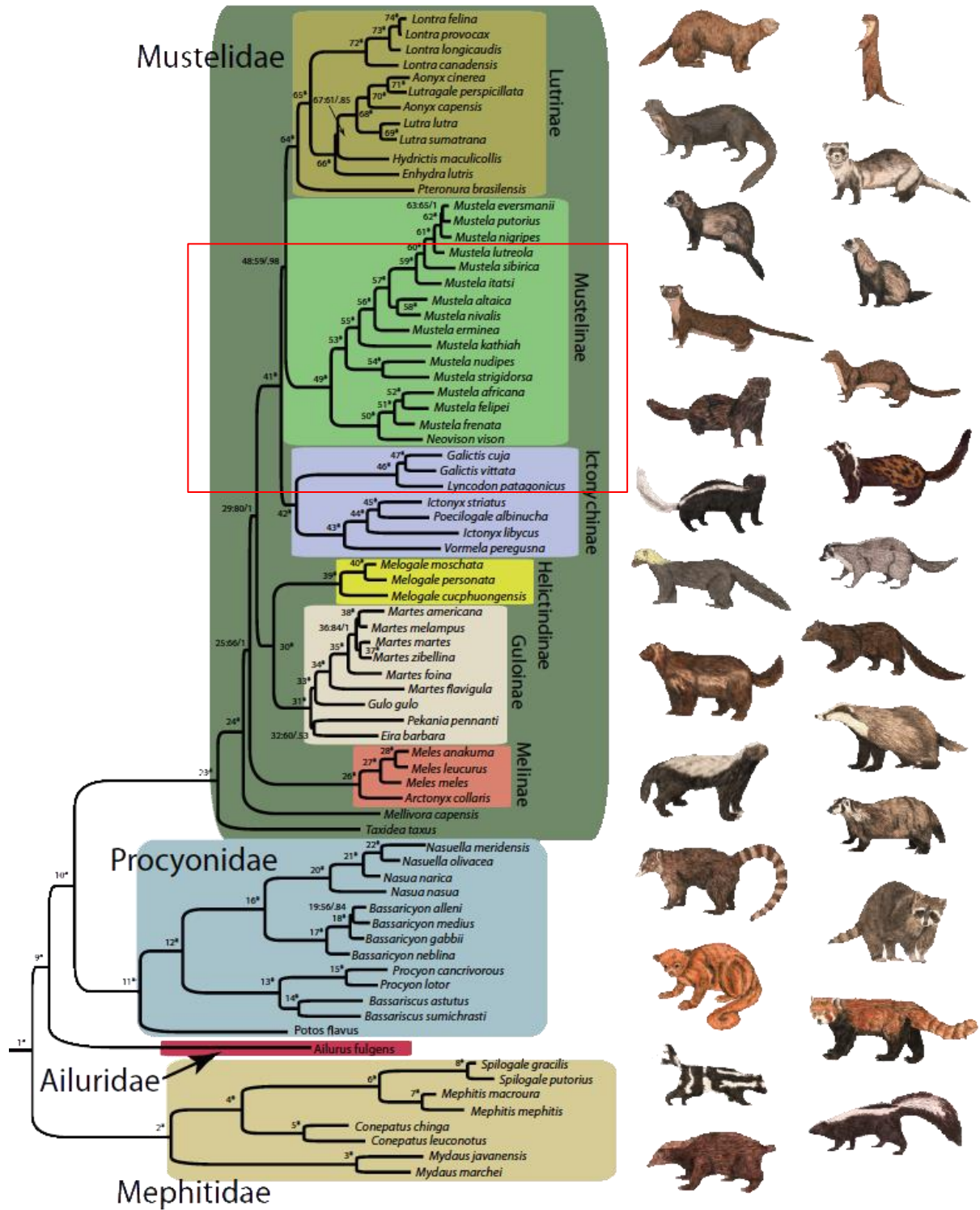


Figure 1. Phylogenetic tree of superfamily Musteloidea with red box outlining subfamily Mustelinae (Modified from Law et al. 2017)

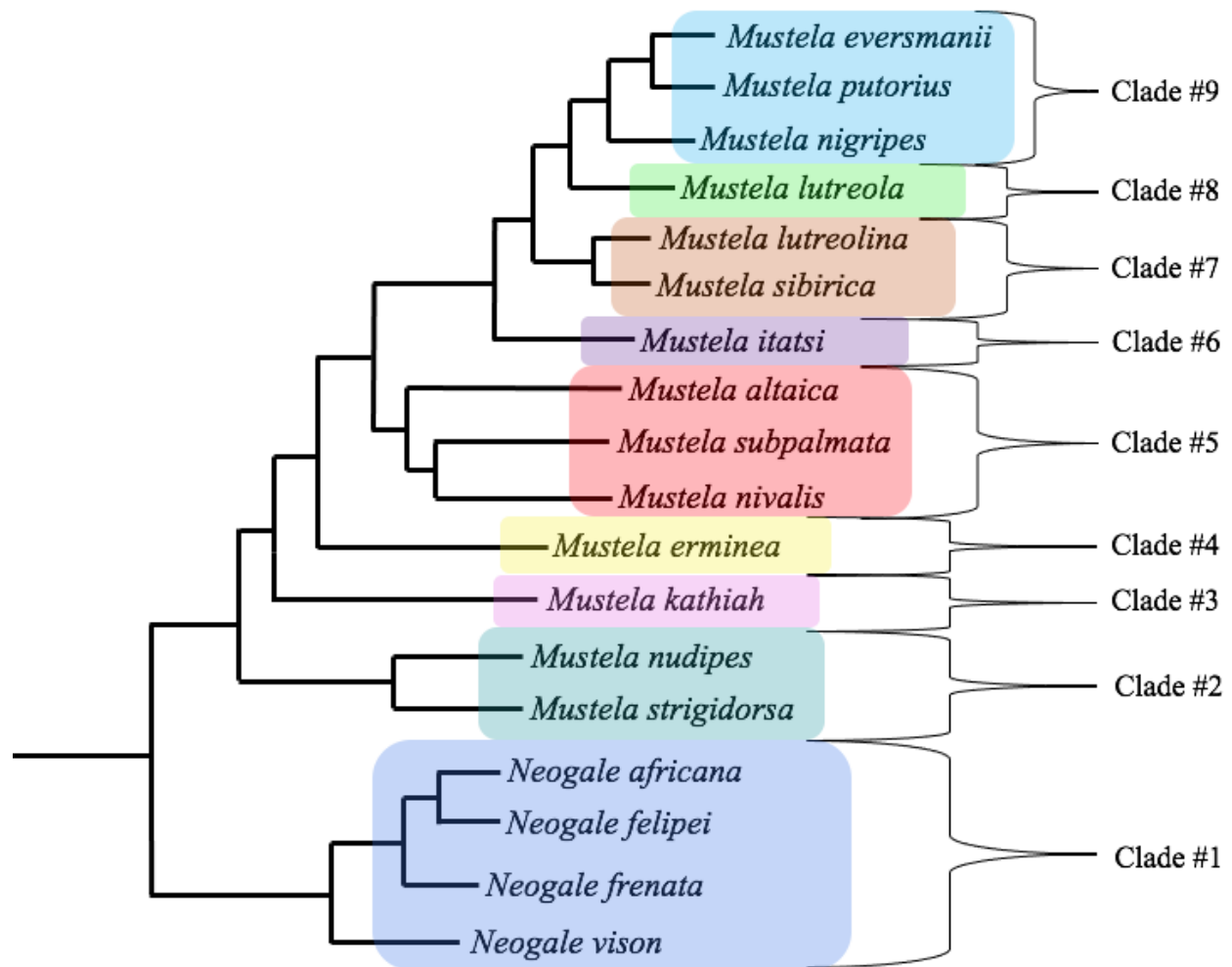


Figure 2. Phylogenetic tree of subfamily Mustelinae and their clade designations used throughout the analysis (Modified from Law et al. 2017 and Patterson et al. 2021)

Many studies have examined the phylogenetic relationships among species of *Mustela*; however, there have been significant differences among subgenera classification. Some studies have placed *Mustela* into two (Ellerman and Morrison-Scott 1951; Heptner et al. 2002; Kurose et al. 2008), four (Pavlinov et al. 1995), or five subgenera (Youngman 1982; Anderson 1989). Abramov (2000) divided the genus into 9 subgenera (*Mustela*, *Gale*, *Putorius*, *Lutreola*, *Kolonokus*, *Pocockictis*, *Gramogale*, *Cabreragale*, *Cryptomustela*) and 17 species (*Mustela erminea*, *frenata*, *nivalis*, *subpalmata*, *altaica*, *kathiah*, *lutreola*, *putorius*, *eversmanii*, *nigripes*,

*sibirica*, *itatsi*, *lutreolina*, *africana*, *felipei*, *nudipes*, *strigidorsa*); however, the phylogeny of *Mustela* is still debated and remains unresolved. For instance, Marmi et al. (2004) proposed that *M. frenata* should be excluded from the subgenus *Mustela*, as that species and *M. erminea* are highly divergent compared with other pairs of *Mustela* species. They also suggested that *M. sibirica* and *M. itatsi* (subgenus *Kolonokus*) be placed together with species in the subgenera *Putorius* (*M. putorius*, *M. eversmannii*, *M. nigripes*) and *Lutreola* (*M. lutreola*) in the same subgenus (Marmi et al. 2004). Some synapomorphic characters that have been used to distinguish *Mustela* include absence of the P1 and p1, absence of the m1 metaconid, and a very reduced m2 (Baskin 1998). Due to similarities in morphological features, all species of mustelines have historically been assigned to *Mustela*; however, recent molecular and phylogenetic studies (Koepfli et al. 2008; Harding and Smith 2009; Law et al. 2017; Hassanin et al. 2021; Patterson et al. 2021) have indicated the need for significant taxonomic revisions among species within this genus. The most recent classification of mustelines, provided by Patterson et al. (2021), is followed here and shown in Figure 2.

There has been long-standing confusion regarding the phylogenetic and taxonomic validity of *Neovison vison*, which was originally placed into *Mustela*. Abramov (2000) morphologically distinguished *M. vison* from the remaining species of *Mustela* by bacular structure, presence of a small metaconid on the m1, and slightly less inflated auditory bullae, thus placing it into its own genus *Neovison*. The results of subsequent studies (Koepfli et al. 2008; Harding and Smith 2009; Sato et al. 2012; Law et al. 2017; Hassanin et al. 2021; Patterson et al. 2021); however, contradict the conclusions of Abramov (2000) and revealed that *N. vison* is a sister to all other *Mustela* only in analyses that do not include its closer relatives, *M. africana*, *M. felipei*, and *M. frenata*. In the only recent phylogenetic analyses to include all four of these

species, Harding and Smith (2009) and Law et al. (2017) concluded a well-supported grouping of *N. vison*, *M. frenata*, *M. africana*, and *M. felipei* as a distinct New World lineage that is sister to the remaining species of *Mustela*, separated first from the two mustelines in Southeast Asia (*M. strigidorsa* and *M. nudipes*), and then from a larger divergent lineage of *Mustela* spanning Eurasia. This phylogenetic pattern led Harding and Smith (2009) to suggest recognizing the New World clade as the genus *Vison* Gray, 1843. More recently, the results of Hassanin et al. (2021) also supported uniting these four species into a distinct genus, though they recommended that the genus be *Grammogale* Cabrera, 1940. Only four synonyms for *Mustela* have been applied to the New World species: *Vison* Gray 1843; *Neogale* Gray 1865; *Grammogale* Cabrera, 1940; and *Cabreragale* Baryshnikov and Abramov, 1997. Furthermore, each of the four species in the New World clade is the type species for a genus-group name: *vison* for *Neovison* Baryshnikov and Abramov, 1997; *frenata* for *Neogale* Gray, 1865; *africana* for *Grammogale* Cabrera, 1940; and *felipei* for *Cabreragale* Baryshnikov and Abramov, 1997. This raises the question of which generic synonym should ultimately apply to the New World clade. Harding and Smith (2009) suggested that priority in synonymy would render the genus name of the clade as *Vison*. However, since the European mink (*M. lutreola*) represents the type species for *Vison* (Baryshnikov and Abramov 1997), Patterson et al. (2021) recognized the senior name for the group to be *Neogale*. They further note that the divergence of extant *Neogale* species (initiated by the split between *N. vison* and *M. frenata*, ~8.69 Ma) precedes the splits in most polytypic mustelid genera (Law et al. 2017), thus arguing the recognition of *Neogale* as a distinct genus and not a subgenus of *Mustela* (Patterson et al. 2021).

To thus rename the members of the New World clade as *Neogale* (*Neogale vison*, *Neogale frenata*, *Neogale africana*, and *Neogale felipei*) distinct from *Mustela*, has two major

effects on the current understanding of New World musteline biogeography. A new genus designation would first recognize a distinct and biogeographically coherent evolutionary lineage that diverged from Eurasian/Holarctic *Mustela* during the late Miocene. Secondly, separating the New World clade from its Eurasian counterparts would help to distinguish among musteline taxa that radiated within and are endemic to the New World versus taxa that are descended from recent immigrations to the Americas (e.g., *M. erminea*, *M. nivalis*, *M. nigripes*) (Harding and Smith 2009). Therefore, the most parsimonious way to resolve the phylogenetic dilemma found in the relationships within *Mustela* is to separate the endemic New World clade as *Neogale*.

## CHAPTER 3. EVOLUTIONARY HISTORY OF MUSTELINES

### *Origin of Mustelidae*

The order Carnivora emerged during the Early Eocene Climatic Optimum (53-51 Ma) with the two major suborders, Caniformia and Feliformia, radiating throughout the Eocene and into the Early Oligocene (Hassanin et al. 2021). The most basal group of the caniform carnivorans is the Mustelidae, which are the most diverse and species-rich carnivoran family today with 59 extant species within 22 genera (King 1989; Koepfli et al. 2008).

A combination of ecological opportunity and rapid diversification occurring right after the Eocene-Oligocene transition (33.5 Ma) gave rise to the first members of Mustelidae (Law et al. 2017) with the oldest known record in North America (*Corumictis wolsani*) dating back to 28.8-25.9 Ma (Paterson et al. 2019). Following the Mid-Miocene Climatic Optimum (~17-15 Ma), these early mustelids underwent extensive diversification, with most studies describing two major bursts of adaptive radiation as being a primary attribution to the incredible ecological and phenotypic diversity in Mustelidae (Sato et al. 2009, 2012; Koepfli et al. 2008). These authors agree that the early divergences during the Late Miocene (~12.5-8.8 Ma) gave rise to most extant lineages while the later divergences during the Pliocene (~5.3-1.8 Ma) resulted in rapid diversification at the genus- and species-level (King 1989; Marmi et al. 2004; Koepfli et al. 2008; Sato et al. 2012).

### *Origin of Mustelinae*

Most phylogenetic studies have concluded the origins of Mustelinae to have begun during the Late Miocene of Eurasia, with dispersal events into North America beginning 6.8-8.6 Ma (Harding and Smith 2009). The time and rate of dispersal of these early mustelines have been hypothesized by several authors to be correlated with the evolution of body elongation as a

response to the Late Miocene diversification of rodents, permitting some species to enter burrows and confined spaces to capture prey (Brown and Lasiewski 1972; King 1989; Koepfli et al. 2008; Sato et al. 2012). Towards the end of the Miocene and into the early Pliocene, open grasslands began to spread and replace forests across much of Eurasia and North America, as the climate cooled and became drier (Retallack 2007; Strömberg 2011). At this time, arvicoline cricetids (voles) dispersed to North America and radiated (Samuels and Hopkins 2017).

Studies such as King (1989), Koepfli et al. (2008) and Sato et al. (2012) suggest it is likely that early mustelines descended from larger marten-like mustelids already existing and soon discovered the advantage in becoming small enough to exploit a new ecological niche of predation via rodent burrows (King 1989; Law et al. 2017). However, additional results from Law et al. (2017) suggested that body elongation within this subclade may have served as an innovation that allowed the group to escape niche competition and rapidly diversify after the onset of ecological opportunity (Law et al. 2017). This hypothesis supported their finding that there is a lack of correspondence in patterns of body length and body mass evolutionary rates within the decoupled mustelid subclade. The increase in the rate of body length evolution, but not body mass evolution, suggested that body elongation might be a key innovation for the exploitation of novel Mid-Miocene habitats and resources and subsequent diversification in some mustelids (Law et al. 2017).

#### *Origin of *Mustela* and *Neogale**

Based on a combination of fossil and molecular evidence (e.g., Baskin 1998; Koepfli et al. 2008; Harding and Smith 2009; Sato et al. 2012; Law et al. 2017), the origin of *Mustela* in Eurasia is estimated to have occurred during the late Miocene, with the oldest fossil evidence of a member of *Mustela* coming from late Miocene deposits of Eurasia (Fortelius 2007; King and



Powell 2007). Members of *Mustela* are believed to have dispersed to North America during the late Miocene around this time as well (Heptner et al. 2002; King and Powell 2007; Koepfli et al. 2008); however, some studies claim that *Mustela* in North America appeared during the early Pliocene due to the oldest fossil evidence of an undoubted species belonging to the genus (*M. rexroadensis*) appearing in North America during the early Blancan (~4.5 Ma) (Tedford et al. 1987; Baskin 1998). One Eurasian lineage began with *M. pliocaenica* during the middle Pliocene, later gave rise to *M. praenivalis* during the late Pliocene, and eventually culminated with the extant *M. nivalis*. Through the middle Pliocene (~4 Ma), a separate Eurasian lineage dispersed into central and western Europe, giving rise to *M. plioerminea* and eventually the extant *M. erminea*. By the late middle Pleistocene (~1.2 Ma), *M. erminea* had spread across Eurasia and into North America.

Members of *Neogale* represent a lineage endemic to North and South America (Patterson et al. 2021). This New World lineage is often represented by the middle Blancan species, *Mustela rexroadensis*, and is believed to be a direct ancestor to *N. frenata* which first appeared in North America during the late Blancan (3.4 Ma) (Kurtén and Anderson 1980; Tedford et al. 1987; Baskin 1998; King and Powell 2007); however, no studies have examined whether or not *M. rexroadensis* is in fact a member of this lineage. Widespread differentiation between species of *Neogale* occurred rapidly through the Pliocene, with *N. africana*, *N. felipei*, and *N. vison* likely originated during this time (Harding and Smith 2009; Law et al. 2017). Further partitioning of *Mustela* species in Eurasia was likely simultaneously occurring during this time as well (Harding and Smith 2009). Continuous dispersal events via the Bering land bridge likely occurred between the Old World and New World lineages, though the lack of a more complete fossil record leaves uncertainty regarding the timing of these events (Koepfli et al. 2008). The

earliest fossil remains identified as *N. vison* are from as far back as the early Pleistocene (Anderson 1989; Larivière 1999); however, molecular estimates for their appearance are earlier than the fossil record suggests (Marmi et al. 2004; Harding and Smith 2009). Molecular evidence across various studies has placed an estimate of the beginning of divergence of *Neogale* from *Mustela* (initiated by the split of *N. vison* from remaining taxa) between 9.9-8.5 Ma (Sato et al. 2003), 9.5-6.6 Ma (Marmi et al. 2004), 14-10 Ma (Hosoda et al, 2000), 6.2-6 Ma (Koepfli et al. 2008), 7.13 Ma (Sato et al. 2012), 8.69 Ma (Law et al. 2017), and 13.4-11.8 Ma (Hassanin et al. 2021), respectively.

## CHAPTER 4. CHARACTERISTICS OF MUSTELINES

### *Skull and Dental Characters of Mustelidae*

Mustelids are very small- to medium-sized arctoid carnivoran mammals, generally with a low braincase, short rostrum, wide occiput, short jaw, small orbits, and forwardly placed carnassials (Kurtén and Anderson 1980; Hall 1981; Radinsky 1982; Baskin 1998). Being a highly ecomorphologically diverse clade of carnivorans, members of this family exhibit diverse diets ranging from the generalist diet of badgers to the specialized diets of the hypercarnivorous weasels and piscivorous otters (Frischia et al. 2007; Law et al. 2018; Macdonald et al. 2018). In addition, they often exhibit a wide range of variation in dental adaptations, though the carnassials are typically sectorial with some groups having been secondarily modified for crushing (Kurtén and Anderson 1980; Hall 1981). Sympleisomorphic skull and dental features characterizing Mustelidae include: a moderately inflated auditory bulla; the presence of a suprameatal fossa in the squamosal; the postglenoid process partially encloses the glenoid fossa, and little (and no rotary) jaw movement is possible; presence of the alisphenoid canal; the dental formula is I3/3, C1/1, P4/4, M2/2; the M1 lacks a postprotocrista and metaconule and has an enlarged parastyle; and the m1 has a reduced metaconid (Kurtén and Anderson 1980; Bryant et al. 1993; Wolsan 1993; Baskin 1998). Additionally, the inner lobe of the M1 is expanded and the M2 is very reduced; the m2 is reduced or absent with a short talonid (Kurtén and Anderson 1980; Baskin 1998).

Members of the stem lineage of Mustelidae are often informally referred to as “Paleomustelidae”, while crown-group (Late Oligocene to Recent) mustelids are referred to as “Neomustelidae” (Baskin 1998; Finarelli 2008; Koepfli et al. 2008; Robles et al. 2009). Paleomustelids are considered to be paraphyletic and are characterized by the ancestral retention

of the P4 carnassial notch, while neomustelids have lost the carnassial notch of the P4 with the paracone connecting continuously with the metacone (Baskin 1998). Additional synapomorphies of neomustelids include an absent M2, absence of the alisphenoid canal, a posterior carotid foramen well anterior of the posterior lacerate foramen, and a very reduced to absent suprameatal fossa (Baskin 1998; Paterson et al. 2019).

#### *Skull and Dental Characters of Mustelinae*

Mustelines are the smallest- and most elongate-bodied group of mustelids and are highly specialized for hypercarnivory (Kurtén and Anderson 1980). The M1 metacone is small and situated close to the paracone with an anteroposteriorly expanded internal cingulum (Bryant et al. 1993; Baskin 1998). Additionally, the m1 has a trenchant talonid and a metaconid that is either absent (*Mustela*) or incipient (*Neogale vison*) (Kurtén and Anderson 1980; Bryant et al. 1993; Baskin 1998; Patterson et al. 2021); and the m2 is single-rooted (Baskin 1998).

#### *Skull and Dental Characters of Mustela*

Members of the genus *Mustela* have retained many of the ancestral characters of Mustelidae (Izor and de la Torre 1978), which has led to its use as a catchall genus despite the results of phylogenetic studies (Koepfli et al. 2008; Harding and Smith 2009; Sato et al. 2012; Law et al. 2018) Nevertheless, *Mustela* can be distinguished from other mustelids by absence of the P1 and p1; a small and anteriorly placed P4 protocone; medial constriction of the M1 with an expanded internal lobe forming a figure-eight occlusal outline and a reduced parastyle; a trenchant talonid on the m1 that is shorter anteroposteriorly relative to the trigonid; absence of the m1 metaconid; a very reduced m2; greatly inflated auditory bullae with paraoccipital processes closely appressed to the bullae; and a palate that is situated behind the upper molars (Figure 3) (Bryant et al. 1993; Baskin 1998). Additionally, the dental formula is I3/3, C1/1, Pm2-

3/3-2, M1/2 = 34; no additional cusp is on the inner side of the main crest of the p4; the longitudinal axes of the crowns of the P4 lie at a significant angle to each other and with the longitudinal axis of the skull; the P2 is very small and corresponds approximately in dimensions to the p1 in *Martes*, but it is not lost, or this occurs only rarely (Hall 1981; Heptner et al. 2001).

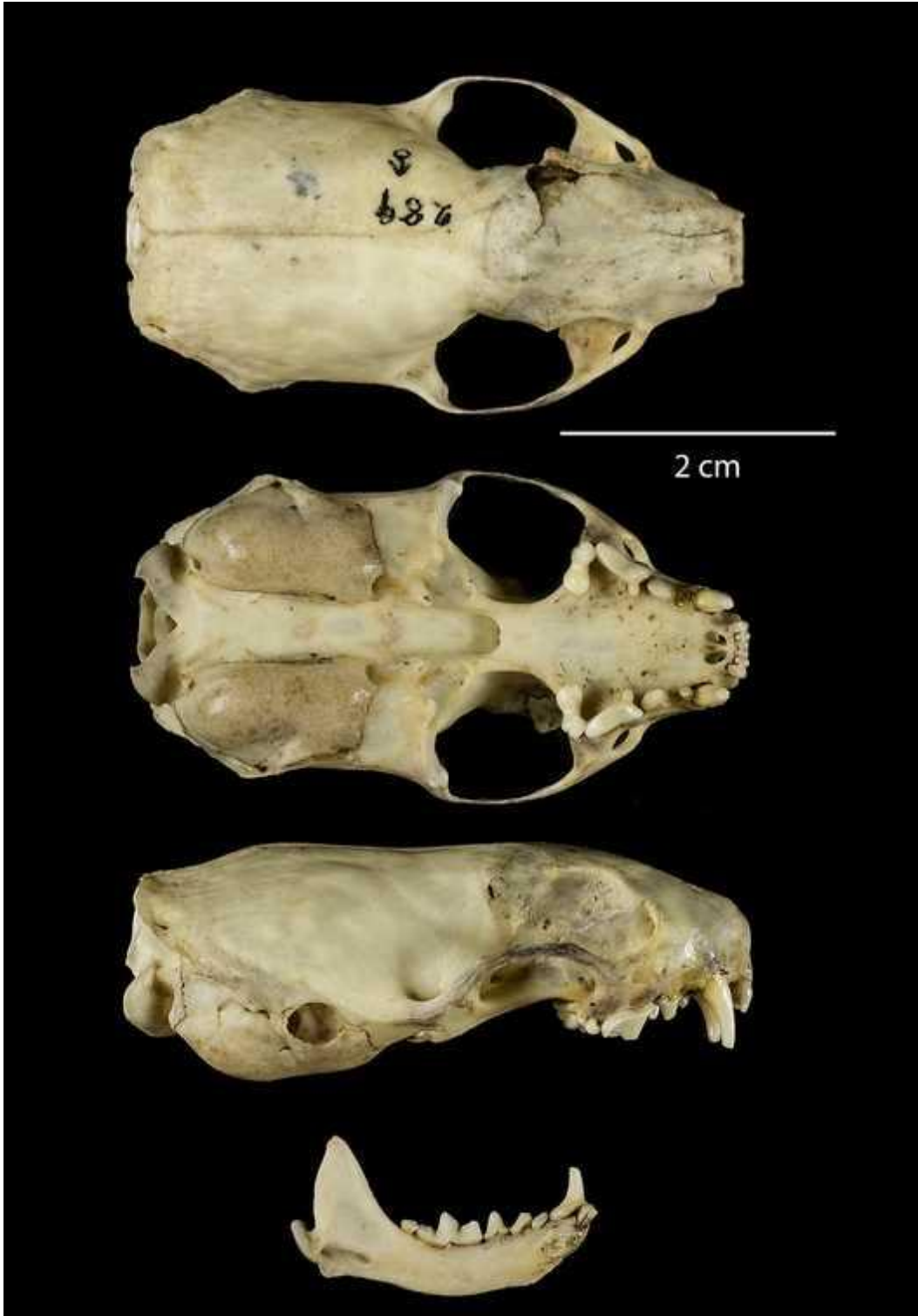


Figure 3. *Mustela erminea* skull in dorsal (top), ventral (center), and right lateral (bottom) views (Museum of Vertebrate Zoology, University of California, Berkeley)

### *Skull and Dental Characters of Neogale*

Members of the genus *Neogale* were formerly placed into *Mustela*; however, recent molecular and phylogenetic analyses (Flynn et al. 2005; Koepfli et al. 2008; Harding and Smith 2009; Sato et al. 2012; Law et al. 2018; Hassanin et al. 2021) support placing the members of this distinct New World clade (*Neogale vison*, *Neogale frenata*, *Neogale africana*, *Neogale felipei*) into a separate genus (Patterson et al. 2021).

Abramov (2000) and Wozencraft (2005) recognized *N. vison* as a separate genus *Neovison* on the basis of its distinctive morphology. Abramov (2000) distinguished *Neovison* from *Mustela* primarily on bacular structure, size of the auditory bullae, and presence of the m1 metaconid; however, this elevation to generic rank was justified by an unsupported phylogenetic tree of relationships suggesting that *Neovison vison* was sister to all species of *Mustela*, which is contradicted by all subsequent phylogenetic studies (Flynn et al. 2005; Koepfli et al. 2008; Harding and Smith 2009; Sato et al. 2012; Law et al. 2018). Diagnostic characters that distinguish *N. vison* from other mustelines include: the braincase is shorter and broader than in subgenera *Kolonokus* and *Lutreola*, but not so strongly built as that of subgenus *Putorius*; the postorbital region of the skull is elongated, and constriction is well marked; and the auditory bullae are small and flattened (Abramov 2000). Additionally, the distance between the upper canines is less than the width of the basioccipital as measured between foramina situated midway along medial sides of the auditory bullae; the teeth are larger and stronger than those of larger *Putorius*; and the P2 has two roots (Figure 4) (Hall 1981; Abramov 2000). *Neogale vison* diagnosis based on skull and dental characters has sometimes be confused with that of *M. nigripes*, but *N. vison* has a larger inner lobe on the M1, a wider occipital region, a larger infraorbital foramen, less inflated auditory bullae, and a wider m1 talonid (Kurtén and Anderson

1980). Also, the upper molars are relatively large (compared to *Mustela*) and the posterior end of the P2 contacts the upper carnassial somewhat more medial to the antero-outer corner of the carnassial (Heptner et al. 2001).

*Neogale africana*, *N. felipei*, and *N. frenata* can be distinguished from one another by the shape of the nasals, the mesopterygoid fossa, inflation of the auditory bullae, orientation of the P3, and size or presence of the p2 (Izor and de la Torre 1978; Sheffield and Thomas 1997; Ramirez-Chavez and Patterson 2014; Ramirez-Chavez et al. 2014). The nasals in *N. africana* form a simple isosceles triangle, whereas in *N. felipei* and *N. frenata* the lateral margins are subparallel anteriorly; the narrower and anteriorly less flaring nasals of *N. felipei* distinguish it from *N. frenata* (Izor and de la Torre 1978). In *N. felipei*, the sides of the mesopterygoid fossa are nearly parallel and the fossa is wide in comparison to *N. africana* and *N. frenata* (Izor and de la Torre 1978; Ramirez-Chavez and Patterson 2014; Ramirez-Chavez et al. 2014). The auditory bullae of *N. felipei* are shorter, broader, and more inflated posteromedially compared to *N. africana* and *N. frenata* (Ramirez-Chavez and Patterson 2014). In *N. felipei*, the buccal margin of the P3 is convex instead of straight or concave as is in *N. africana* and *N. frenata* (Izor and de la Torre 1978). The p2 is very reduced in size compared to *N. frenata* and is absent in *N. africana* (Izor and de la Torre 1978; Ramirez-Chavez and Patterson 2014; Ramirez-Chavez et al. 2014).

The phylogenetic studies previously mentioned were incredibly necessary to identify which species belong to *Neogale* since there are such morphological disparities among the group. And since this taxonomical revision is so recent, morphological synapomorphies and a robust group diagnosis has not yet been identified (Patterson et al. 2021).





Figure 4. *Neogale vison* skull in dorsal (top), ventral (center), and right lateral (bottom) views (Museum of Vertebrate Zoology, University of California, Berkeley)

## CHAPTER 5. ECOLOGY OF MUSTELINES

### *Habitat and Distribution*

Today mustelines are distributed across a variety of habitats within a wide geographic range spanning Europe, northern Africa, Asia (including Java, Sumatra, and Borneo), North America, and northern South America (Kurtén and Anderson 1980; Nowak 2005) (Figure 5). The northern limit of the New World range includes the whole mainland and the entire Arctic Archipelago and the northern and northeastern part of Greenland. The southern limit passes along the northern and northwestern parts of South America, spanning Venezuela and southwestern Colombia to the south and Peru and Bolivia to the west (Heptner et al. 2002). In the Old World, their range occupies all of Europe except Iceland, the Arctic Islands and the islands of the Mediterranean Sea. In Asia, the northern limit of their range spans the entire mainland, to the south, Palestine, Syria, and Iraq (Heptner et al. 2002). Continuing eastward, their range occupies across northern Iran and the entire Himalayas from Kashmir through Nepal, Sikkim, Bhutan, and Assam. In southeast Asia, their range includes Myanmar, the Indochinese Peninsula, Tenasserim, Malacca and the islands of Sumatra, Java, and Borneo (Heptner et al. 2002). Moving eastward, the mainland range reaches the Pacific Ocean and includes the islands of Karangin, Kuril, Shantar, Sakhalin, Japan, the Ryukyus, Taiwan, and Hainan (Heptner et al. 2002).

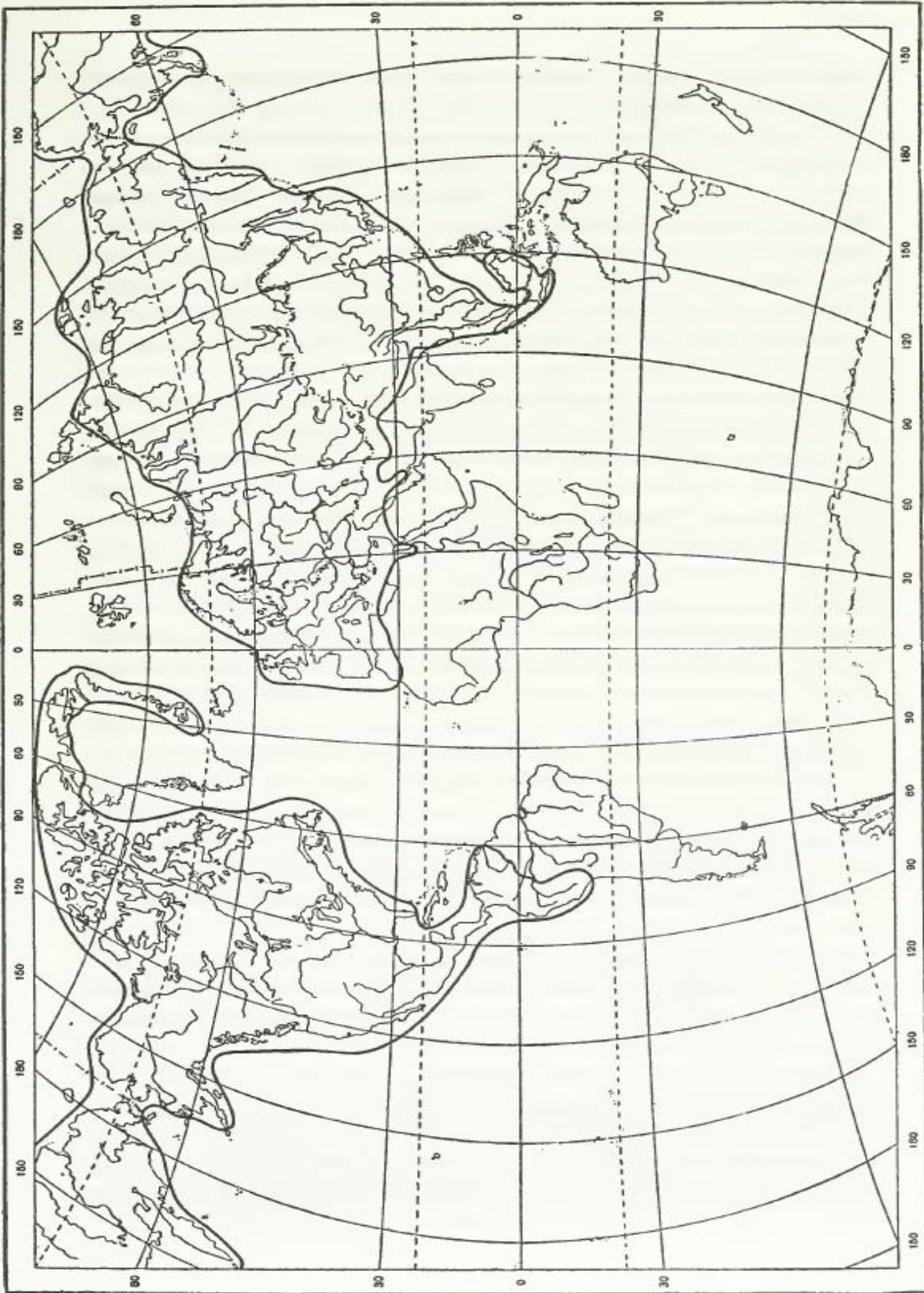


Figure 5. Current world range of Mustelinae (reproduced from Heptner et al. 2001)

Mustelines occupy a wide variety of habitats including tundra, taiga, forest-steppe zones (most common), grassy steppes, deserts, tropical forests, and mountain ranges. (Heptner et al. 2002). Habitat selection is very reliant on prey abundance, and differences in habitat use between mustelines and their prey has led to shifts in occupied niches and variation of diet (King and Powell 2007; Zub et al. 2008).

### *Dietary Ecology*

Mustelines exhibit a hypercarnivorous (>70% vertebrate prey) diet and have evolved as specialist predators of small to medium-sized rodents and lagomorphs, although they may occasionally prey on some reptiles, birds, and their eggs (Heptner et al. 2002; King and Powell 2007; Law et al. 2018). The vast and scattered scientific literature on mustelines contains many descriptions of their diet; however, the interpretation of diet can often be hazardous due to biases toward habitat, season, species, age, and sex (King and Powell 2007). This is evident when examining prey abundance in relation to the size of populations of mustelines. They often demonstrate an exceptionally interdependent relationship with local rodent populations, although levels of dependence can vary significantly among species making it difficult to deduce useful information from their diet (Erlinge 1975; Korpimaki et al. 1991; King and Powell 2007). It is evident that some populations of musteline species have become more specialized while others remain filling a more generalized ecological niche (King and Powell 2007). *M. nivalis* is considered a specialist predator of microtine rodents and other mice (Sheffield and King 1994). Due to its usual association with aquatic environments, the diet of *N. vison* is typically comprised mostly of fish, amphibians, and crustaceans with fewer numbers of small mammals; however, its diet will nevertheless reflect the local prey base (Larivière 1999). Studies documenting the diets of *M. nigripes* populations provide a close affinity for *Cynomys* spp. and their predation does not

seem to significantly reduce *Cynomys* populations, because *M. nigripes*, unlike many other species of mustelines, do not often exhibit surplus predation (Hillman and Clark 1980). *M. erminea* are often considered specialist predators of small mammals, though some studies have revealed some populations of *M. erminea* taking a wider variety of prey species in different proportions, thus considering them to be more of a 'semi-generalist' predator (King 1983; Korpimaki et al. 1991). *N. frenata* is the least-specialized member of the small carnivore guild (Rosenzweig 1966). As a generalist predator, they feed on a wide variety of prey and are able to switch to alternative prey when normal abundance is low (Sheffield and Thomas 1997; King and Powell 2007).

### *Sexual Dimorphism*

Sexual dimorphism in body size is a characteristic feature of all mustelines, with males always being larger than females (Erlinge 1979; Moors 1980; King and Powell 2007). The extent of dimorphism varies between species, as well as geographically within species (Moors 1980). It has been hypothesized by Brown and Lasiewski (1972) that the elongate body of mustelines and their sexual dimorphism has evolved together and that the energetic cost of their elongate body shape has been compensated for by differential food exploitation of the two sexes. The authors' hypothesis expected mustelines to display intra- but not intersexual territoriality, though no field data were available to test the hypothesis. Respectively, Erlinge (1979) and Moors (1980) later provided evidence suggesting the difference in size between sexes has evolved primarily as an adaptation for their different roles in reproduction. It was hypothesized that small females (alone rearing the young) are selectively advantageous, as they can exploit small rodent tunnels and have low absolute food requirements (Erlinge 1979; Moors 1980). In males, large body size is favored by sexual selection, as such males are dominant; by monopolizing areas including

several females, or by social dominance, these males will successfully have more mates (Erlinge 1979; Moors 1980). Considering the evolution of size difference in males and females, the opportunity has come for the two sexes to exploit different food and habitats, which has given further selective advantages to small-sized females and large-sized males and therefore may have enlarged the dimorphism (Erlinge 1979). Moreover, Moors (1980) claimed these patterns indicate that the optimum sizes of males and females result from different selective pressures and are likely to vary independently. However, Ralls and Harvey (1985) argued that the primary factors influencing geographic variation in sexual dimorphism of body size are correlated with prey size, prey abundance, and hunting efficiency. Furthermore, they discovered that male and female size do covary within each species (Ralls and Harvey 1985). With an indication that these factors influence the body size of both male and female North American *Mustela* spp., Ralls and Harvey (1985) rejected the previously stated claim by Moors (1980), suggesting that the influencing factors are similar for both sexes.

Although these studies are broadly supported, the striking degree of sexual dimorphism displayed by mustelines continues to be a controversial topic, as continuing research has resulted in a broad array of possible explanations (King and Powell 2007). Dayan and Simberloff (1994) further extended this list of possible explanations by arguing based on patterns in canine sizes that sexual dimorphism in mustelids evolved to reduce competition between the sexes for food (King and Powell 2007). However, Holmes (1988) analyzed both cranial and post-cranial measurements from North American *Mustela* spp. and found almost no significant differences in morphology between sexes except that skull morphology was disproportionately more similar in size than expected. This indicated that those features most critically involved in mastication, particularly the jaws and teeth, showed less sexual dimorphism than did body size (Holmes

1988; King and Powell 2007). With all of these patterns in consideration, King and Powell (2007) proposed that sexual selection drives the evolution of large body size in males, that efficiency of reproduction drives the evolution of small body size in females, and that the diet of males and females are more similar than expected from their differences in body size.

### *Geographic Variation*

In addition to displaying pronounced sexual dimorphism, mustelines also exhibit a high degree of spatial variation in body size (Abramov and Puzachenko 2009). They are particularly sensitive to thermal stress at low temperatures due to their small, elongate bodies (King and Powell 2007). This metabolic inefficiency may persuade one to suggest that mustelines are very likely to follow Bergmann's Rule, which states that populations found in higher latitudes tend to be larger in species of mammals and birds than populations of the same species found in lower latitudes (McNab 1971). However, a simple comparison between skull size and latitude indicates that mustelines surprisingly often do not follow Bergmann's Rule (King and Powell 2007); only *M. erminea* in North America has been observed to follow Bergmann's Rule (Rosenzweig 1966; McNab 1971; Ralls and Harvey 1985; Eger 1990). Nevertheless, the northern populations of *M. erminea* in North America displaying this pattern can be said to be so only by comparison with their extraordinarily small relatives further south in North America; they are not larger than their relatives at the same latitudes in eastern Eurasia (King 1989; King and Powell 2007).

Many authors have studied geographic variation in the body size of mammals in an attempt to reveal potential spatial patterns, with MacPherson (1965), Rosenzweig (1966), and McNab (1971) notably being among the earliest to address this phenomenon in mustelines. MacPherson (1965) specifically examined arctic mammals and suggested that the current broad patterns of geographic variation among each species are due largely to historical processes of

isolation and divergence in refugia of the Wisconsin glaciation. Likewise, Reig (1997) found based on statistical analyses that the isolation of *M. nivalis* in North America during the glaciations, rather than ecological factors, seems to be the key determinant of geographic variation in skull size. Moreover, the patterns of variation in *M. nivalis* populations from North America, Central Europe, and Siberia, based on skull size and morphology, supported the existence of four distinct groups: *rixosa*, *eskimo*, *vulgaris*, and *subpalmata* (Reig 1997). He suggested that *rixosa* and *subpalmata* each represent a very distinct taxon and therefore deserve consideration as a separate species (Reig 1997).

Eger (1990) further evaluated this refugium hypothesis using a statistical analysis of geographic variation in the skull size and morphology of *M. erminea* in North America. She suggested that the patterns of geographic variation now exhibited by *M. erminea* could be influenced not only by differentiation in refugia, as hypothesized by MacPherson (1965), but also by several other factors, including location prior to postglacial dispersion, current geographic barriers to gene flow, isolation by distance, and climate (Eger 1990). Given that skull size varies closely with current ecology, as well as the likely ability of *M. erminea* to adapt rapidly to changes in its environment, results found post-Wisconsin ecogeographic adaptation to be the primary determinant of geographic variation in skull size in current populations in North America (Eger 1990). Conversely, patterns of variation in skull morphology were more consistent with divergence in refugia of the Wisconsin glaciation (Eger 1990), as hypothesized by MacPherson (1965).

Alternatively, Rosenzweig (1966) suggested that hunting strategy, prey size, and interspecific competition among carnivoran mammals may contribute to various gradations in body size, which allows these sympatric populations of closely related carnivorans to coexist.



Contrary to this hypothesis, he observed sympatric populations of *M. nivalis*, *M. erminea*, and *N. frenata* in North America and discovered only minuscule differences in prey size among each species, consequently leading him to suggest that their successful coexistence may be attributed to differential prey specialization (Rosenzweig 1966). He also discovered latitude to be a climatic variable accurate at predicting body size in *M. erminea* only (Rosenzweig 1968). Similarly, McNab (1971) observed geographic variation in North American musteline species and reported that *M. erminea* and *M. nivalis* increase in body size at latitudes above 50° while *N. frenata* and *M. nigripes* have body sizes independent of latitude in the region from 30° to 50°. Despite this observation, he proposed an alternative explanation to the increase in size at higher latitudes exhibited by *M. erminea*, challenging the suggestions made by Rosenzweig (1966). McNab (1971) stated that *M. erminea* can increase in size at higher latitudes because of the absence of *N. frenata*; it is no longer under constraints to keep its trophic “distance”, thus resulting in character displacement. However, Ralls and Harvey (1985) conducted a statistical analysis of variance including North American species of mustelines and determined that *M. erminea* increases in size with latitude regardless of the presence or absence of *N. frenata* or *M. nivalis*, thus suggesting there is no evidence for character displacement between any pair of species. There was no apparent covariation between *N. frenata*, *M. erminea*, and *M. nivalis* body size when it is sympatric with either of the other two species; however, both sexes within each species did show evidence of covariation in size (Ralls and Harvey 1985). Additionally, they discovered that *M. nivalis* does not increase in size with latitude, contrary to the claim made by McNab (1971) (Ralls and Harvey 1985).

Despite the analyses of Ralls and Harvey (1985), there have been numerous authors report what they view as tentative evidence for character displacement in some populations of *M.*

*erminea*, particularly in the British Isles (Hutchinson 1959; Williamson 1972; Fairley 1981; Dayan et al. 1989; Dayan and Simberloff 1994). Hutchinson (1959) and Williamson (1972) mention that *M. erminea* is smaller in Ireland, where it occurs alone, than on the British mainland, where it is sympatric with *M. nivalis*. However, it later became apparent that *M. erminea* from the south of Ireland are similar in body size to those on the British mainland—it was only in the north of Ireland that *M. erminea* was significantly small (Fairley 1981; Ralls and Harvey 1985). Dayan et al. (1989) and Dayan and Simberloff (1994) searched for possible community-wide character displacement in musteline species of North America and the British Isles, respectively. Both studies suggested evidence of character displacement among sympatric *Mustela* spp. in North America and Great Britain, although not in Ireland. Results that led to this conclusion were evidenced by equal size ratios for condylobasal skull length and maximal diameter of the upper canine among sympatric populations (Dayan et al. 1989; Dayan and Simberloff 1994). However, both groups of authors acknowledge that many critical data remain uncollected (Dayan et al. 1989; Dayan and Simberloff 1994).

## CHAPTER 6. METHODOLOGY

### *Measurements and Statistical Analyses*

Linear measurements from 311 skulls of all 18 extant species of *Mustela* and *Neogale* were collected from the Smithsonian Natural History Museum (USNM) and the East Tennessee State University Museum of Natural History (ETMNH) (Table 1, Figure 6a, 6b; Appendix). An even ratio of adult males and females, as well as an even spatial distribution of specimens covering the entirety of each one's current range, were attempted to account for intraspecific differentiation accounted by high degrees of sexual dimorphism and geographic variation. No juvenile specimens were selected for this study; specimens were determined to be adult based on examination of tooth eruption. Each specimen used in the analysis can be found in the Appendix on pp. 135-143.

Specimens of the extinct sea mink (*'Neovison' macrodon*) were also studied from the USNM collection. The sea mink specimens are the most complete known of a fossil musteline and provide an excellent opportunity for evaluating classification of fossil specimens based on their morphology. Note that the sea mink is referred to as *'Neovison'*, since the name *Neovison* is considered invalid according to the Patterson et al. (2021) taxonomy used here. Additional measurements compiled from literary sources were taken of fossil specimens of extinct taxa, including: *M. gazini* (from Hibbard 1958), *M. jacksoni* (from Storer 2004), *M. meltoni* (from Bjork 1973), and *M. rexroadensis* (from Hibbard 1950; Hibbard 1952; Bjork 1970).

Measurements from Pleistocene fossil specimens of extant species include *M. erminea* (from Getz 1960; Harris 1993a; Anderson 1977; Baryshnikov and Alekseeva 2017), *N. frenata* (from Harris 1993b), *M. nivalis* (from Baryshnikov and Alekseeva 2017), *M. nigripes* (from Anderson et al. 1986; Harris 1993b; Owen et al. 2000; Fox 2014), and *N. vison* (from Gidley and Gazin

1938; Anderson 1977), which were compiled to examine potential morphological differences between Pleistocene and Holocene individuals of the same species. Measurements from two Blancan-aged fossils labeled *Mustela* sp. were also taken to examine potential classification. Lastly, measurements from the left P4 and M1 of a taxonomically unknown musteline recently uncovered from the early Pliocene (late Hemphillian or early Blancan) Gray Fossil Site (GFS) in eastern Tennessee were collected to attempt classification of its taxonomic status.

Table 1. Definitions of Osteological Measurements Used in the Analysis and Their Abbreviations

| <b>Definition</b>  | <b>Abbreviation</b> |
|--|---------------------|
| Length of upper third premolar   | P3L                 |
| Width of upper third premolar  | P3W                 |
| Length of upper carnassial   | P4L                 |
| Width of upper carnassial at protocone   | P4ProW              |
| Width of upper carnassial at paracone  | P4ParW              |
| Width of upper first molar   | M1W                 |
| Length of upper first molar at lingual lobe  | M1LinL              |
| Length of upper first molar at buccal lobe   | M1BucL              |
| Upper grinding area (occlusal surface area of upper first molar)   | UGA                 |
| Length of lower fourth premolar  | p4L                 |
| Width of lower fourth premolar   | p4W                 |
| Length of lower carnassial   | m1L                 |
| Length of trigonid of lower carnassial   | m1TriL              |
| Length of talonid of lower carnassial  | m1TalL              |
| Width of lower carnassial  | m1W                 |
| Lower grinding area (occlusal surface area of talonid of lower carnassial and m2)                          | LGA                 |
| Mandibular depth between p4 and m1   | MD                  |
| Moment arm of temporalis muscle (distance between mandibular condyle and apex of coronoid process)         | MAT                 |
| Moment arm of masseter muscle (distance between mandibular condyle and ventral border of mandibular angle) | MAM                 |
| Condylbasal length of skull  | CBL                 |
| Maximum cranial width  | MCW                 |



Figure 6a. Linear measurements of skull used in the analysis. Image is not to scale. Measurements modified from Friscia et al. 2007.

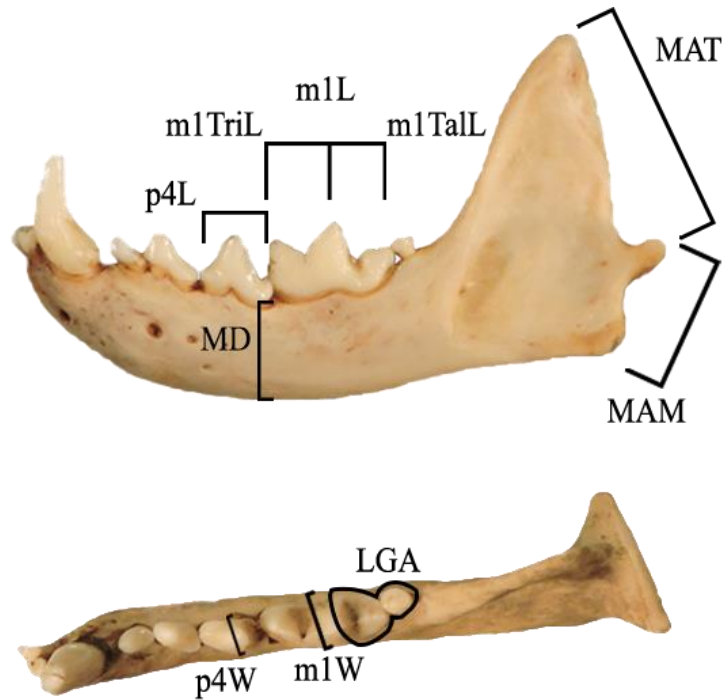


Figure 6b. Linear measurements of mandible used in the analysis. Image is not to scale. Measurements modified from Friscia et al. 2007.

Measurements chosen for this analysis were modified from Anderson et al. (1986) and Friscia et al. (2007) and recorded to the nearest 0.01 mm using either digital calipers or from digital photographs of the specimens. Photographs were taken in dorsal, lateral, and ventral views, and positioned with the palate parallel to the photographic plane with a scale bar included. Measurements from the photographs were scaled and obtained using ImageJ image processing and analysis software (Rasband 1997-2018). When available, scaled photographs of the fossil specimens were also analyzed using ImageJ to collect any additional measurements not already provided in the literature. Selected raw measurements were then combined and calculated into ratios to interpret proportional differentiation (Table 2). Measurements were averaged across the individuals of each species and a geometric mean (GM) transformation was applied to each

individual to correct for body size, examine allometry, and allow for potential strong relationships to become more interpretable (Frischia et al. 2007). A separate GM transformation was applied to each extinct taxon analysis to separately examine the classification of the specific target variable being analyzed. Each extinct taxon was run as an ungrouped case in the analysis. Due to the fragmentary nature of the fossil specimens, an averaged composite score of measurements for each extinct species was calculated to allow for each measurement to be run in the analysis. A stepwise discriminant function analysis (DFA) was used to classify each individual at the genus- and species-level. Additionally, a third DFA was used to classify each individual by clade (Table 3). Bivariate scatterplots of the log-transformed variables were used for visual interpretation of data. All analyses were performed using IBM SPSS Statistical Package, Version 28.

Table 2. Definitions of Ratios Used in the Analysis and Their Abbreviations (modified from Friscia et al., 2007)

| <b>Definition</b>  | <b>Abbreviation</b> |
|--|---------------------|
| Length divided by width of upper carnassial                                  | P4L/W               |
| Width of parastyle divided by width of protocone of upper carnassial         | P4PastW/ProW        |
| Length divided by width of upper first molar                                 | M1L/W               |
| Length of lingual lobe divided by length of buccal lobe of upper first molar | M1LinL/BucL         |
| Length of upper carnassial divided by width of upper first molar             | P4L/M1W             |
| Length divided by width of lower fourth premolar                             | p4L/W               |
| Length divided by width of lower carnassial                                  | m1L/W               |
| Length of trigonid divided by length of talonid of lower carnassial          | m1TriL/TalL         |
| Length of lower carnassial divided by length of lower fourth premolar        | m1L/p4L             |
| Condylbasal length of skull divided by maximum cranial width                 | CBL/MCW             |

Table 3. Evolutionary Clades of Mustelines (from Harding and Smith 2009 and Law et al. 2018)

| Clade # | Taxa   |
|---------|--|
| 1       | <i>N. africana</i> , <i>N. felipei</i> , <i>N. frenata</i> , <i>N. vison</i> |
| 2       | <i>M. nudipes</i> , <i>M. strigidorsa</i>                                    |
| 3       | <i>M. kathiah</i>  |
| 4       | <i>M. erminea</i>  |
| 5       | <i>M. altaica</i> , <i>M. nivalis</i> , <i>M. subpalmata</i>                 |
| 6       | <i>M. itatsi</i>   |
| 7       | <i>M. lutreolina</i> , <i>M. sibirica</i>                                    |
| 8       | <i>M. lutreola</i>   |
| 9       | <i>M. eversmanii</i> , <i>M. nigripes</i> , <i>M. putorius</i>               |

#### Character State Analysis

In addition to a statistical analysis, a qualitative analysis was conducted to potentially distinguish *Mustela* and *Neogale* using a total of 43 skull and tooth morphological characters (Table 4). An additional analysis targeting *N. vison* was completed to examine for potential characters distinguishing it from other mustelines due to its well-known semi-aquatic ecology (Larivière 1999). Characters used in the analysis are listed and defined below and were compiled from Bryant et al. (1993) and Wolsan (1993) to assess phylogenetic relationships between both extant and extinct groups within Mustelidae. A “state” of each character was scored for each individual and organized into a data matrix to observe potential distinguishing characters at the genus- and species-level and to examine intraspecific variation in expression of these traits.



Table 4. Definitions of Skull and Tooth Characters Used in the Analysis (modified from Bryant et al. 1993 and Wolsan 1993)

| <b>Character</b>  | <b>a</b>   | <b>b</b>  | <b>c</b> | <b>d</b> | <b>e</b> |
|---|--|---|----------|----------|----------|
| <b>(1) Form of postorbital region</b>   | postorbital region not elongated in adults, shorter than its greatest width        | postorbital region greatly elongated in adults                            |          |          |          |
| <b>(2) Pattern of dorsal cranial crests</b>   | Y-shaped in adults, sagittal crest present   | crests parallel to X-shaped in adults, strong parasagittal crests present |          |          |          |
| <b>(3) Occurrence of postlateral sulcus of brain</b>  | present  | absent  |          |          |          |
| <b>(4) Anterior opening of palatine canal</b>   | at maxilla-palatine suture   | more anterior through maxilla   |          |          |          |
| <b>(5) Posterior margin of secondary palate</b>   | well posterior of posterior margin of M1   | level with the posterior margin of M1                                     |          |          |          |
| <b>(6) Sagittal partition of nasal cavity by the vomer</b>                                      | posterior edge well-forward of posterior end of the horizontal lamina of the vomer | posterior edge at or adjacent to posterior end of horizontal lamina       |          |          |          |
| <b>(7) Caliber of infraorbital canal</b>  | small  | intermediate  | large    |          |          |
| <b>(8) Orientation of anterior opening of infraorbital canal</b>                                | faces anteriorly   | faces anteroventrally   |          |          |          |
| <b>(9) Positional relationship between sphenopalatine canal and posterior palatine foramina</b> | in a distinct, common fossa  | not in a common fossa   |          |          |          |
| <b>(10) Occurrence of alisphenoid canal</b>   | present  | absent  |          |          |          |
| <b>(11) Position of posterior carotid foramen</b>   | joined to fossa leading to posterior lacerate foramen                              | separated from fossa leading to posterior lacerate foramen                |          |          |          |

|  |  |  |   |
|--|--|--|---|
| <b>(12) Size of posterior lacerate foramen</b>         | not enlarged, smaller than lateral opening of external auditory meatus   | greatly enlarged, greater than lateral opening of external auditory meatus   |   |
| <b>(13) Posterior extension of caudal entotympanic</b> | smallest width of auditory bulla between stylomastoid foramen and fossa leading to posterior lacerate foramen smaller than greatest diameter of stylomastoid foramen | smallest width of auditory bulla between stylomastoid foramen and fossa leading to posterior lacerate foramen greater than greatest diameter of stylomastoid foramen, posterior border of caudal entotympanic situated in front of that of fossa leading to posterior lacerate foramen | smallest width of auditory bulla between stylomastoid foramen and fossa leading to posterior lacerate foramen greater than greatest diameter of stylomastoid foramen, posterior border of caudal entotympanic situated behind that of fossa leading to posterior lacerate foramen |
| <b>(14) Lateral extension of ectotympanic</b>          | meatal trough of ossified ectotympanic not differentiated  | meatal trough of ossified ectotympanic short, its smallest mediolateral dimension smaller than one-third of bullar width   | meatal trough of ossified ectotympanic long, its smallest mediolateral dimension greater than one-third of bullar width   |
| <b>(15) Hamulus</b>                                    | not connected to auditory bulla  | with bony connection to auditory bulla   |   |
| <b>(16) Stylomastoid foramen</b>                       | tympanohyal in a common fossa with, or immediately posteromedial to, the foramen   | tympanohyal separated from foramen by a bridge of bone   |   |
| <b>(17) Lateral extension of epitympanic recess</b>    | epitympanic recess anterior to fossa for incudal processus brevis not floored by squamosal   | lateral part of epitympanic recess anterior to fossa for incudal processus brevis floored by squamosal   |   |

|   |  |   |  |
|---|--|---|--|
| <b>(18) Paroccipital process</b>                                  | moderately to strongly developed, projecting posteriorly or posteroventrally                               | absent  |  |
| <b>(19) Lateral swelling of cranium dorsal to mastoid process</b> | absent   | present   |  |
| <b>(20) Condylod canal</b>  | present  | absent  |  |
| <b>(21) Osseous tentorium</b>                                     | present  | absent  |  |
| <b>(22) Auditory bulla</b>  | restricted to immediately medial to the external auditory meatus, probably involving only the ectotympanic | inflation increased, medially, anteriorly and especially posteriorly, involving primarily the caudal entotympanic |  |
| <b>(23) Suprameatal fossa</b>                                     | well-developed but closed ventrally  | moderately to extremely reduced   |  |
| <b>(24) Pm1 occurrence</b>  | present  | absent  |  |
| <b>(25) pm1 occurrence</b>  | present  | absent  |  |
| <b>(26) Pm2 occurrence</b>  | present  | absent  |  |
| <b>(27) pm2 occurrence</b>  | present  | absent  |  |
| <b>(28) Pm4 carnassial notch occurrence</b>                       | present  | absent  |  |
| <b>(29) Pm4 medial shelf</b>                                      | absent   | moderately developed, especially anteriorly   | extensive, projecting strongly medially and extending posteriorly to the end of the metastylar blade, or nearly so |
| <b>(30) Pm4 protocone</b>   | no prominent cusp, but a raised ridge or cuspule present, smaller in width than the parastyle              | small cusp, larger in width than the parastyle  | large, high cusp   |

|  |   |   |   |   |   |
|--|---|---|---|---|---|
| <b>(31) Pm4 hypocone</b>               | absent  | present   |   |   |   |
| <b>(32) Pm4 shape</b>                  | large with size similar to that of M1, with metastyle well-developed  | large with size similar to that of M1, with metastyle reduced   | anteroposterior length reduced, much shorter than M1, with metastyle reduced  |   |   |
| <b>(33) Pm4 accessory cusp</b>         | present   | absent  |   |   |   |
| <b>(34) Size relation of M1 to Pm4</b> | M1 clearly larger than Pm4  | M1 subequal in size to Pm4  | M1 clearly smaller than Pm4   |   |   |
| <b>(35) Pattern of M1</b>              | lingual half of M1 crown shorter than buccal half, anterior and posterior borders of lingual half not parallel to each other  | lingual half of M1 crown shorter than buccal half, anterior and posterior borders of lingual half parallel to each other  | lingual half of M1 crown subequal in length to buccal half, both halves separated from each other by anteroposterior constriction | lingual half of M1 crown longer than buccal half, both halves separated from each other by anteroposterior constriction | lingual half of M1 crown subequal in length to buccal half, no anteroposterior constriction |
| <b>(36) M1 lingual cingulum</b>        | anterior and posterior cingula of M1 not continuous around lingual lobe   | anterior and posterior cingula of M1 continuous around lingual lobe   |   |   |   |
| <b>(37) m1 talonid morphology</b>      | rim complete with strong hypoconid, poorly developed lingual cusps and shallow basin  | lingual rim absent and prominent hypoconid  | no basin, strong central hypoconid, entoconid, and buccal cingulum  | strong rim and basin, cusps poorly developed  | prominent basin and rim, hypoconid and entoconid well-developed                             |
| <b>(38) Pattern of m1 talonid</b>      | entoconid and entoconulid poorly differentiated (ridge-like or cuspule-like), anterior and posterior halves of lingual wall of talonid subequal in height to each other | entoconid and entoconulid poorly differentiated (ridge-like or cuspule-like) or not differentiated, anterior half of lingual wall of talonid distinctly lower than posterior half | entoconid prominent (cusp-like)   |   |   |
| <b>(39) m1 metaconid</b>               | large   | much smaller than the other trigonid cusps and often positioned posteriorly   | absent  |   |   |

|  |  |   |
|--|--|---|
| <b>(40) Relation of m1 trigonid to talonid</b> | trigonid less than three times as long as talonid                                | trigonid more than three times as long as talonid               |
| <b>(41) M1 postprotocrista</b>                 | present, may be weak posterobuccally   | absent or minimally developed                                   |
| <b>(42) M1 preprotocrista</b>                  | extends lingually to posterolingually from the parastyle region to the protocone | extends mostly posteriorly, elongated and divided into cuspules |
| <b>(43) m2 occurrence</b>                      | present  | absent  |

## CHAPTER 7. RESULTS

### *Character State Analysis*

A character state analysis using 43 skull and tooth morphological characters was conducted to qualitatively identify potential distinguishing characters within *Mustela* and *Neogale*. Two characters, #27 (pm2 occurrence) and #40 (relation of m1 trigonid to talonid), showed consistent differences that can aid in distinguishing between the two genera (Table 5). For #27, 192 (100%) of *Mustela* showed *a* (present); 61 (97%) of *Neogale* showed *a* and 2 (3%) showed *b* (absent) (Table 6). For #40, 157 (84%) of *Mustela* showed *a* (trigonid less than three times as long as talonid) and 29 (16%) showed *b* (trigonid more than three times as long as talonid); 62 (100%) of *Neogale* showed *a* (Table 6).

A total of four characters, #30 (P4 protocone), #34 (size relation of M1 to P4), #35 (pattern of M1), and #39 (m1 metaconid), proved successful in distinguishing *N. vison* and *N. macrodon* from all other musteline taxa (Table 7). For #30, 151 (87%) of *Mustela* showed *a* (no prominent cusp, but a raised ridge or cuspule present, smaller in width than the parastyle) and 22 (13%) showed *b* (small cusp, larger in width than the parastyle); 26 (84%) of *Neogale* (excluding *N. vison*) showed *a* and 5 (16%) showed *b*; 29 (100%) of *N. vison* showed *b*; and 5 (100%) of *N. macrodon* showed *b* (Table 7). For #34, 56 (30%) of *Mustela* showed *b* (M1 subequal in size to P4) and 128 (70%) showed *c* (M1 clearly smaller than P4); 14 (44%) of *Neogale* (excluding *N. vison*) showed *b* and 18 (56%) showed *c*; 23 (82%) of *N. vison* showed *b* and 5 (18%) showed *c*; and 3 (100%) of *N. macrodon* showed *b* (Table 7). For #35, 101 (55%) of *Mustela* showed *c* (lingual half of M1 crown subequal in length to buccal half, both halves separated from each other by anteroposterior constriction) and 84 (45%) showed *d* (lingual half of M1 crown longer than buccal half, both halves separated from each other by anteroposterior constriction); 18

(56%) of *Neogale* (excluding *N. vison*) showed *c* and 14 (44%) showed *d*; 4 (14%) of *N. vison* showed *c* and 24 (86%) showed *d*; and 3 (100%) of *N. macrodon* showed *c*. For #39, 188 (100%) of *Mustela* showed *c* (absent); 32 (100%) of *Neogale* (excluding *N. vison*) showed *c*; 31 (100%) of *N. vison* showed *b* (much smaller than the other trigonid cusps and often positioned posteriorly); and 21 (100%) of *N. macrodon* showed *c* (Table 7).

Table 5. Character State Distribution Among *Mustela*, *Neogale*, and *Neogale vison* With Distinguishing Characters Highlighted

| Character state  | <i>Mustela</i> | <i>Neogale</i> | <i>N. vison</i> |
|--|----------------|----------------|-----------------|
| (1) Form of postorbital region   | a              | a              | a               |
| (2) Pattern of dorsal cranial crests   | a              | a              | a               |
| (3) Occurrence of postlateral sulcus of brain  | b              | b              | b               |
| (4) Anterior opening of palatine canal   | b              | b              | b               |
| (5) Posterior margin of secondary palate   | a              | a              | a               |
| (6) Sagittal partition of nasal cavity by the vomer                                      | a              | a              | a               |
| (7) Caliber of infraorbital canal  | a              | a              | a               |
| (8) Orientation of anterior opening of infraorbital canal                                | a              | a              | a               |
| (9) Positional relationship between sphenopalatine canal and posterior palatine foramina | a              | a              | a               |
| (10) Occurrence of alisphenoid canal   | b              | b              | b               |
| (11) Position of posterior carotid foramen   | b              | b              | b               |
| (12) Size of posterior lacerate foramen  | a              | a              | a               |
| (13) Posterior extension of caudal entotympanic  | c              | c              | c               |
| (14) Lateral extension of ectotympanic   | b              | b              | b               |
| (15) Hamulus   | a              | a              | a               |
| (16) Stylomastoid foramen  | a              | a              | a               |
| (17) Lateral extension of epitympanic recess   | b              | b              | b               |
| (18) Paroccipital process  | b              | b              | b               |
| (19) Lateral swelling of cranium dorsal to mastoid process                               | a              | a              | a               |
| (20) Condylloid canal  | a              | a              | a               |
| (21) Osseous tentorium   | a              | a              | a               |
| (22) Auditory bulla  | b              | b              | b               |
| (23) Suprameatal fossa   | a              | a              | a               |
| (24) P1 occurrence   | b              | b              | b               |
| (25) p1 occurrence   | b              | b              | b               |
| (26) P2 occurrence   | a              | a              | a               |

|   |    |    |    |
|---|----|----|----|
| (27) p2 occurrence                      | a  | ab | a  |
| (28) P4 carnassial notch occurrence     | b  | b  | b  |
| (29) P4 medial shelf                    | a  | a  | a  |
| (30) P4 protocone                       | ab | ab | b  |
| (31) P4 hypocone                        | a  | a  | a  |
| (32) P4 shape                           | a  | a  | a  |
| (33) P4 accessory cusp                  | b  | b  | b  |
| (34) Size relation of M1 to P4          | bc | bc | bc |
| (35) Pattern of M1                      | cd | cd | cd |
| (36) M1 lingual cingulum                | b  | b  | b  |
| (37) m1 talonid morphology              | b  | b  | b  |
| (38) Pattern of m1 talonid              | b  | b  | b  |
| (39) m1 metaconid                       | c  | c  | b  |
| (40) Relation of m1 trigonid to talonid | ab | a  | a  |
| (41) M1 postprotocrista                 | b  | b  | b  |
| (42) M1 preprotocrista                  | a  | a  | a  |
| (43) m2 occurrence                      | a  | a  | a  |

Table 6. Percentages of Distinguishing Characters Between *Mustela* and *Neogale*

| Genus          | 27            |           | 30           |             | 34          |              | 35           |             | 39          |               | 40           |             |
|----------------|---------------|-----------|--------------|-------------|-------------|--------------|--------------|-------------|-------------|---------------|--------------|-------------|
|                | a             | b         | a            | b           | b           | c            | c            | d           | b           | c             | a            | b           |
| <i>Mustela</i> | 192<br>(100%) | –         | 151<br>(87%) | 22<br>(13%) | 56<br>(30%) | 128<br>(70%) | 101<br>(55%) | 84<br>(45%) | –           | 188<br>(100%) | 157<br>(84%) | 29<br>(16%) |
| <i>Neogale</i> | 61<br>(97%)   | 2<br>(3%) | 26<br>(43%)  | 34<br>(57%) | 37<br>(62%) | 23<br>(38%)  | 22<br>(37%)  | 38<br>(63%) | 31<br>(49%) | 32<br>(51%)   | 62<br>(100%) | –           |



Table 7. Percentages of Distinguishing Characters Among Holocene Musteline Taxa. Species of *Mustela* are highlighted in green, *Neogale* in blue, and ‘*Neovison*’ *macrodon* in orange.

| Taxon                                  | 27           |             | 30           |              | 34          |             | 35          |             | 39           |              | 40           |             |
|--|--------------|-------------|--------------|--------------|-------------|-------------|-------------|-------------|--------------|--------------|--------------|-------------|
|  | a            | b           | a            | b            | b           | c           | c           | d           | b            | c            | a            | b           |
| <i>M. altaica</i>                      | 16<br>(100%) | –           | 15<br>(94%)  | 1 (6%)       | 1 (6%)      | 15<br>(94%) | 11<br>(69%) | 5<br>(31%)  | –            | 16<br>(100%) | 11<br>(69%)  | 5<br>(31%)  |
| <i>M. erminea</i>                      | 31<br>(100%) | –           | 20<br>(71%)  | 8<br>(29%)   | 26<br>(93%) | 2 (7%)      | 9<br>(31%)  | 20<br>(69%) | –            | 33<br>(100%) | 26<br>(84%)  | 5<br>(16%)  |
| <i>M. eversmanii</i>                   | 11<br>(100%) | –           | 9<br>(100%)  | –            | 2<br>(22%)  | 7<br>(78%)  | 8<br>(89%)  | 1<br>(11%)  | –            | 10<br>(100%) | 8<br>(80%)   | 2<br>(20%)  |
| <i>M. itatsi</i>                       | 17<br>(100%) | –           | 17<br>(100%) | –            | 1 (6%)      | 16<br>(94%) | 3<br>(18%)  | 14<br>(82%) | –            | 17<br>(100%) | 17<br>(100%) | –           |
| <i>M. kathiah</i>                      | 5<br>(100%)  | –           | 5<br>(100%)  | –            | 3<br>(60%)  | 2<br>(40%)  | 3<br>(60%)  | 2<br>(40%)  | –            | 5<br>(100%)  | 5<br>(100%)  | –           |
| <i>M. lutreola</i>                     | 4<br>(100%)  | –           | 4<br>(100%)  | –            | 2<br>(50%)  | 2<br>(50%)  | 2<br>(50%)  | 2<br>(50%)  | –            | 4<br>(100%)  | 4<br>(100%)  | –           |
| <i>M. lutreolina</i>                   | 2<br>(100%)  | –           | 1<br>(100%)  | –            | 2<br>(100%) | –           | 1<br>(50%)  | 1<br>(50%)  | –            | 2<br>(100%)  | 2<br>(100%)  | –           |
| <i>M. nigripes</i>                     | 13<br>(100%) | –           | 10<br>(100%) | –            | 1 (7%)      | 13<br>(93%) | 12<br>(86%) | 2<br>(14%)  | –            | 13<br>(100%) | 13<br>(100%) | –           |
| <i>M. nivalis</i>                      | 27<br>(100%) | –           | 20<br>(83%)  | 4<br>(17%)   | 5<br>(21%)  | 19<br>(79%) | 11<br>(46%) | 13<br>(54%) | –            | 26<br>(100%) | 23<br>(88%)  | 3<br>(12%)  |
| <i>M. nudipes</i>                      | 5<br>(100%)  | –           | 5<br>(100%)  | –            | 2<br>(40%)  | 3<br>(60%)  | 5<br>(100%) | –           | –            | 5<br>(100%)  | 5<br>(100%)  | –           |
| <i>M. putorius</i>                     | 19<br>(100%) | –           | 18<br>(95%)  | 1 (5%)       | 6<br>(32%)  | 13<br>(68%) | 10<br>(53%) | 9<br>(47%)  | –            | 19<br>(100%) | 15<br>(79%)  | 4<br>(21%)  |
| <i>M. sibirica</i>                     | 22<br>(100%) | –           | 16<br>(94%)  | 1 (6%)       | 1 (5%)      | 20<br>(95%) | 9<br>(43%)  | 12<br>(57%) | –            | 18<br>(100%) | 18<br>(100%) | –           |
| <i>M. strigidorsa</i>                  | 1<br>(100%)  | –           | 1<br>(100%)  | –            | 1<br>(100%) | –           | 1<br>(100%) | –           | –            | 1<br>(100%)  | 1<br>(100%)  | –           |
| <i>M. subpalmata</i>                   | 19<br>(100%) | –           | 10<br>(59%)  | 7<br>(41%)   | 3<br>(16%)  | 16<br>(84%) | 16<br>(84%) | 3<br>(16%)  | –            | 19<br>(100%) | 9<br>(47%)   | 10<br>(53%) |
| <i>N. africana</i>                     | –            | 2<br>(100%) | 1 (50%)      | 1<br>(50%)   | 2<br>(100%) | –           | 2<br>(100%) | –           | –            | 2<br>(100%)  | 2<br>(100%)  | –           |
| <i>N. felipei</i>                      | 2<br>(100%)  | –           | 2<br>(100%)  | –            | 2<br>(100%) | –           | 1<br>(50%)  | 1<br>(50%)  | –            | 2<br>(100%)  | 1<br>(100%)  | –           |
| <i>N. frenata</i>                      | 28<br>(100%) | –           | 23<br>(85%)  | 4<br>(15%)   | 10<br>(36%) | 18<br>(64%) | 15<br>(54%) | 13<br>(46%) | –            | 28<br>(100%) | 28<br>(100%) | –           |
| <i>N. vison</i>                        | 31<br>(100%) | –           | –            | 29<br>(100%) | 23<br>(82%) | 5<br>(18%)  | 4<br>(14%)  | 24<br>(86%) | 31<br>(100%) | –            | 31<br>(100%) | –           |
| ‘ <i>Neovison</i> ’<br><i>macrodon</i> | 21<br>(100%) | –           | –            | 5<br>(100%)  | 3<br>(100%) | –           | 3<br>(100%) | –           | 21<br>(100%) | –            | 20<br>(100%) | –           |

### *Extant Taxa Analysis*

A stepwise DFA of genus, species, and clade classification was performed using the ratios and GM-transformed linear measurements for each extant musteline taxon. Additionally, Pleistocene-aged specimens of each North American taxon (*M. erminea*, *N. frenata*, *M. nigripes*, *M. nivalis*, and *N. vison*) were included in the analysis as unclassified cases.

#### *Genus Classification*

For genus classification, a total of nine of the 31 indices are included in the stepwise discriminant model (Table 8). The DFA separated each genus fairly well (Wilks'  $\lambda = 0.513$ ,  $p < 0.001$ ) and yielded one discriminant function with an eigenvalue of 0.948 and a canonical correlation of 0.698. The discriminant function (DF1) was positively correlated with P4PastW/ProW, CBL, m1TriL/TalL, m1L/W, and P3W, and negatively correlated with LGA, M1W, m1TalL, and p4L. Members of *Mustela* had both negative and positive scores with most cases scoring slightly to moderately positive, while nearly all members of *Neogale* had moderately to highly negative scores (Figure 7). Boxplots and bivariate plots showed significant differences in indices between genera and are illustrated in Figure 8. The ability of the discriminant model to separate musteline taxa into genus was determined using the classification matrix (Table 9). The classification showed 94.6% correct classification of *Mustela* and 82.5% correct classification of *Neogale*. When cross-validated, the classification showed 94% correct classification of *Mustela* and 80.7% correct classification of *Neogale*. Regarding the Pleistocene specimens, *M. erminea*, *N. frenata*, *M. nigripes*, and *M. nivalis* were classified as *Mustela* and *N. vison* was classified as *Neogale* (Table 14).

Table 8. Extant Genus Structure Matrix, Eigenvalue, Percent Variance Explained, and Wilks'  $\lambda$  for Discriminant Function 1

| <b>Index</b>          | <b>DF 1</b> |
|-----------------------|-------------|
| P4PastW/ProW          | 0.462       |
| CBL                   | 0.448       |
| m1TriL/TalL           | 0.382       |
| LGA                   | -0.291      |
| m1L/W                 | 0.259       |
| P3W                   | 0.177       |
| M1W                   | -0.093      |
| m1TalL                | -0.085      |
| p4L                   | -0.027      |
| Eigenvalue            | 0.948       |
| % variance explained  | 100         |
| Canonical correlation | 0.698       |
| Wilks' $\lambda$      | 0.513       |
| <i>p</i> -value       | < 0.001     |

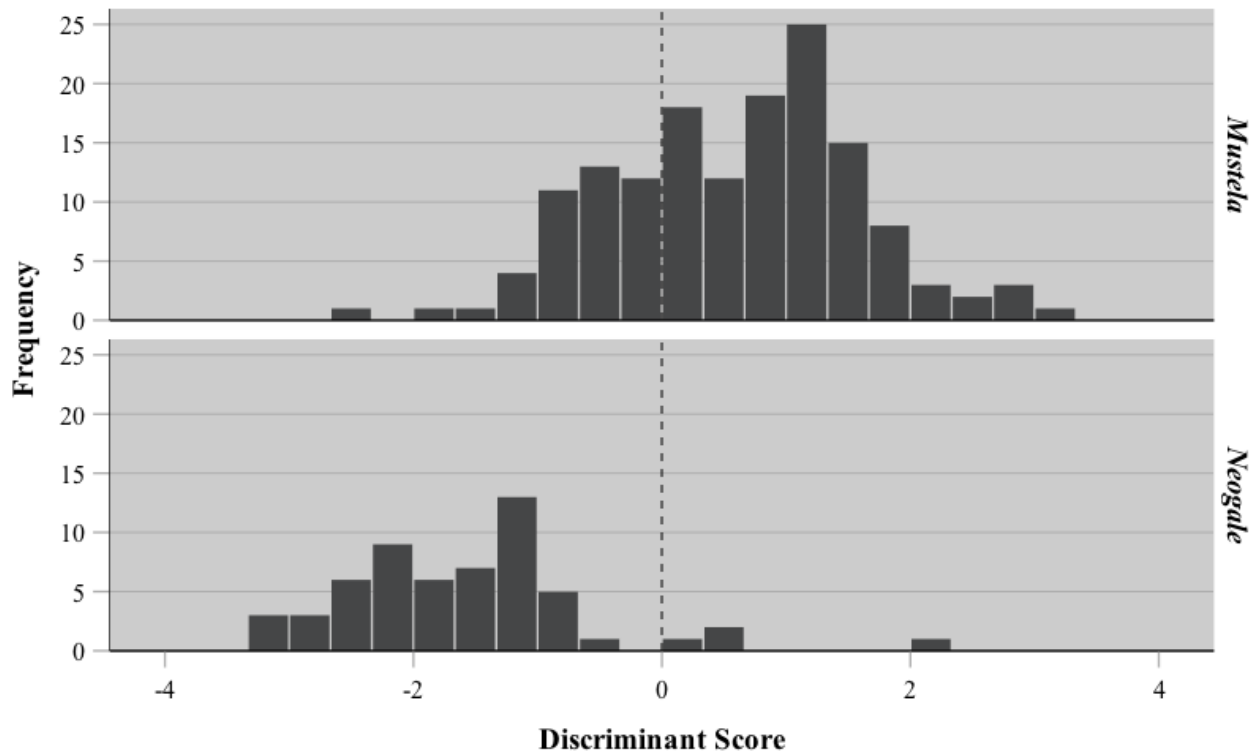
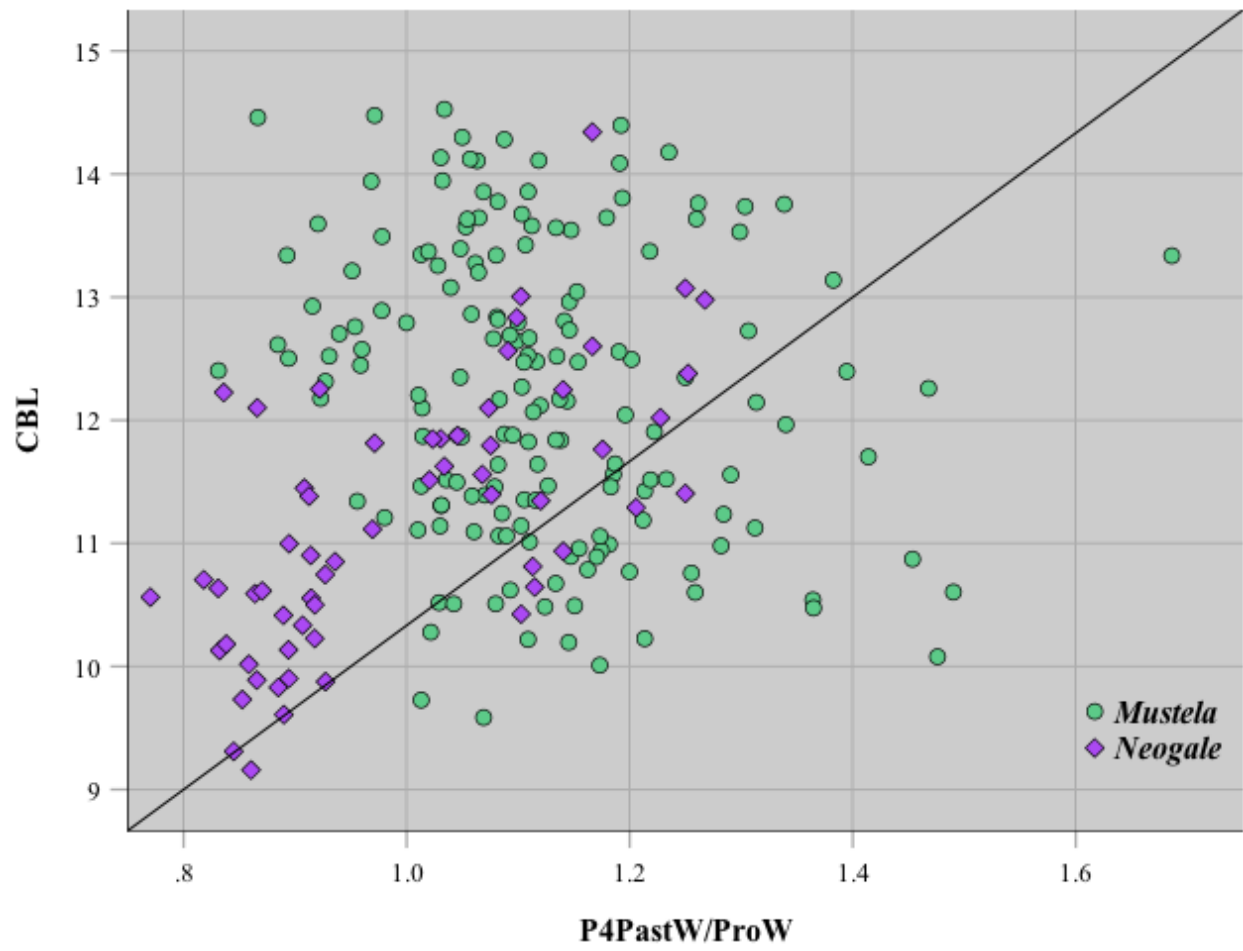


Figure 7. Discriminant scores from DF1 for extant genus analysis



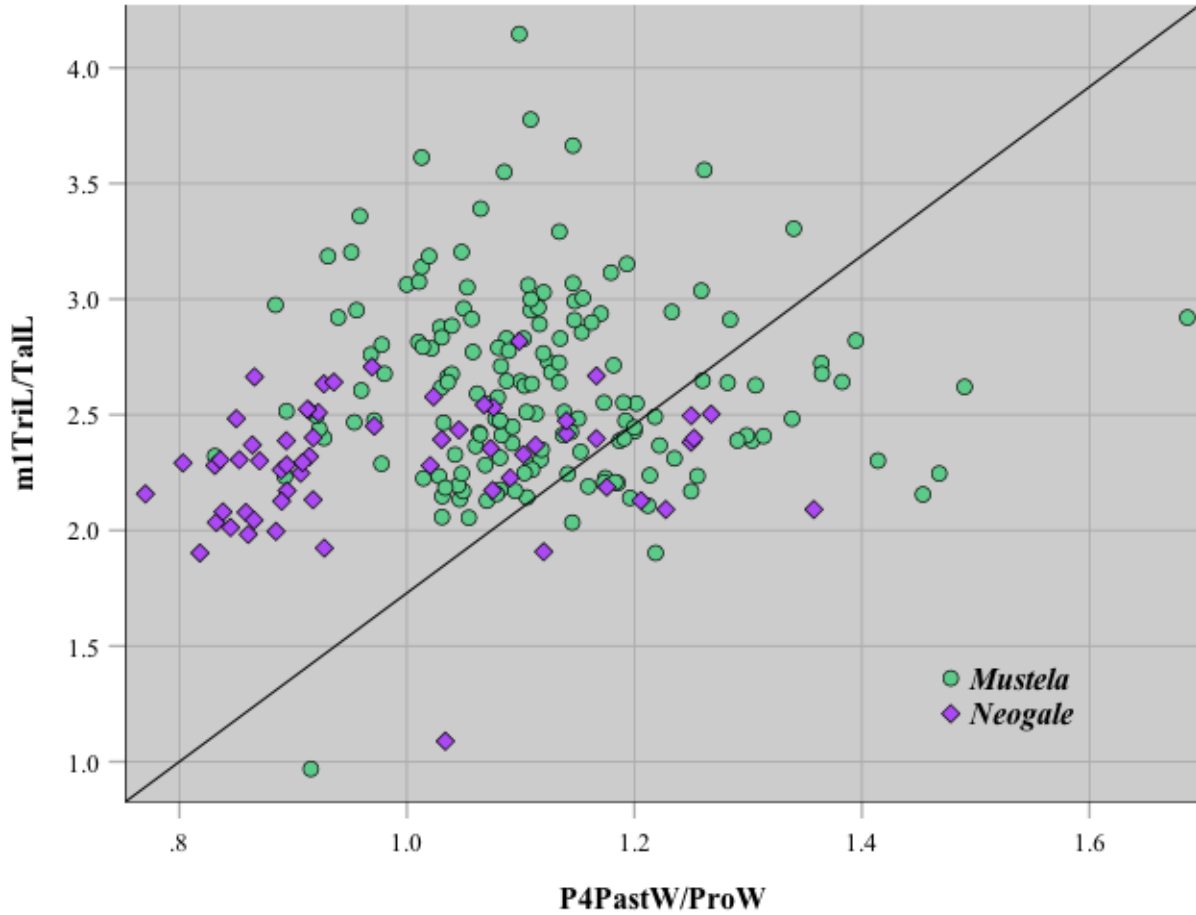


Figure 8. Bivariate plots comparing P4PastW/ProW and CBL and P4PastW/ProW and m1TriL/TalL. The y-axis represents the numerator and x-axis represents the denominator. Units are in mm.

Table 9. Extant Genus Analysis Classification Matrix

|                 |                | Predicted genus |                |                |       |
|-----------------|----------------|-----------------|----------------|----------------|-------|
|                 |                | % Correct       | <i>Mustela</i> | <i>Neogale</i> | Total |
| Original        | <i>Mustela</i> | 94.6            | 141            | 8              | 149   |
|                 | <i>Neogale</i> | 82.5            | 10             | 47             | 57    |
| Cross-validated | <i>Mustela</i> | 94              | 140            | 9              | 149   |
|                 | <i>Neogale</i> | 80.7            | 11             | 46             | 57    |

### *Species Classification*

For species classification, a total of 12 of the 31 indices are included in the stepwise discriminant model (Table 10 ). Overall, the DFA separated each species well and was significant (Wilks'  $\lambda = 0.000$ ,  $P < 0.001$ ). The classification showed all but seven species (*M. erminea*, *M. eversmannii*, *N. frenata*, *M. lutreola*, *M. nivalis*, *M. subpalmata*, and *N. vison*) being 100% correctly classified, with *M. erminea* and *M. nivalis* particularly showing notable overlap (Table 11; Figure 9 ). Only two Pleistocene specimens were correctly classified (*N. vison* and *M. nigripes*); *M. erminea* was classified as *M. subpalmata*, *N. frenata* was classified as *M. nigripes*, and *M. nivalis* was classified as *M. subpalmata* (Table 14). The analysis yielded four discriminant functions with eigenvalues  $>1$  and accounted for 85.9% of the variance in the data set.

Table 10. Extant Species Analysis Structure Matrix, Eigenvalue, Percent Variance Explained, and Wilks'  $\lambda$  for Discriminant Functions 1, 2, 3, and 4

| <b>Index</b>          | <b>DF 1</b> | <b>DF 2</b> | <b>DF 3</b> | <b>DF 4</b> |
|-----------------------|-------------|-------------|-------------|-------------|
| UGA                   | 0.778       | -0.049      | -0.083      | 0.381       |
| LGA                   | 0.703       | 0.055       | -0.125      | -0.030      |
| m1L                   | -0.545      | 0.553       | 0.171       | 0.056       |
| CBL/MCW               | -0.082      | 0.527       | -0.551      | 0.195       |
| M1W                   | -0.336      | 0.008       | 0.067       | 0.624       |
| P4WPar                | -0.079      | -0.079      | 0.363       | 0.115       |
| M1L/W                 | 0.332       | -0.001      | -0.466      | -0.015      |
| P4WPro                | -0.068      | -0.273      | -0.103      | 0.246       |
| P4PastW/ProW          | -0.070      | 0.316       | 0.181       | -0.457      |
| m1TriL/TalL           | -0.086      | -0.034      | 0.384       | -0.133      |
| p4L/W                 | -0.113      | 0.340       | -0.132      | 0.114       |
| P3W                   | 0.030       | -0.276      | -0.087      | -0.331      |
| Eigenvalue            | 8.562       | 2.861       | 2.420       | 1.908       |
| % variance explained  | 46.7        | 15.6        | 13.2        | 10.4        |
| Canonical correlation | 0.946       | 0.861       | 0.841       | 0.810       |
| Wilks' $\lambda$      | 0.000       | 0.003       | 0.012       | 0.042       |
| <i>p</i> -value       | < 0.001     | < 0.001     | < 0.001     | < 0.001     |

Table 11. Extant Species Analysis Classification Matrix. Taxa with 100% correct classification not listed.

| Taxon                | % Correct | Predicted Species |                   |                |                |                 |                |                |                 |                   |              | Total |
|----------------------|-----------|-------------------|-------------------|----------------|----------------|-----------------|----------------|----------------|-----------------|-------------------|--------------|-------|
|                      |           | <i>erminea</i>    | <i>eversmanii</i> | <i>frenata</i> | <i>kathiah</i> | <i>lutreola</i> | <i>nivalis</i> | <i>nudipes</i> | <i>putorius</i> | <i>subpalmata</i> | <i>vison</i> |       |
| <i>M. erminea</i>    | 71        | 17                | -                 | 1              | -              | -               | 6              | -              | -               | -                 | -            | 24    |
| <i>M. eversmanii</i> | 75        | -                 | 3                 | -              | -              | -               | -              | -              | 1               | -                 | -            | 4     |
| <i>N. frenata</i>    | 85        | 3                 | -                 | 22             | -              | -               | 1              | -              | -               | -                 | -            | 26    |
| <i>M. lutreola</i>   | 80        | -                 | -                 | -              | -              | 4               | -              | -              | 1               | -                 | -            | 5     |
| <i>M. nivalis</i>    | 70        | 3                 | -                 | 2              | 1              | -               | 14             | -              | -               | -                 | -            | 20    |
| <i>M. subpalmata</i> | 94        | -                 | -                 | -              | -              | -               | 1              | -              | -               | 16                | -            | 17    |
| <i>N. vison</i>      | 96        | -                 | -                 | -              | -              | -               | -              | 1              | -               | -                 | 26           | 27    |



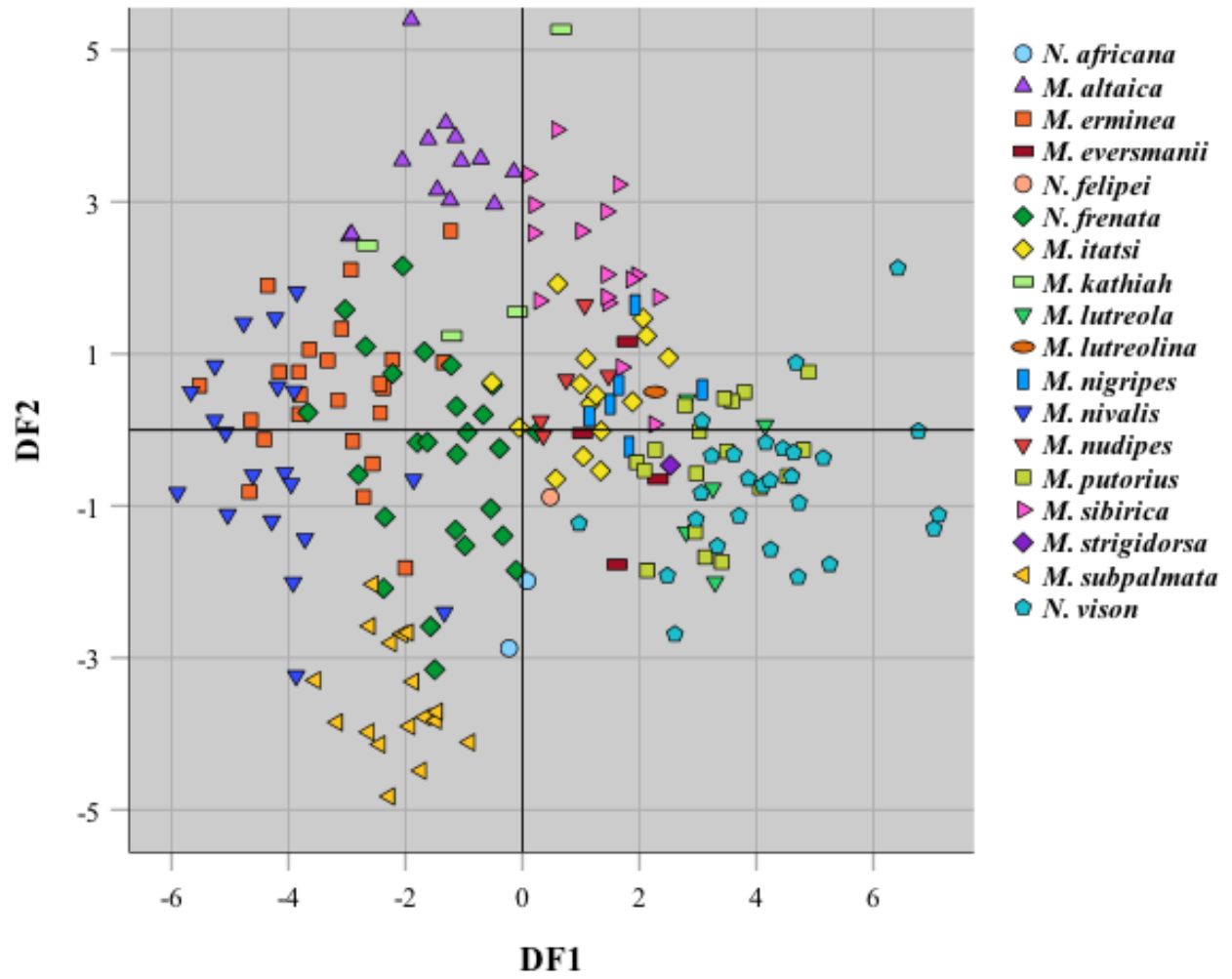


Figure 9. Extant species analysis scatterplot comparing DF1 vs. DF2

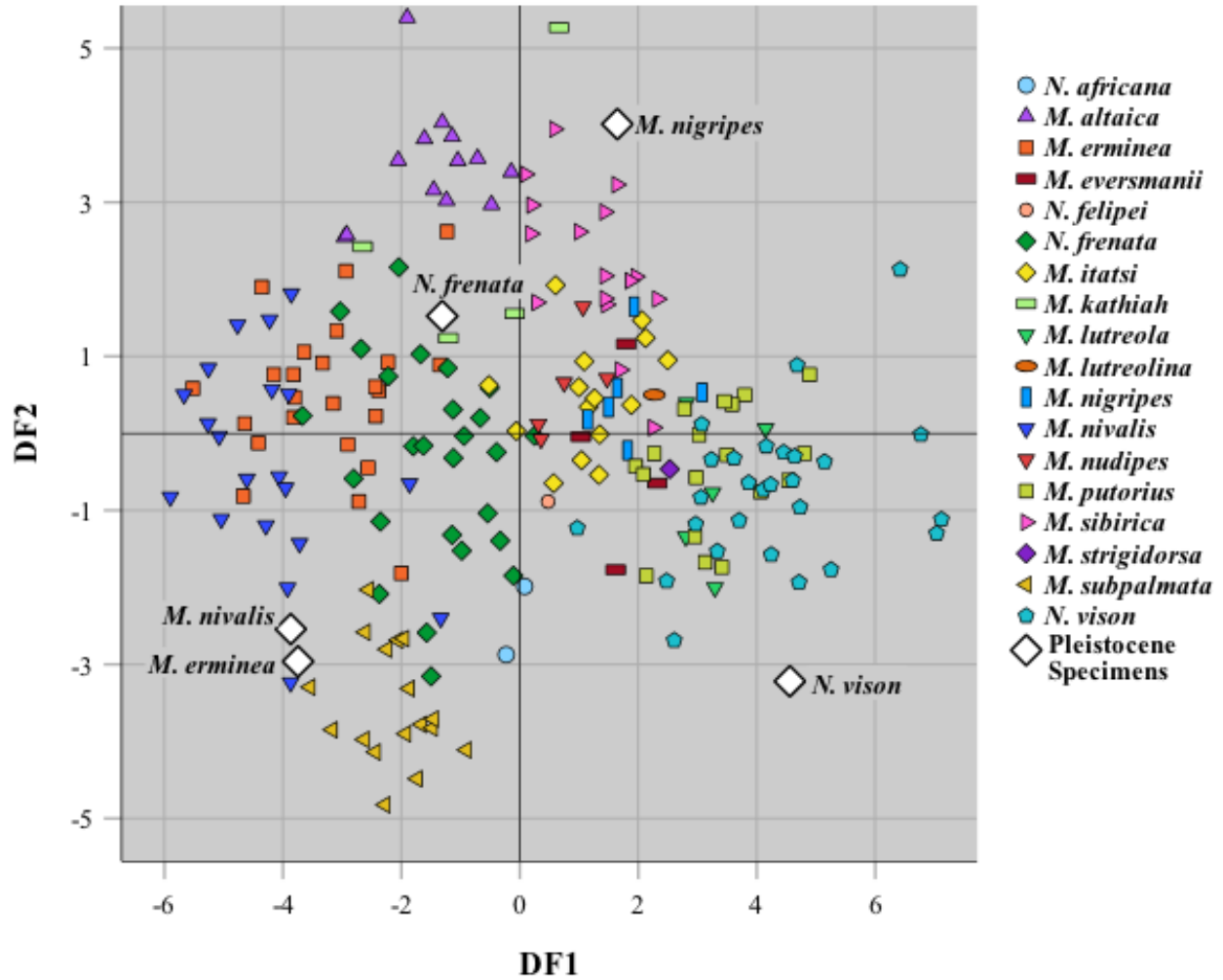


Figure 10. Pleistocene specimens of extant species analysis scatterplot comparing DF1 vs. DF2

DF1 accounted for 46.7% of the variance, was positively correlated with UGA, LGA, M1L/W, and P3W, and negatively correlated with m1L, CBL/MCW, M1W, P4WPar, P4WPro, P4PastW/ProW, m1TriL/TalL, and p4L/W. *N. africana* had slightly positive to slightly negative scores, *M. altaica* had slightly negative to moderately negative scores, *M. erminea* had slightly to highly negative scores, *M. eversmanii* had slightly to moderately positive scores, *N. felipei* had slightly positive scores, *N. frenata* had slightly to highly negative scores, *M. itatsi* had moderately positive to slightly negative scores, *M. kathiah* had slightly positive to moderately negative scores, *M. lutreola* had moderately to highly positive scores, *M. lutreolina* had

moderately positive scores, *M. nigripes* had slightly to moderately positive scores, *M. nivalis* had slightly to highly negative scores, *M. nudipes* had slightly positive scores, *M. putorius* had moderately to highly positive scores, *M. sibirica* had slightly to moderately positive scores, *M. strigidorsa* had moderately positive scores, *M. subpalmata* had slightly to moderately negative scores, and *N. vison* had slightly to highly positive scores.

DF2 accounted for 15.6% of the variance, was positively correlated with LGA, m1L, CBL/MCW, M1W, P4PastW/ProW, and p4L/W, and negatively correlated with UGA, P4WPar, M1L/W, P4WPro, m1TriL/TalL, and P3W. *N. africana* had moderately negative scores, *M. altaica* had moderately to highly positive scores, *M. erminea* had moderately positive to moderately negative scores, *M. eversmanii* had slightly positive to moderately negative scores, *N. felipei* had slightly negative scores, *N. frenata* had moderately positive to highly negative scores, *M. itatsi* had moderately positive to slightly negative scores, *M. kathiah* had moderately to highly positive scores, *M. lutreola* had slightly positive to moderately negative scores, *M. lutreolina* had slightly positive scores, *M. nigripes* had moderately positive to slightly negative scores, *M. nivalis* had moderately positive to highly negative scores, *M. nudipes* had moderately positive to slightly negative scores, *M. putorius* had slightly positive to moderately negative scores, *M. sibirica* had slightly to highly positive scores, *M. subpalmata* had moderately to highly negative scores, and *N. vison* had moderately positive to moderately negative scores.

DF3 accounted for 13.2% of the variance, was positively correlated with m1L, M1W, P4WPar, P4PastW/ProW, and m1TriL/TalL, and negatively correlated with UGA, LGA, CBL/MCW, M1L/W, P4WPro, p4L/W, and P3W. *N. africana* had slightly positive to slightly negative scores, *M. altaica* had slightly to highly positive scores, *M. erminea* had moderately positive to highly negative scores, *M. eversmanii* had moderately to highly positive scores, *N.*

*felipei* had slightly negative scores, *N. frenata* had moderately positive to moderately negative scores, *M. itatsi* had moderately to highly negative scores, *M. kathiah* had slightly positive to highly negative scores, *M. lutreola* had moderately positive to moderately negative scores, *M. lutreolina* had moderately negative scores, *M. nigripes* had moderately to highly positive scores, *M. nivalis* had moderately positive to moderately negative scores, *M. nudipes* had slightly positive to slightly negative scores, *M. putorius* had moderately to highly positive scores, *M. sibirica* had slightly to highly negative scores, *M. strigidorsa* had highly negative scores, *M. subpalmata* had moderately positive to slightly negative scores, and *N. vison* had slightly positive to moderately negative scores.

DF4 accounted for 10.4% of the variance, was positively correlated with UGA, m1L, CBL/MCW, M1W, P4WPar, P4WPro, p4L/W, and negatively correlated with LGA, M1L/W, P4PastW/ProW, m1TriL/TalL, and P3W. *N. africana* had slightly positive scores, *M. altaica* had moderately positive to moderately negative scores, *M. erminea* had highly positive to moderately negative scores, *M. eversmanii* had moderately negative scores, *N. felipei* had slightly negative scores, *N. frenata* moderately positive to moderately negative scores, *M. itatsi* had slightly to highly negative scores, *M. kathiah* had slightly to moderately positive scores, *M. lutreola* had slightly to moderately negative scores, *M. lutreolina* had moderately negative scores, *M. nigripes* had moderately to highly negative scores, *M. nivalis* had moderately positive to slightly negative scores, *M. nudipes* had moderately positive to slightly negative scores, *M. putorius* had slightly positive to moderately negative scores, *M. sibirica* had slightly positive to moderately negative scores, *M. strigidorsa* had slightly positive scores, *M. subpalmata* had slightly positive to moderately negative scores, and *N. vison* had slightly to highly positive scores.

### Clade Classification

For clade classification, a total of 11 of the 31 indices are included in the stepwise discriminant model (Table 12). The DFA separated each clade fairly well and was significant (Wilks'  $\lambda = 0.015$ ,  $P < 0.001$ ); however, there was notable overlap among Clades #4 and #5 (Table 13; Figure 11). Three of the Pleistocene specimens (*M. nigripes*, *M. nivalis*, and *N. vison*) were correctly classified; *M. erminea* was assigned to Clade #5 and *N. frenata* was assigned to Clade #9; however, the analysis yielded correct classification for both taxa when predicting the second most likely clade (Table 14). The analysis yielded three discriminant functions with eigenvalues  $>1$  and accounted for 84.6% of the variance in the data set.

Table 12. Extant Clade Structure Matrix, Eigenvalue, Percent Variance Explained, and Wilks'  $\lambda$  for Discriminant Functions 1, 2, and 3

| <b>Index</b>          | <b>DF 1</b> | <b>DF 2</b> | <b>DF 3</b> |
|-----------------------|-------------|-------------|-------------|
| CBL/MCW               | 0.579       | 0.253       | -0.275      |
| CBL                   | 0.570       | -0.539      | 0.285       |
| MCW                   | 0.141       | -0.601      | 0.408       |
| M1W                   | 0.225       | -0.526      | -0.460      |
| m1TriL/TalL           | -0.047      | -0.283      | 0.344       |
| P4PastW/ProW          | 0.010       | 0.143       | 0.355       |
| P4WPar                | -0.117      | -0.323      | 0.084       |
| P4WPro                | 0.061       | -0.109      | -0.240      |
| m1TalL                | 0.194       | 0.023       | -0.177      |
| P3W                   | -0.060      | 0.064       | 0.331       |
| M1LinL/M1BucL         | 0.177       | 0.126       | -0.114      |
| Eigenvalue            | 2.568       | 2.302       | 1.196       |
| % variance explained  | 35.8        | 32.1        | 16.7        |
| Canonical correlation | 0.848       | 0.835       | 0.738       |
| Wilks' $\lambda$      | 0.015       | 0.053       | 0.176       |
| <i>p</i> -value       | $< 0.001$   | $< 0.001$   | $< 0.001$   |

Table 13. Extant Clade Classification Matrix

| Clade  | % Correct | Predicted Clade |   |   |    |    |    |    |   |    | Total |
|--|-----------|-----------------|---|---|----|----|----|----|---|----|-------|
|  |           | 1               | 2 | 3 | 4  | 5  | 6  | 7  | 8 | 9  |       |
| 1 ( <i>M. africana</i> , <i>M. felipei</i> , <i>M. frenata</i> , <i>N. vison</i> ) | 86.2      | 50              | - | - | -  | 7  | -  | -  | 1 | -  | 58    |
| 2 ( <i>M. nudipes</i> , <i>M. strigidorsa</i> )                                    | 50        | 2               | 3 | - | -  | 1  | -  | -  | - | -  | 6     |
| 3 ( <i>M. kathiah</i> )  | 75        | 1               | - | 3 | -  | -  | -  | -  | - | -  | 4     |
| 4 ( <i>M. erminea</i> )  | 59.3      | -               | - | - | 16 | 11 | -  | -  | - | -  | 27    |
| 5 ( <i>M. altaica</i> , <i>M. nivalis</i> , <i>M. subpalmata</i> )                 | 78.4      | -               | - | 1 | 10 | 40 | -  | -  | - | -  | 51    |
| 6 ( <i>M. itatsi</i> )   | 88.2      | -               | - | - | -  | -  | 15 | 2  | - | -  | 17    |
| 7 ( <i>M. lutreolina</i> , <i>M. sibirica</i> )                                    | 100       | -               | - | - | -  | -  | -  | 17 | - | -  | 17    |
| 8 ( <i>M. lutreola</i> )   | 80        | 1               | - | - | -  | -  | -  | -  | 4 | -  | 5     |
| 9 ( <i>M. eversmanii</i> , <i>M. nigripes</i> , <i>M. putorius</i> )               | 93.5      | 2               | - | - | -  | -  | -  | -  | - | 29 | 31    |

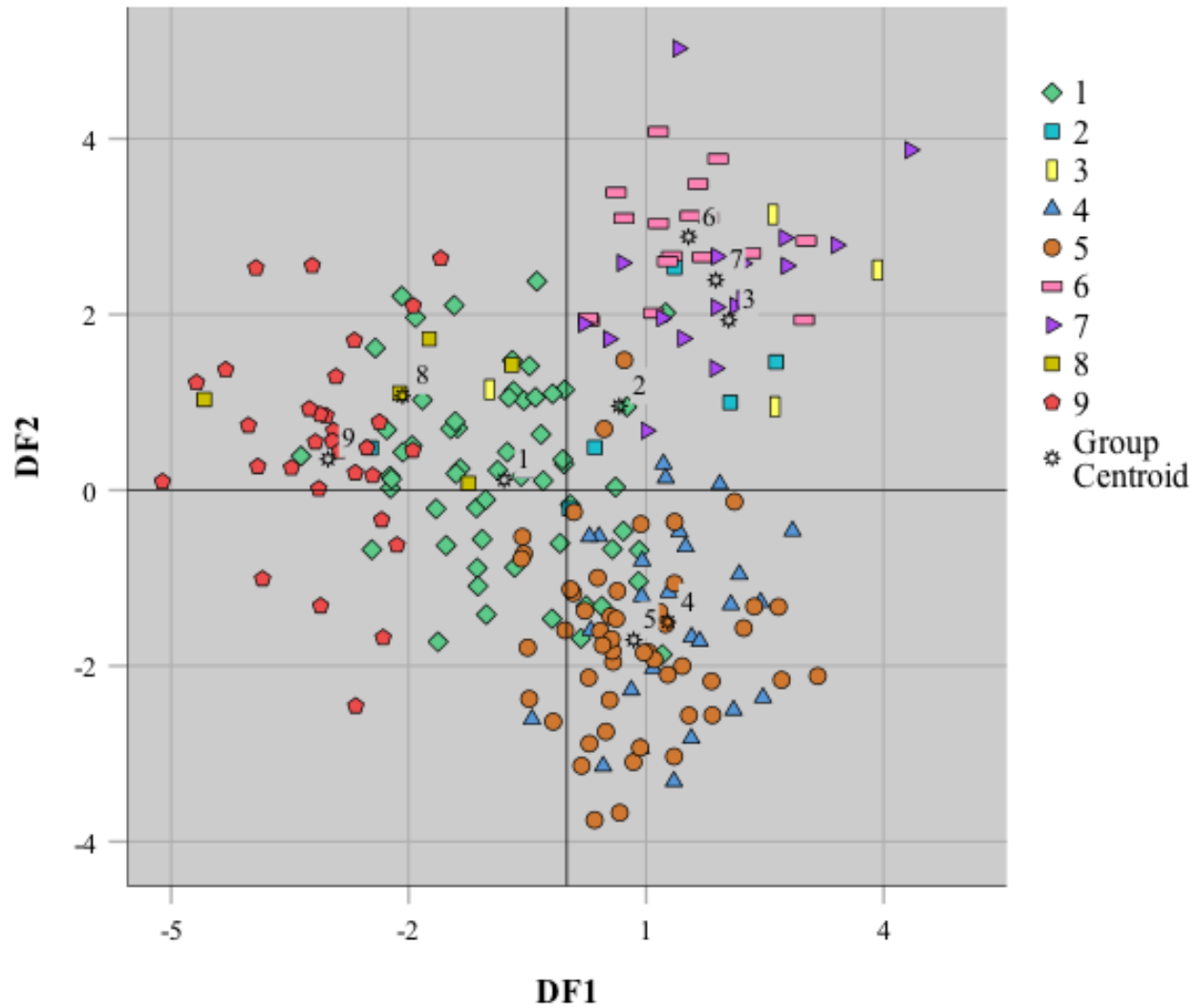


Figure 11. Extant clade analysis scatterplot comparing DF1 vs. DF2. Clade 1 = *N. africana*, *N. felipei*, *N. frenata*, *N. vison*; Clade 2 = *M. nudipes*, *M. strigidorsa*; Clade 3 = *M. kathiah*; Clade 4 = *M. erminea*; Clade 5 = *M. altaica*, *M. nivalis*, *M. subpalmata*; Clade 6 = *M. itatsi*; Clade 7 = *M. lutreolina*, *M. sibirica*; Clade 8 = *M. lutreola*; and Clade 9 = *M. eversmanii*, *M. nigripes*, *M. putorius*.

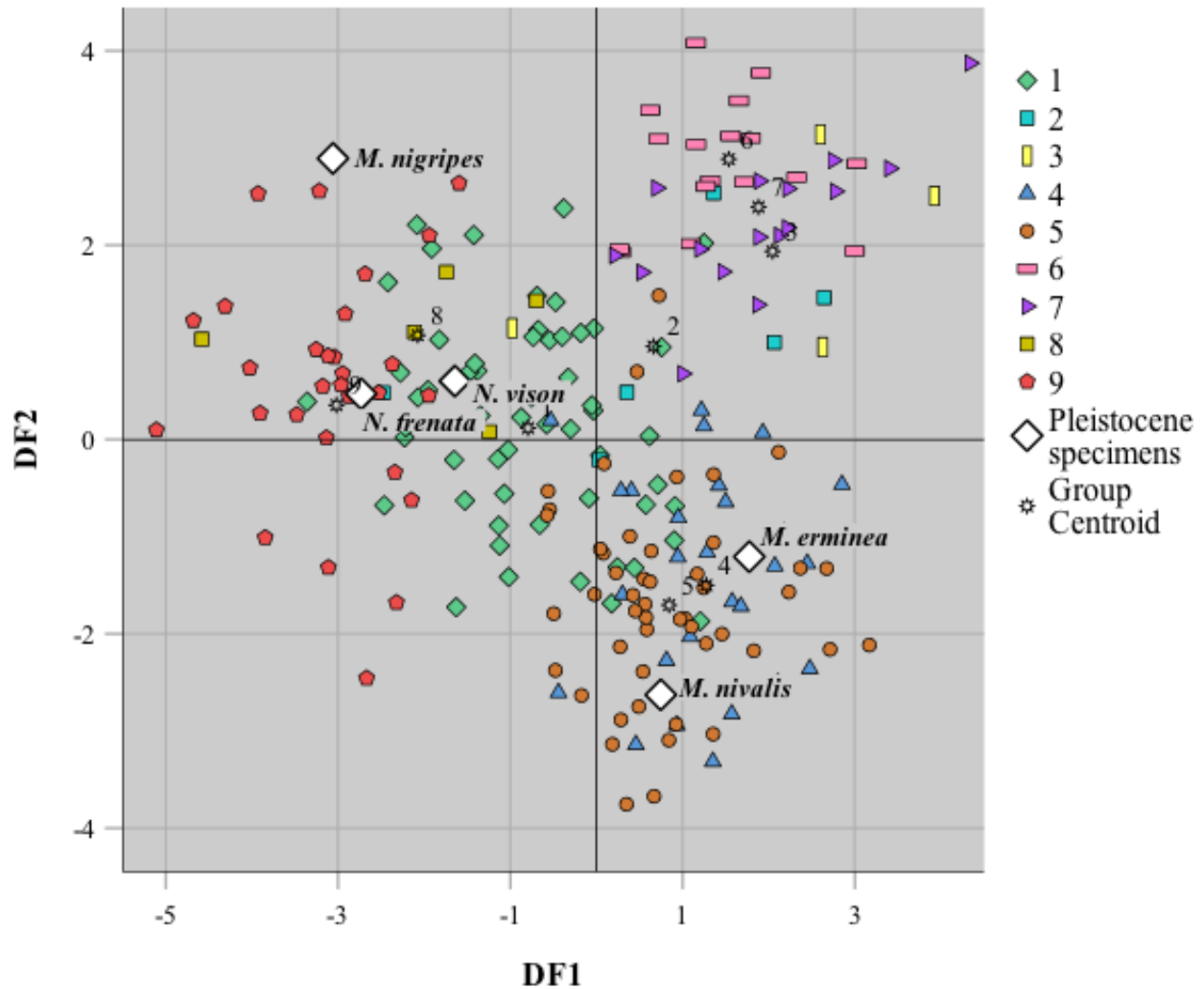


Figure 12. Pleistocene specimens of extant species clade analysis scatterplot comparing DF1 vs. DF2. Clade 1 = *N. africana*, *N. felipei*, *N. frenata*, *N. vison*; Clade 2 = *M. nudipes*, *M. strigidorsa*; Clade 3 = *M. kathiah*; Clade 4 = *M. erminea*; Clade 5 = *M. altaica*, *M. nivalis*, *M. subpalmata*; Clade 6 = *M. itatsi*; Clade 7 = *M. lutreolina*, *M. sibirica*; Clade 8 = *M. lutreola*; and Clade 9 = *M. eversmanii*, *M. nigripes*, *M. putorius*.



Table 14. Summary of Pleistocene Specimens of Extant Species Classification Matrix

| <b>Pleistocene specimens</b> | <b>Predicted genus</b> | <b>Predicted species</b> | <b>2nd most likely species</b> | <b>Predicted clade</b> | <b>2nd most likely clade</b> |
|------------------------------|------------------------|--------------------------|--------------------------------|------------------------|------------------------------|
| <i>N. vison</i>              | <i>Neogale</i>         | <i>N. vison</i>          | <i>N. africana</i>             | 1                      | 2                            |
| <i>M. erminea</i>            | <i>Mustela</i>         | <i>M. subpalmata</i>     | <i>M. nivalis</i>              | 5                      | 4                            |
| <i>N. frenata</i>            | <i>Mustela</i>         | <i>M. nigripes</i>       | <i>M. eversmanii</i>           | 9                      | 1                            |
| <i>M. nigripes</i>           | <i>Mustela</i>         | <i>M. nigripes</i>       | <i>M. eversmanii</i>           | 9                      | 7                            |
| <i>M. nivalis</i>            | <i>Mustela</i>         | <i>M. subpalmata</i>     | <i>M. nivalis</i>              | 5                      | 4                            |

DF1 accounted for 35.8% of the variance, was positively correlated with CBL/MCW, CBL, MCW, M1W, P4PastW/ProW, P4WPro, m1TalL, and M1LinL/BucL, and negatively correlated with m1TriL/TalL, P4WPar, and P3W. Clade #1 had slightly positive to moderately negative scores, Clade #2 had slightly to moderately negative scores, Clade #3 had highly positive to slightly negative scores, Clade #4 had moderately positive to slightly negative scores, Clade #5 had moderately positive to slightly negative scores, Clade #6 had slightly to highly positive scores, Clade #7 had slightly to highly positive scores, Clade #8 had slightly to highly negative scores, and Clade #9 had moderately to highly negative scores.

DF2 accounted for 32.1% of the variance, was positively correlated with CBL/MCW, P4PastW/ProW, P4WPro, m1TalL, and M1LinL/BucL, and negatively correlated with CBL, MCW, M1W, m1TriL/TalL, P4WPar, and P4WPro. Clade #1 had moderately positive to moderately negative scores, Clade #2 had slightly negative to moderately positive scores, Clade #3 had slightly to highly positive scores, Clade #4 had slightly positive to highly negative scores, Clade #5 had moderately positive to highly negative scores, Clade #6 had moderately to highly

positive scores, Clade #7 had slightly to highly positive scores, Clade #8 had slightly to moderately positive scores, and Clade #9 had moderately positive to moderately negative scores.

DF3 accounted for 16.7% of the variance, was positively correlated with CBL, MCW, m1TriL/TalL, P4PastW/ProW, P4WPar, and P3W, and negatively correlated with CBL/MCW, M1W, P4WPro, m1TalL, and M1LinL/BucL. Clade #1 had moderately positive to highly negative scores, Clade #2 had moderately positive to highly negative scores, Clade #3 had slightly to highly negative scores, Clade #4 had moderately positive to moderately negative scores, Clade #5 had highly positive to moderately negative scores, Clade #6 had highly positive to slightly negative scores, Clade #7 had moderately positive to slightly negative scores, Clade #8 had slightly positive to slightly negative scores, and Clade #9 had moderately positive to slightly negative scores.

#### *'Neovison' macrodon Analysis*

A stepwise DFA of genus and clade classification was performed using the ratios and GM-transformed linear measurements for each extant musteline taxon, as well as a composite of *'Neovison' macrodon* included as an unclassified case.

#### *Genus Classification*

A total of seven of the 26 indices are included in the stepwise discriminant model (Table 15). The DFA separated each genus fairly well (Wilks'  $\lambda = 0.608$ ,  $P < 0.001$ ). and yielded one discriminant function with an eigenvalue of 0.643 and a canonical correlation of 0.626. The discriminant function (DF1) was positively correlated with P4L/M1W, P4PastW/ProW, m1TriL/TalL, p4L, and m1TalL, and negatively correlated with UGA and M1L/W. The classification showed 95.8% correct classification of *Mustela* and 59.3% correct classification of *Neogale*, with *N. macrodon* being classified as *Neogale* (Table 16). When cross-validated, the

classification showed 95.2% correct classification of *Mustela* and 57.6% correct classification of *Neogale*.

Table 15. ‘*Neovison*’ *macrodon* Genus Analysis Structure Matrix, Eigenvalue, Percent Variance Explained, and Wilks’  $\lambda$  for Discriminant Function 1

| <b>Index</b>          | <b>DF 1</b> |
|-----------------------|-------------|
| P4L/M1W               | 0.517       |
| UGA                   | -0.513      |
| P4PastW/ProW          | 0.511       |
| m1TriL/TalL           | 0.407       |
| M1L/W                 | -0.193      |
| p4L                   | 0.020       |
| m1TalL                | 0.004       |
| Eigenvalue            | 0.643       |
| % variance explained  | 100         |
| Canonical correlation | 0.626       |
| Wilks' $\lambda$      | 0.608       |
| <i>p</i> -value       | < 0.001     |

Table 16. ‘*Neovison*’ *macrodon* Genus Analysis Classification Matrix

|                        |                    | <b>Predicted genus</b> |                       |                       |              |
|------------------------|--------------------|------------------------|-----------------------|-----------------------|--------------|
|                        |                    | <b>% Correct</b>       | <b><i>Mustela</i></b> | <b><i>Neogale</i></b> | <b>Total</b> |
| <b>Original</b>        | <i>Mustela</i>     | 95.8                   | 161                   | 7                     | 168          |
|                        | <i>Neogale</i>     | 59.3                   | 24                    | 35                    | 59           |
|                        | <i>N. macrodon</i> | -                      | -                     | 1                     | 1            |
| <b>Cross-validated</b> | <i>Mustela</i>     | 95.2                   | 160                   | 8                     | 168          |
|                        | <i>Neogale</i>     | 57.6                   | 25                    | 34                    | 59           |

### *Clade Classification*

A total of 11 of the 26 indices are included in the stepwise discriminant model (Table 17). The DFA separated each clade fairly well and was significant (Wilks'  $\lambda = 0.031$ ,  $P < 0.001$ ). The classification showed *N. macrodon* being assigned to Clade #1 (Table 18). The analysis yielded two discriminant functions with eigenvalues  $>1$  and accounted for 71.1% of the variance in the data set. DF1 accounted for 41.7% of the variance, was positively correlated with UGA, M1L/W, P4PastW/ProW, and P3W, and negatively correlated with M1W, m1L, m1TriL/TalL, p4L/W, P4WPar, P4WPro, and M1LinL. DF2 accounted for 29.4% of the variance, was positively correlated with m1L, M1L/W, p4L/W, P4PastW/ProW, P3W, and M1LinL, and negatively correlated with M1W, UGA, m1TriL/TalL, P4WPar, and P4WPro. *N. macrodon* had a moderately positive score for DF1 and a moderately negative score for DF2 (Figure 13).

Table 17. ‘*Neovison*’ *macrodon* Clade Analysis Structure Matrix, Eigenvalue, Percent Variance Explained, and Wilks’  $\lambda$  for Discriminant Functions 1 and 2

| <b>Index</b>          | <b>DF 1</b> | <b>DF 2</b> |
|-----------------------|-------------|-------------|
| M1W                   | -0.646      | -0.063      |
| UGA                   | 0.526       | -0.289      |
| m1L                   | -0.484      | 0.180       |
| M1L/W                 | 0.342       | 0.271       |
| m1TriL/TalL           | -0.170      | -0.160      |
| p4L/W                 | -0.116      | 0.168       |
| P4WPar                | -0.300      | -0.274      |
| P4PastW/ProW          | 0.145       | 0.039       |
| P3W                   | 0.060       | 0.060       |
| P4WPro                | -0.198      | -0.084      |
| M1LinL                | -0.023      | 0.225       |
| Eigenvalue            | 2.317       | 1.631       |
| % variance explained  | 41.7        | 29.4        |
| Canonical correlation | 0.836       | 0.787       |
| Wilks' $\lambda$      | 0.031       | 0.103       |
| <i>p</i> -value       | < 0.001     | < 0.001     |

Table 18. ‘*Neovison*’ *macrodon* Clade Analysis Classification Matrix

| <b>Clade</b>   | <b>% Correct</b> | <b>Predicted Clade</b> |          |          |          |          |          |          |          |          | <b>Total</b> |
|--|------------------|------------------------|----------|----------|----------|----------|----------|----------|----------|----------|--------------|
|  |                  | <b>1</b>               | <b>2</b> | <b>3</b> | <b>4</b> | <b>5</b> | <b>6</b> | <b>7</b> | <b>8</b> | <b>9</b> |              |
| <i>N. macrodon</i>   | -                | 1                      | -        | -        | -        | -        | -        | -        | -        | -        | 1            |
| 1 ( <i>N. africana</i> , <i>N. felipei</i> , <i>N. frenata</i> , <i>N. vison</i> ) | 77.2             | 44                     | -        | -        | 1        | 9        | -        | 2        | -        | 1        | 57           |
| 2 ( <i>M. nudipes</i> , <i>M. strigidorsa</i> )                                    | 0                | 5                      | -        | -        | -        | -        | -        | -        | -        | 1        | 6            |
| 3 ( <i>M. kathiah</i> )  | 80               | -                      | -        | 4        | -        | 1        | -        | -        | -        | -        | 5            |
| 4 ( <i>M. erminea</i> )  | 66.7             | -                      | -        | -        | 18       | 9        | -        | -        | -        | -        | 27           |
| 5 ( <i>M. altaica</i> , <i>M. nivalis</i> , <i>M. subpalmata</i> )                 | 76.8             | 2                      | -        | 1        | 8        | 43       | -        | -        | -        | 2        | 56           |
| 6 ( <i>M. itatsi</i> )   | 88.2             | 1                      | -        | -        | -        | -        | 15       | 1        | -        | -        | 17           |
| 7 ( <i>M. lutreolina</i> , <i>M. sibirica</i> )                                    | 77.8             | 2                      | -        | -        | -        | -        | 1        | 14       | -        | 1        | 18           |
| 8 ( <i>M. lutreola</i> )   | 80               | 1                      | -        | -        | -        | -        | -        | -        | 4        | -        | 5            |
| 9 ( <i>M. eversmanii</i> , <i>M. nigripes</i> , <i>M. putorius</i> )               | 81.3             | 3                      | -        | -        | -        | 1        | -        | 2        | -        | 26       | 32           |

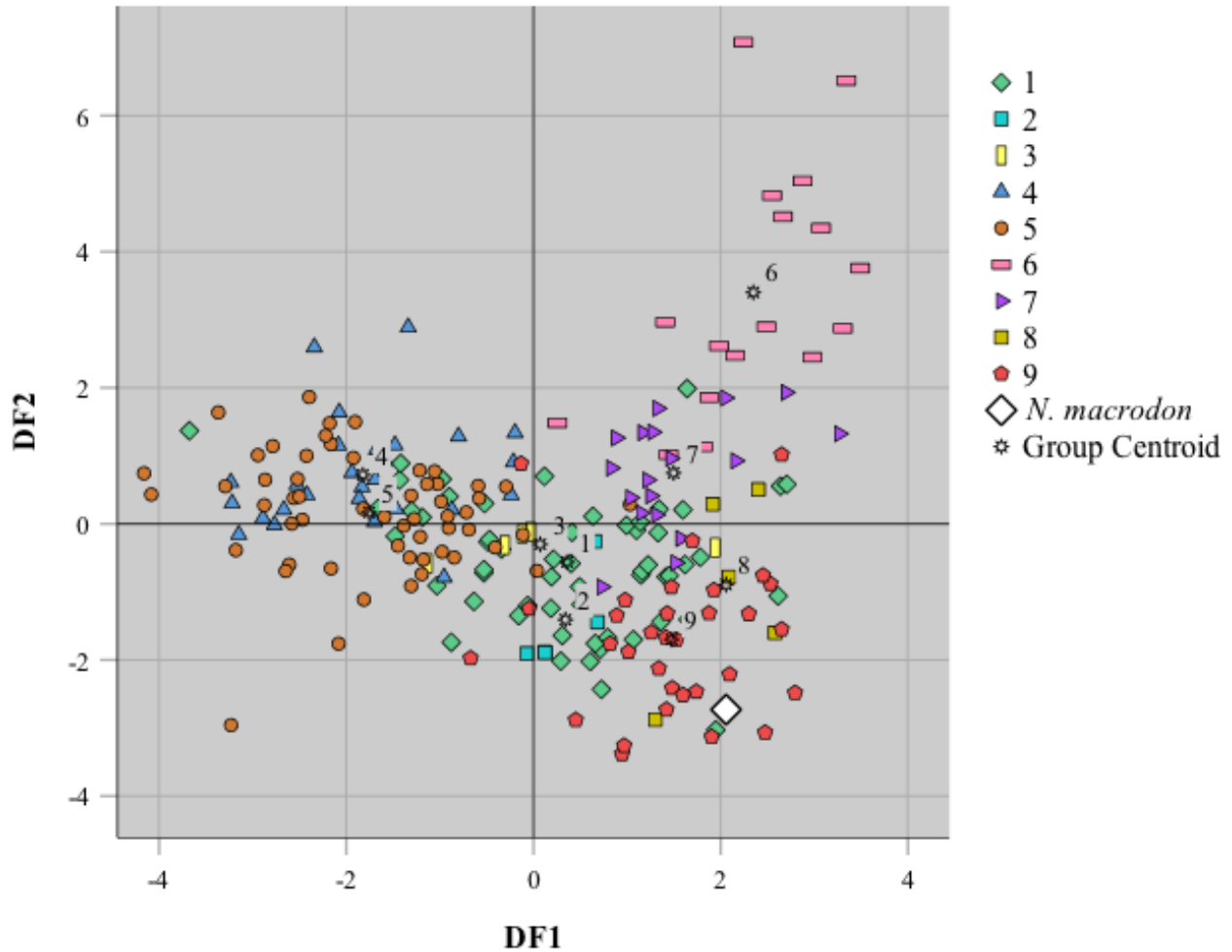


Figure 13. ‘*Neovison*’ *macrodon* clade analysis scatterplot comparing DF1 vs. DF2. Clade 1 = *N. africana*, *N. felipei*, *N. frenata*, *N. vison*; Clade 2 = *M. nudipes*, *M. strigidorsa*; Clade 3 = *M. kathiah*; Clade 4 = *M. erminea*; Clade 5 = *M. altaica*, *M. nivalis*, *M. subpalmata*; Clade 6 = *M. itatsi*; Clade 7 = *M. lutreolina*, *M. sibirica*; Clade 8 = *M. lutreola*; and Clade 9 = *M. eversmanii*, *M. nigripes*, *M. putorius*.

#### *Mustela rexroadensis* Analysis

A stepwise DFA of genus and clade classification was performed using the ratios and GM-transformed linear measurements for each extant musteline taxon, as well as a composite of *Mustela rexroadensis* included as an unclassified case.

### Genus Classification

A total of four of the 18 indices are included in the stepwise discriminant model (Table 19). The DFA separated each genus fairly well (Wilks'  $\lambda = 0.674$ ,  $P < 0.001$ ) and the analysis yielded one discriminant function with an eigenvalue of 0.485 and a canonical correlation of 0.571. DF1 was positively correlated with P4PastW/ProW, m1L/p4L, and m1TriL/TalL, and negatively correlated with m1TalL. The classification showed 94.6% correct classification of *Mustela* and 55.9% correct classification of *Neogale*, with *M. rexroadensis* being classified as *Neogale* (Table 20). When cross-validated, the classification showed 93.4% correct classification of *Mustela* and 55.9 % correct classification of *Neogale*.

Table 19. *Mustela rexroadensis* Genus Analysis Structure Matrix, Eigenvalue, Percent Variance Explained, and Wilks'  $\lambda$  for Discriminant Function 1

| <b>Index</b>          | <b>DF 1</b> |
|-----------------------|-------------|
| P4PastW/ProW          | 0.589       |
| m1L/p4L               | 0.530       |
| m1TriL/TalL           | 0.468       |
| m1TalL                | -0.024      |
| Eigenvalue            | 0.485       |
| % variance explained  | 100         |
| Canonical correlation | 0.571       |
| Wilks' $\lambda$      | 0.674       |
| <i>p</i> -value       | < 0.001     |

Table 20. *Mustela rexroadensis* Genus Analysis Classification Matrix

|                        |                        | Predicted genus |                |                | Total |
|------------------------|------------------------|-----------------|----------------|----------------|-------|
|                        |                        | % Correct       | <i>Mustela</i> | <i>Neogale</i> |       |
| <b>Original</b>        | <i>Mustela</i>         | 94.6            | 158            | 9              | 167   |
|                        | <i>Neogale</i>         | 55.9            | 26             | 33             | 59    |
|                        | <i>M. rexroadensis</i> | -               | -              | 1              | 1     |
| <b>Cross-validated</b> | <i>Mustela</i>         | 93.4            | 156            | 11             | 167   |
|                        | <i>Neogale</i>         | 55.9            | 26             | 33             | 59    |

### Clade Classification

For clade classification, a total of six of the 18 indices are included in the stepwise discriminant model (Table 21). The DFA separated most clades fairly well and was significant (Wilks'  $\lambda = 0.137$ ,  $P < 0.001$ ). The classification showed *M. rexroadensis* being assigned to Clade #4 (Table 22). The analysis yielded one discriminant function with an eigenvalue  $>1$  and accounted for 65.4% of the variance in the data set. DF1 was positively correlated with m1L, P4L, P4WPar, and p4W, and negatively correlated with P4PastW/ProW, and MD. DF2 had an eigenvalue of 0.536, accounted for 17.6% of the variance, was positively correlated with P4WPar, P4PastW/ProW, MD, and p4W, and negatively correlated with m1L, and P4L. *M. rexroadensis* had a moderately positive score for DF1 and a moderately negative score for DF2 (Figure 14).



Table 21. *Mustela rexroadensis* Clade Analysis Structure Matrix, Eigenvalue, Percent Variance Explained, and Wilks'  $\lambda$  for Discriminant Functions 1 and 2

| <b>Index</b>          | <b>DF 1</b> | <b>DF 2</b> |
|-----------------------|-------------|-------------|
| m1L                   | 0.577       | -0.426      |
| P4L                   | 0.531       | -0.274      |
| P4WPar                | 0.264       | 0.610       |
| P4PastW/ProW          | -0.119      | 0.191       |
| MD                    | -0.138      | 0.515       |
| p4W                   | 0.084       | 0.401       |
| Eigenvalue            | 1.986       | 0.536       |
| % variance explained  | 65.4        | 17.6        |
| Canonical correlation | 0.816       | 0.591       |
| Wilks' $\lambda$      | 0.137       | 0.408       |
| <i>p</i> -value       | < 0.001     | < 0.001     |

Table 22. *Mustela rexroadensis* Clade Analysis Classification Matrix

| <b>Clade</b>   | <b>% Correct</b> | <b>Predicted Clade</b> |          |          |          |          |          |          |          |          | <b>Total</b> |
|--|------------------|------------------------|----------|----------|----------|----------|----------|----------|----------|----------|--------------|
|  |                  | <b>1</b>               | <b>2</b> | <b>3</b> | <b>4</b> | <b>5</b> | <b>6</b> | <b>7</b> | <b>8</b> | <b>9</b> |              |
| <i>M. rexroadensis</i>   | -                | -                      | -        | -        | 1        | -        | -        | -        | -        | -        | 1            |
| 1 ( <i>N. africana</i> , <i>N. felipei</i> , <i>N. frenata</i> , <i>N. vison</i> ) | 69               | 40                     | -        | -        | 2        | 9        | -        | 2        | -        | 5        | 58           |
| 2 ( <i>M. nudipes</i> , <i>M. strigidorsa</i> )                                    | 0                | 4                      | -        | -        | -        | 1        | -        | 1        | -        | -        | 6            |
| 3 ( <i>M. kathiah</i> )  | 60               | 1                      | -        | 3        | -        | 1        | -        | -        | -        | -        | 5            |
| 4 ( <i>M. erminea</i> )  | 66.7             | 1                      | -        | -        | 18       | 6        | -        | 2        | -        | -        | 27           |
| 5 ( <i>M. altaica</i> , <i>M. nivalis</i> , <i>M. subpalmata</i> )                 | 75               | 5                      | -        | 1        | 6        | 42       | -        | -        | -        | 2        | 56           |
| 6 ( <i>M. itatsi</i> )   | 52.9             | 4                      | -        | -        | -        | -        | 9        | 2        | 1        | 1        | 17           |
| 7 ( <i>M. lutreolina</i> , <i>M. sibirica</i> )                                    | 38.9             | 7                      | -        | -        | 1        | -        | 2        | 7        | -        | 1        | 18           |
| 8 ( <i>M. lutreola</i> )   | 80               | -                      | -        | -        | -        | -        | -        | -        | 4        | 1        | 5            |
| 9 ( <i>M. eversmanii</i> , <i>M. nigripes</i> , <i>M. putorius</i> )               | 65.6             | 6                      | -        | -        | -        | 2        | 3        | -        | -        | 21       | 32           |

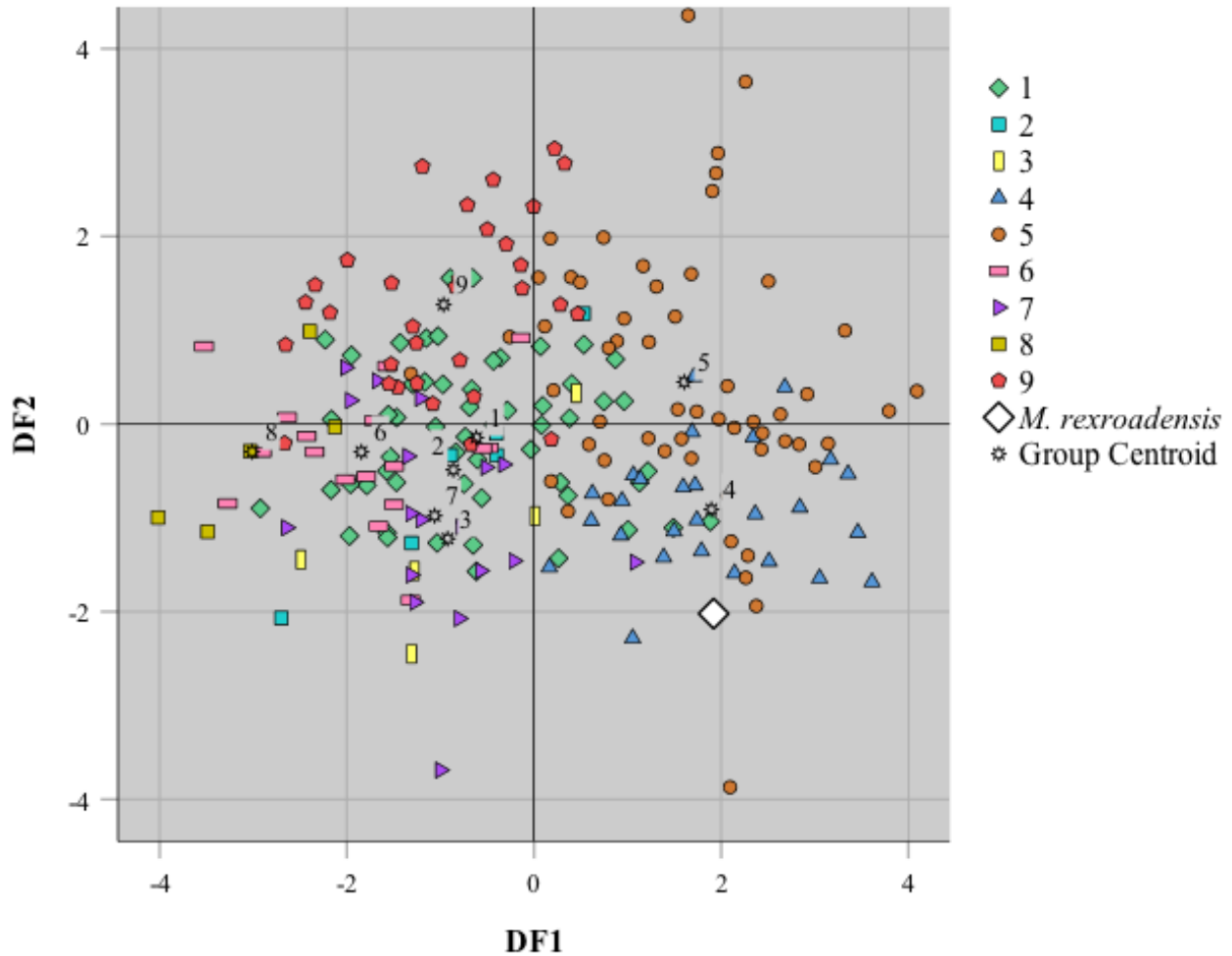


Figure 14. *Mustela rexroadensis* clade analysis scatterplot comparing DF1 vs. DF2. Clade 1 = *N. africana*, *N. felipei*, *N. frenata*, *N. vison*; Clade 2 = *M. nudipes*, *M. strigidorsa*; Clade 3 = *M. kathiah*; Clade 4 = *M. erminea*; Clade 5 = *M. altaica*, *M. nivalis*, *M. subpalmata*; Clade 6 = *M. itatsi*; Clade 7 = *M. lutreolina*, *M. sibirica*; Clade 8 = *M. lutreola*; and Clade 9 = *M. eversmanii*, *M. nigripes*, *M. putorius*.

#### *Mustela meltoni* Analysis

A stepwise DFA of genus and clade classification was performed using the ratios and GM-transformed linear measurements for each extant musteline taxon, as well as a composite of *M. meltoni* included as an unclassified case.

*Genus Classification*

A total of three of the 12 indices are included in the stepwise discriminant model (Table 23). The analysis yielded one discriminant function with an eigenvalue of 0.350 and a canonical correlation of 0.509. The discriminant function (DF1) was positively correlated with m1L/p4L and m1TriL/TalL, and negatively correlated with m1TalL. The DFA correctly classified *Mustela* well (91.7%); however, only 45.9% of *Neogale* were correctly classified (Wilks'  $\lambda = 0.741$ ,  $p < 0.001$ ). *M. meltoni* was classified as *Mustela* (Table 24). When cross-validated, the classification still showed 91.7% correct classification of *Mustela* and 45.9% correct classification of *Neogale*.

Table 23. *Mustela meltoni* Genus Analysis Structure Matrix, Eigenvalue, Percent Variance Explained, and Wilks'  $\lambda$  for Discriminant Function 1

| <b>Index</b>          | <b>DF 1</b> |
|-----------------------|-------------|
| m1L/p4L               | 0.638       |
| m1TriL/TalL           | 0.541       |
| m1TalL                | -0.008      |
| Eigenvalue            | 0.350       |
| % variance explained  | 100         |
| Canonical correlation | 0.509       |
| Wilks' $\lambda$      | 0.741       |
| <i>p</i> -value       | < 0.001     |

Table 24. *Mustela meltoni* Genus Analysis Classification Matrix

|                        |                   | <b>Predicted genus</b> |                       |                       |              |
|------------------------|-------------------|------------------------|-----------------------|-----------------------|--------------|
|                        |                   | <b>% Correct</b>       | <b><i>Mustela</i></b> | <b><i>Neogale</i></b> | <b>Total</b> |
| <b>Original</b>        | <i>Mustela</i>    | 91.7                   | 166                   | 15                    | 181          |
|                        | <i>Neogale</i>    | 45.9                   | 33                    | 28                    | 61           |
|                        | <i>M. meltoni</i> | -                      | 1                     | -                     | 1            |
| <b>Cross-validated</b> | <i>Mustela</i>    | 91.7                   | 166                   | 15                    | 181          |
|                        | <i>Neogale</i>    | 45.9                   | 33                    | 28                    | 61           |

### Clade Classification

A total of five of the 12 indices are included in the stepwise discriminant model (Table 25). The DFA did not separate most clades well except for Clades #1, #5, and #9 (Wilks'  $\lambda = 0.215$ ,  $P < 0.001$ ). The classification showed *M. meltoni* being assigned to Clade #1 (Table 26). The analysis yielded one discriminant function with an eigenvalue  $>1$  and accounted for 61.1% of the variance in the data set. DF1 was positively correlated with all indices. DF2 had an eigenvalue of 0.513, accounted for 24.2% of the variance, was positively correlated with m1L/p4L, m1TriL/TalL, and p4W, and negatively correlated with m1L and m1L/W. *M. meltoni* had a slightly negative score for DF1 and a slightly positive score for DF2 (Figure 15).

Table 25. *Mustela meltoni* Clade Analysis Structure Matrix, Eigenvalue, Percent Variance Explained, and Wilks'  $\lambda$  for Discriminant Functions 1 and 2

| <b>Index</b>          | <b>DF 1</b> | <b>DF2</b> |
|-----------------------|-------------|------------|
| m1L                   | 0.826       | -0.167     |
| m1L/W                 | 0.390       | -0.100     |
| m1L/p4L               | 0.325       | 0.356      |
| m1TriL/TalL           | 0.316       | 0.572      |
| p4W                   | 0.189       | 0.167      |
| Eigenvalue            | 1.295       | 0.513      |
| % variance explained  | 61.1        | 24.2       |
| Canonical correlation | 0.751       | 0.582      |
| Wilks' $\lambda$      | 0.215       | 0.495      |
| <i>p</i> -value       | $< 0.001$   | $< 0.001$  |

Table 26. *Mustela meltoni* Analysis Clade Classification Matrix

| Clade  | % Correct | Predicted Clade |   |   |    |    |   |   |   |    | Total |
|--|-----------|-----------------|---|---|----|----|---|---|---|----|-------|
|  |           | 1               | 2 | 3 | 4  | 5  | 6 | 7 | 8 | 9  |       |
| <i>M. meltoni</i>  | -         | 1               | - | - | -  | -  | - | - | - | -  | 1     |
| 1 ( <i>N. africana</i> , <i>N. felipei</i> , <i>N. frenata</i> , <i>N. vison</i> ) | 73.3      | 44              | - | - | -  | 10 | 4 | 1 | - | 1  | 60    |
| 2 ( <i>M. nudipes</i> , <i>M. strigidorsa</i> )                                    | 0         | 3               | - | - | -  | 2  | - | 1 | - | -  | 6     |
| 3 ( <i>M. kathiah</i> )  | 0         | 1               | - | - | -  | 2  | - | 1 | - | 1  | 5     |
| 4 ( <i>M. erminea</i> )  | 40        | 1               | - | - | 12 | 16 | - | 1 | - | -  | 30    |
| 5 ( <i>M. altaica</i> , <i>M. nivalis</i> , <i>M. subpalmata</i> )                 | 62.1      | 6               | - | - | 11 | 36 | - | 1 | - | 4  | 58    |
| 6 ( <i>M. itatsi</i> )   | 17.6      | 11              | - | - | -  | 2  | 3 | 1 | - | -  | 17    |
| 7 ( <i>M. lutreolina</i> , <i>M. sibirica</i> )                                    | 42.1      | 7               | - | - | -  | 2  | 1 | 8 | - | 1  | 19    |
| 8 ( <i>M. lutreola</i> )   | 0         | 5               | - | - | -  | -  | - | - | - | -  | 5     |
| 9 ( <i>M. eversmanii</i> , <i>M. nigripes</i> , <i>M. putorius</i> )               | 62.5      | 8               | - | - | -  | 5  | 1 | 1 | - | 25 | 40    |

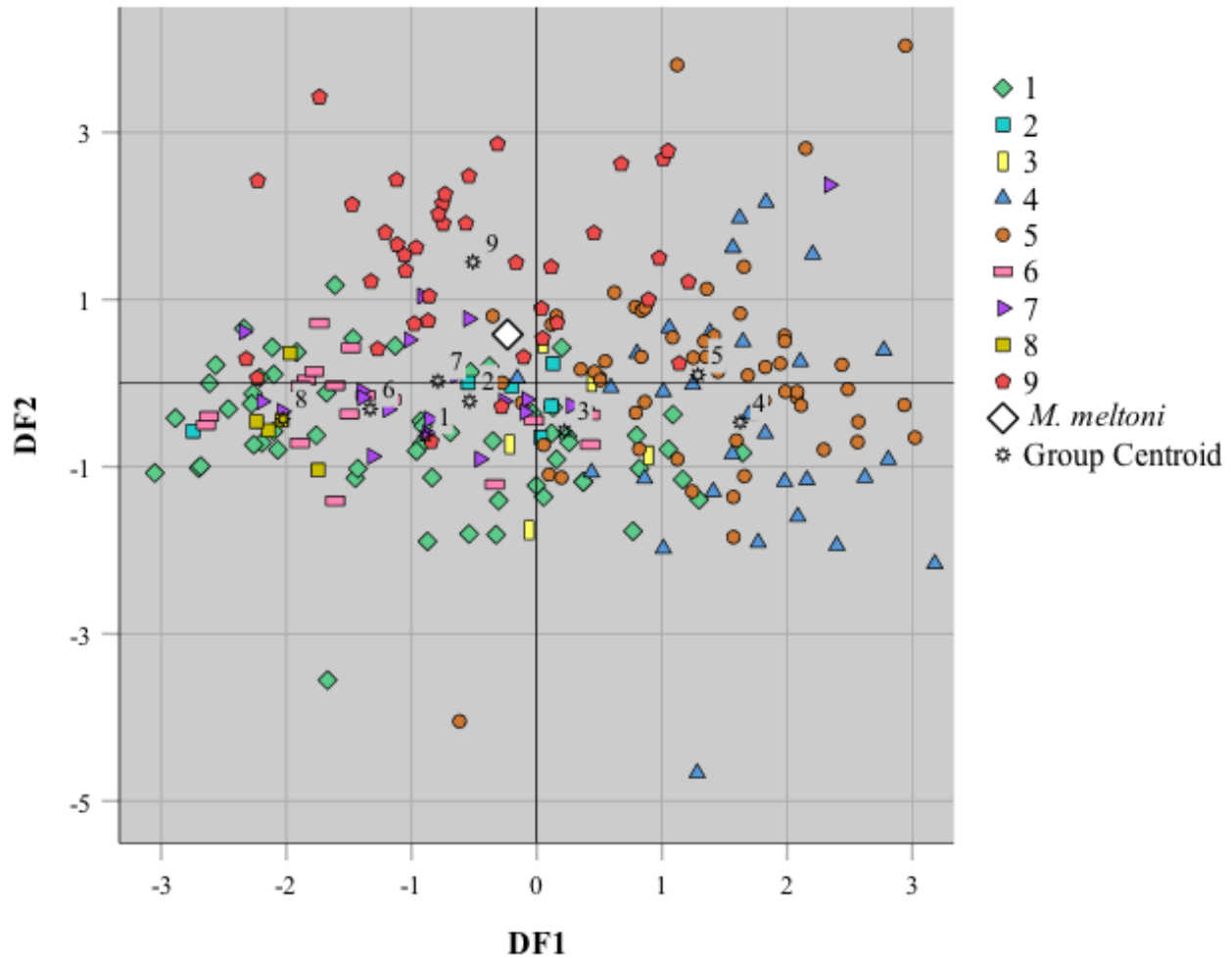


Figure 15. *Mustela meltoni* clade analysis scatterplot comparing DF1 vs. DF2. Clade 1 = *N. africana*, *N. felipei*, *N. frenata*, *N. vison*; Clade 2 = *M. nudipes*, *M. strigidorsa*; Clade 3 = *M. kathiah*; Clade 4 = *M. erminea*; Clade 5 = *M. altaica*, *M. nivalis*, *M. subpalmata*; Clade 6 = *M. itatsi*; Clade 7 = *M. lutreolina*, *M. sibirica*; Clade 8 = *M. lutreola*; and Clade 9 = *M. eversmanii*, *M. nigripes*, *M. putorius*.

#### GFS Musteline Analysis

A stepwise DFA of genus, species, and clade classification was performed using the ratios and GM-transformed linear measurements for each extant musteline taxon, as well as the GFS musteline included as an unclassified case.

### Genus Classification

A total of three of the 11 indices are included in the stepwise discriminant model (Table 27). Overall, The DFA correctly classified *Mustela* well (97.7%); however, only 53.2% of *Neogale* were correctly classified (Wilks'  $\lambda = 0.533$ ,  $P < 0.001$ ). When cross-validated, the classification showed 96.6% correct classification of *Mustela* and 54.8% correct classification of *Neogale*. The analysis yielded one discriminant function with an eigenvalue of 0.396 and a canonical correlation of 0.533. DF1 was positively correlated with UGA and negatively correlated with P4PastW/ProW and M1W. The GFS musteline was classified as *Neogale* (Table 28).

Table 27. GFS Musteline Genus Analysis Structure Matrix, Eigenvalue, Percent Variance Explained, and Wilks'  $\lambda$  for Discriminant Function 1

| <b>Index</b>          | <b>DF 1</b> |
|-----------------------|-------------|
| P4PastW/ProW          | -0.638      |
| UGA                   | 0.581       |
| M1W                   | -0.158      |
| Eigenvalue            | 0.404       |
| % variance explained  | 100         |
| Canonical correlation | 0.396       |
| Wilks' $\lambda$      | 0.533       |
| <i>p</i> -value       | < 0.001     |

Table 28. GFS Musteline Genus Analysis Classification Matrix

|                        |                | Predicted genus |                |                | Total |
|------------------------|----------------|-----------------|----------------|----------------|-------|
|                        |                | % Correct       | <i>Mustela</i> | <i>Neogale</i> |       |
| <b>Original</b>        | <i>Mustela</i> | 97.7            | 170            | 4              | 174   |
|                        | <i>Neogale</i> | 53.2            | 29             | 33             | 62    |
|                        | GFS Musteline  | -               | -              | 1              | 1     |
| <b>Cross-validated</b> | <i>Mustela</i> | 96.6            | 168            | 6              | 174   |
|                        | <i>Neogale</i> | 54.8            | 28             | 34             | 62    |

### Clade Classification

A total of six of the 11 indices are included in the stepwise discriminant model (Table 29). The DFA did not separate some clades well; however, Clades #1, #3, #5, #6, and #9 were separated fairly well (Wilks'  $\lambda = 0.116$ ,  $P < 0.001$ ). The classification showed the GFS musteline being assigned to Clade #4; however, Clade #4 was only 46.6% correctly classified (Table 30). The analysis yielded one discriminant function with an eigenvalue  $>1$  (1.666) and accounted for 53.5% of the variance in the data set. DF1 was positively correlated with P4WPar, M1W, and M1LinL, and negatively correlated with UGA, M1L/W, and P4PastW/ProW. DF2 had an eigenvalue of 0.705, accounted for 22.6% of the variance, was positively correlated with UGA, M1L/W, P4PastW/ProW, and M1LinL, and negatively correlated with P4WPar and M1W. The GFS musteline had a slightly positive score for both DF1 and DF2 (Figure 16).



Table 29. GFS Musteline Clade Analysis Structure Matrix, Eigenvalue, Percent Variance Explained, and Wilks'  $\lambda$  for Discriminant Function 1

| <b>Index</b>          | <b>DF 1</b> | <b>DF2</b> |
|-----------------------|-------------|------------|
| UGA                   | -0.699      | 0.332      |
| M1L/W                 | -0.110      | 0.660      |
| P4WPar                | 0.145       | -0.556     |
| P4PastW/ProW          | -0.145      | 0.239      |
| M1W                   | 0.494       | -0.492     |
| M1LinL                | 0.355       | 0.411      |
| Eigenvalue            | 1.666       | 0.705      |
| % variance explained  | 53.5        | 22.6       |
| Canonical correlation | 0.791       | 0.643      |
| Wilks' $\lambda$      | 0.116       | 0.310      |
| <i>p</i> -value       | < 0.001     | < 0.001    |

Table 30. GFS Musteline Clade Analysis Classification Matrix

| <b>Clade</b>   | <b>% Correct</b> | <b>Predicted Clade</b> |          |          |          |          |          |          |          |          | <b>Total</b> |
|--|------------------|------------------------|----------|----------|----------|----------|----------|----------|----------|----------|--------------|
|  |                  | <b>1</b>               | <b>2</b> | <b>3</b> | <b>4</b> | <b>5</b> | <b>6</b> | <b>7</b> | <b>8</b> | <b>9</b> |              |
| GFS musteline  | -                | -                      | -        | -        | 1        | -        | -        | -        | -        | -        | 1            |
| 1 ( <i>N. africana</i> , <i>N. felipei</i> , <i>N. frenata</i> , <i>N. vison</i> ) | 72.1             | 44                     | -        | -        | -        | 13       | -        | 1        | -        | 3        | 61           |
| 2 ( <i>M. nudipes</i> , <i>M. strigidorsa</i> )                                    | 0                | 5                      | -        | -        | -        | -        | -        | -        | -        | 1        | 6            |
| 3 ( <i>M. kathiah</i> )  | 60               | 1                      | -        | 3        | -        | 1        | -        | -        | -        | -        | 5            |
| 4 ( <i>M. erminea</i> )  | 46.4             | 2                      | -        | -        | 13       | 13       | -        | -        | -        | -        | 28           |
| 5 ( <i>M. altaica</i> , <i>M. nivalis</i> , <i>M. subpalmata</i> )                 | 73.7             | 1                      | -        | 2        | 9        | 42       | 1        | -        | -        | 2        | 57           |
| 6 ( <i>M. itatsi</i> )   | 58.8             | 2                      | -        | -        | -        | -        | 10       | 5        | -        | -        | 17           |
| 7 ( <i>M. lutreolina</i> , <i>M. sibirica</i> )                                    | 27.8             | 4                      | -        | -        | 1        | 3        | 4        | 5        | -        | 1        | 18           |
| 8 ( <i>M. lutreola</i> )   | 40               | -                      | 1        | -        | -        | -        | -        | 1        | 2        | 1        | 5            |
| 9 ( <i>M. eversmanii</i> , <i>M. nigripes</i> , <i>M. putorius</i> )               | 89.2             | 2                      | -        | -        | -        | 1        | -        | 1        | -        | 33       | 37           |

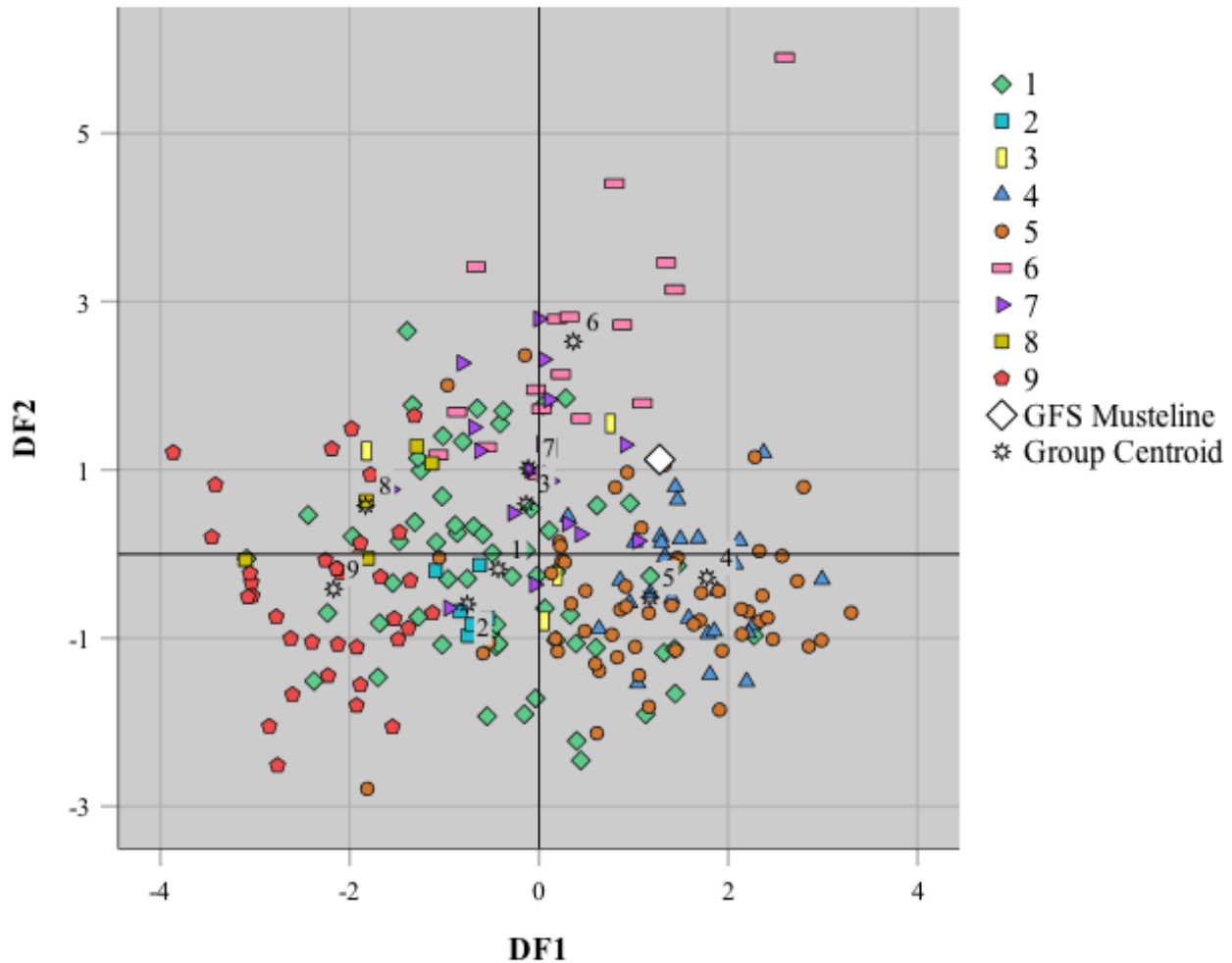


Figure 16. GFS musteline clade analysis scatterplot comparing DF1 vs. DF2. Clade 1 = *N. africana*, *N. felipei*, *N. frenata*, *N. vison*; Clade 2 = *M. nudipes*, *M. strigidorsa*; Clade 3 = *M. kathiah*; Clade 4 = *M. erminea*; Clade 5 = *M. altaica*, *M. nivalis*, *M. subpalmata*; Clade 6 = *M. itatsi*; Clade 7 = *M. lutreolina*, *M. sibirica*; Clade 8 = *M. lutreola*; and Clade 9 = *M. eversmanii*, *M. nigripes*, *M. putorius*.

#### *Extinct Pleistocene Taxa Analysis*

A stepwise DFA of genus and clade classification was performed using the ratios and GM-transformed linear measurements for each extant musteline taxon, as well as two extinct Pleistocene taxa, *Mustela gazini* and *Mustela jacksoni*, as unclassified cases.

### Genus Classification

A total of three of the 12 indices are included in the stepwise discriminant model (Table 31). The analysis yielded one discriminant function with an eigenvalue of 0.350 and a canonical correlation of 0.509. DF1 was positively correlated with m1L/p4L and m1TriL/TalL, and negatively correlated with m1TalL. The DFA separated members of *Mustela* well but not *Neogale* (Wilks'  $\lambda = 0.741$ ,  $P < 0.001$ ); classification showed 91.7% correct classification of *Mustela* and 45.9% correct classification of *Neogale*, with both *M. gazini* and *M. jacksoni* being classified as *Mustela* (Table 32). When cross-validated, the classification showed 91.7% correct classification of *Mustela* and 45.9% correct classification of *Neogale*.

Table 31. Extinct Pleistocene Genus Analysis Structure Matrix, Eigenvalue, Percent Variance Explained, and Wilks'  $\lambda$  for Discriminant Function 1

| <b>Index</b>          | <b>DF 1</b> |
|-----------------------|-------------|
| m1L/p4L               | 0.638       |
| m1TriL/TalL           | 0.541       |
| m1TalL                | -0.008      |
| Eigenvalue            | 0.350       |
| % variance explained  | 100         |
| Canonical correlation | 0.509       |
| Wilks' $\lambda$      | 0.741       |
| <i>p</i> -value       | < 0.001     |

Table 32. Extinct Pleistocene Genus Analysis Classification Matrix

|                        |                    | Predicted genus |                |                |       |
|------------------------|--------------------|-----------------|----------------|----------------|-------|
|                        |                    | % Correct       | <i>Mustela</i> | <i>Neogale</i> | Total |
| <b>Original</b>        | <i>Mustela</i>     | 91.7            | 166            | 15             | 181   |
|                        | <i>Neogale</i>     | 45.9            | 33             | 28             | 61    |
|                        | <i>M. gazini</i>   | -               | 1              | -              | 1     |
|                        | <i>M. jacksoni</i> | -               | 1              | -              | 1     |
| <b>Cross-validated</b> | <i>Mustela</i>     | 91.7            | 166            | 15             | 181   |
|                        | <i>Neogale</i>     | 45.9            | 33             | 28             | 61    |

### Species Classification

A total of seven of the 12 indices are included in the stepwise discriminant model (Table 33). The DFA separated each species fairly well and was significant (Wilks'  $\lambda = 0.021$ ,  $P < 0.001$ ). *M. gazini* was classified as *M. itatsi* and *M. jacksoni* was classified as *M. subpalmata*. The analysis yielded two discriminant functions with eigenvalues  $>1$  and accounted for 71% of the variance in the data set. DF1 accounted for 50.8% of the variance, was positively correlated with MD, and negatively correlated with m1L, m1L/W, m1L/p4L, m1TriL/TalL, p4L, and p4W. *M. gazini* had a highly positive score for DF1 while *M. jacksoni* had a moderately negative score. DF2 accounted for 20.2% of the variance, was positively correlated with m1L, m1L/p4L, m1TriL/TalL, MD, and p4W, and negatively correlated with m1L/W and p4L. *M. gazini* had a highly positive score for DF2 while *M. jacksoni* had a moderately positive score (Figure 17).

Table 33. Extinct Pleistocene Species Analysis Structure Matrix, Eigenvalue, Percent Variance Explained, and Wilks'  $\lambda$  for Discriminant Functions 1 and 2

| <b>Index</b>          | <b>DF 1</b> | <b>DF 2</b> |
|-----------------------|-------------|-------------|
| m1L                   | -0.910      | 0.090       |
| m1L/W                 | -0.578      | -0.218      |
| m1L/p4L               | -0.274      | 0.243       |
| m1TriL/TalL           | -0.098      | 0.306       |
| p4L                   | -0.317      | -0.133      |
| MD                    | 0.187       | 0.562       |
| p4W                   | -0.003      | 0.451       |
| Eigenvalue            | 3.361       | 1.334       |
| % variance explained  | 50.8        | 20.2        |
| Canonical correlation | 0.878       | 0.756       |
| Wilks' $\lambda$      | 0.021       | 0.091       |
| <i>p</i> -value       | < 0.001     | < 0.001     |

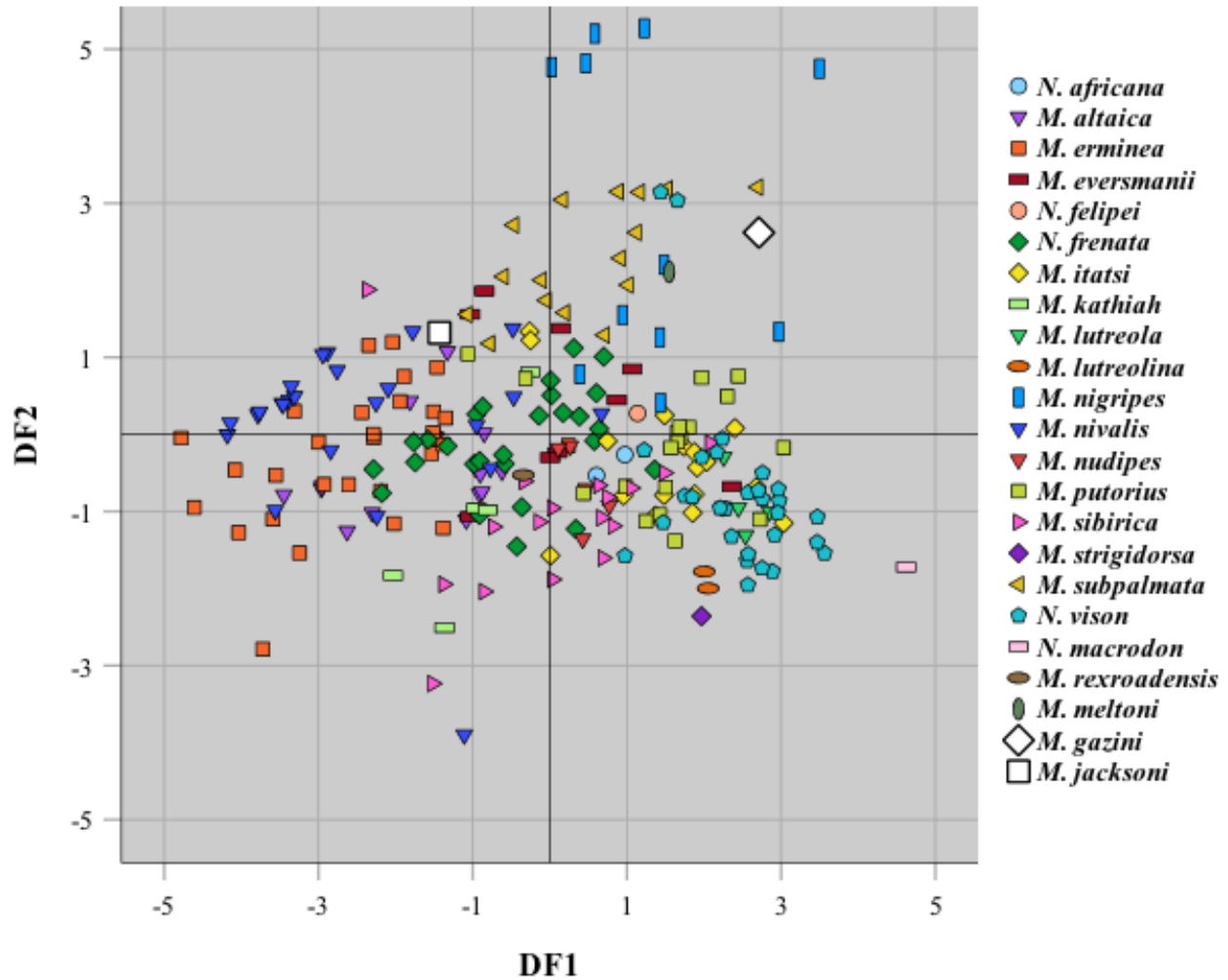


Figure 17. Extinct Pleistocene species analysis scatterplot comparing DF1 vs. DF2

### Clade Classification

A total of five of the 12 indices are included in the stepwise discriminant model (Table 34). The DFA did not separate most clades well; however, Clades #1, #5, and #9 were separated fairly well (Wilks'  $\lambda = 0.215$ ,  $P < 0.001$ ). The classification showed *M. gazini* being assigned to Clade #1 and *M. jacksoni* being assigned to Clade #5 (Table 35). The analysis yielded one discriminant function with an eigenvalue  $>1$  and accounted for 61.1% of the variance in the data set. DF1 was positively correlated with all indices (m1L, p4W, m1L/W, m1L/p4L, and

m1TriL/TalL). DF2 had an eigenvalue of 0.513, accounted for 24.2% of the variance, was positively correlated with p4W, m1L/p4L, and m1TriL/TalL, and negatively correlated with m1L and m1L/W. *M. gazini* had a slightly negative score for both DF1 and DF2. *M. jacksoni* had a moderately positive score for DF1 and a slightly negative score for DF2 (Figure 18).

Table 34. Extinct Pleistocene Clade Analysis Structure matrix, Eigenvalue, Percent Variance Explained, and Wilks'  $\lambda$  for Discriminant Functions 1 and 2

| <b>Index</b>          | <b>DF 1</b> | <b>DF2</b> |
|-----------------------|-------------|------------|
| m1L                   | 0.826       | -0.167     |
| p4W                   | 0.189       | 0.167      |
| m1L/W                 | 0.390       | -0.100     |
| m1L/p4L               | 0.325       | 0.356      |
| m1TriL/TalL           | 0.316       | 0.572      |
| Eigenvalue            | 1.295       | 0.513      |
| % variance explained  | 61.1        | 24.2       |
| Canonical correlation | 0.751       | 0.582      |
| Wilks' $\lambda$      | 0.215       | 0.495      |
| <i>p</i> -value       | < 0.001     | < 0.001    |

Table 35. Extinct Pleistocene Clade Analysis Classification Matrix

| Clade  | % Correct | Predicted Clade |   |   |    |    |   |   |   |    | Total |
|--|-----------|-----------------|---|---|----|----|---|---|---|----|-------|
|  |           | 1               | 2 | 3 | 4  | 5  | 6 | 7 | 8 | 9  |       |
| <i>M. gazini</i>   | -         | 1               | - | - | -  | -  | - | - | - | -  | 1     |
| <i>M. jacksoni</i>   | -         | -               | - | - | -  | 1  | - | - | - | -  | 1     |
| 1 ( <i>N. africana</i> , <i>N. felipei</i> , <i>N. frenata</i> , <i>N. vison</i> ) | 73.3      | 44              | - | - | -  | 10 | 4 | 1 | - | 1  | 60    |
| 2 ( <i>M. nudipes</i> , <i>M. strigidorsa</i> )                                    | 0         | 3               | - | - | -  | 2  | - | 1 | - | -  | 6     |
| 3 ( <i>M. kathiah</i> )  | 0         | 1               | - | - | -  | 2  | - | 1 | - | 1  | 5     |
| 4 ( <i>M. erminea</i> )  | 40        | 1               | - | - | 12 | 16 | - | 1 | - | -  | 30    |
| 5 ( <i>M. altaica</i> , <i>M. nivalis</i> , <i>M. subpalmata</i> )                 | 62.1      | 6               | - | - | 11 | 36 | - | 1 | - | 4  | 58    |
| 6 ( <i>M. itatsi</i> )   | 17.6      | 11              | - | - | -  | 2  | 3 | 1 | - | -  | 17    |
| 7 ( <i>M. lutreolina</i> , <i>M. sibirica</i> )                                    | 42.1      | 7               | - | - | -  | 2  | 1 | 8 | - | 1  | 19    |
| 8 ( <i>M. lutreola</i> )   | 0         | 5               | - | - | -  | -  | - | - | - | -  | 5     |
| 9 ( <i>M. eversmanii</i> , <i>M. nigripes</i> , <i>M. putorius</i> )               | 62.5      | 8               | - | - | -  | 5  | 1 | 1 | - | 25 | 40    |



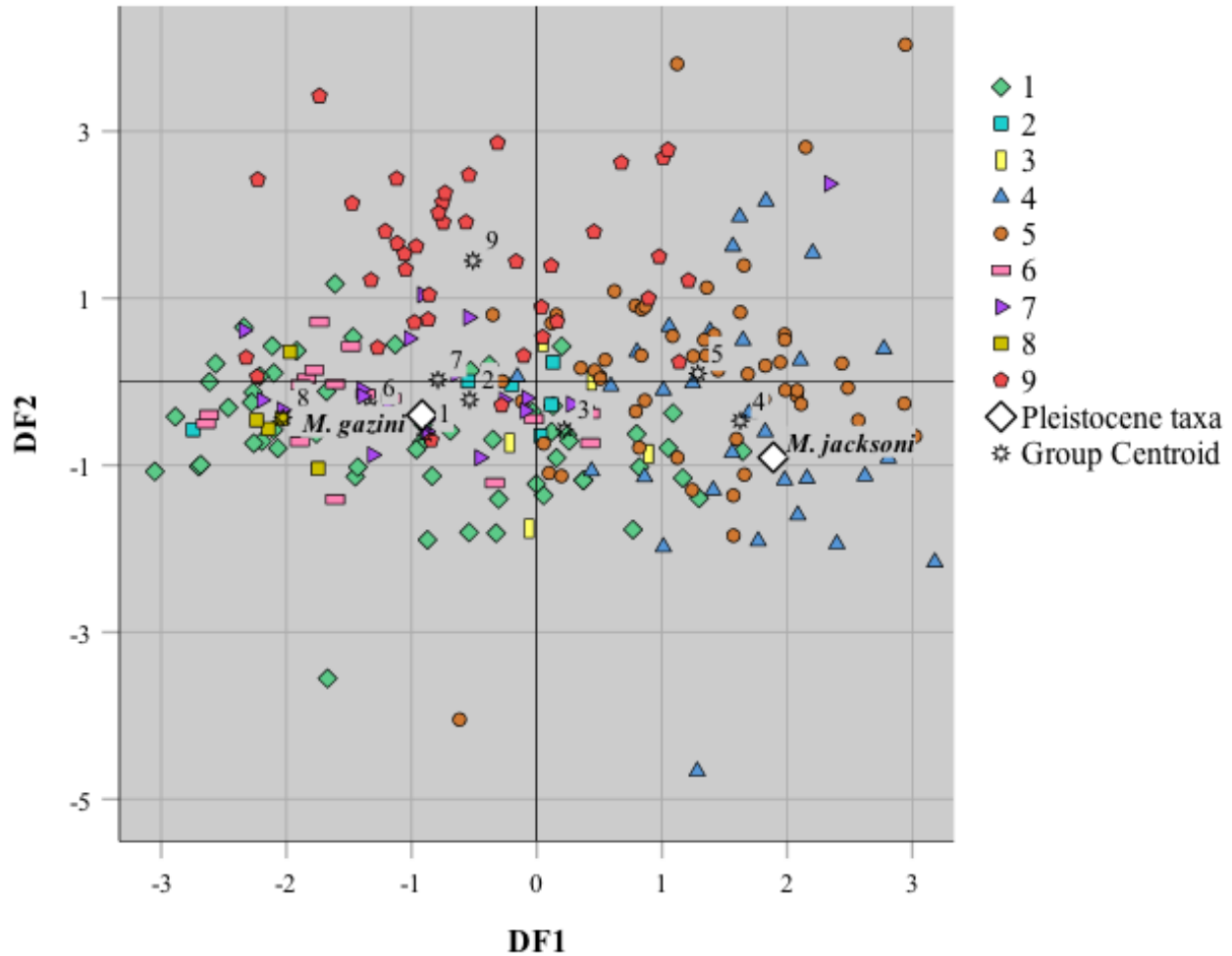


Figure 18. Extinct Pleistocene clade analysis scatterplot comparing DF1 vs. DF2. Clade 1 = *N. africana*, *N. felipei*, *N. frenata*, *N. vison*; Clade 2 = *M. nudipes*, *M. strigidorsa*; Clade 3 = *M. kathiah*; Clade 4 = *M. erminea*; Clade 5 = *M. altaica*, *M. nivalis*, *M. subpalmata*; Clade 6 = *M. itatsi*; Clade 7 = *M. lutreolina*, *M. sibirica*; Clade 8 = *M. lutreola*; and Clade 9 = *M. eversmanii*, *M. nigripes*, *M. putorius*.

#### *Mustela sp. Analysis*

A stepwise DFA of genus, species, and clade classification was performed using the ratios and GM-transformed linear measurements for two Blancan-aged specimens labeled *Mustela sp. aff. M. rexroadensis* as unclassified cases. In addition to each extant taxon, *N. macrodon*, *M. rexroadensis*, and *M. meltoni*, were also included in the analysis for comparison.

### *Genus Classification*

A total of two of the seven indices are included in the stepwise discriminant model (Table 36).

The DFA separated *Mustela* well but did not perform as well at separating *Neogale* (Wilks'  $\lambda = 0.829$ ,  $P < 0.001$ ). The analysis yielded one discriminant function with an eigenvalue of 0.206 and a canonical correlation of 0.413. DF1 was positively correlated with both indices, p4L and m1L. The classification showed 93.3% correct classification of *Mustela* and 25.4% correct classification of *Neogale*, with both specimens of *Mustela* sp. being classified as *Mustela* (Table 37). When cross-validated, the classification showed 93.3% correct classification of *Mustela* and 25.4% correct classification of *Neogale*.

Table 36. *Mustela* sp. Genus Analysis Structure Matrix, Eigenvalue, Percent Variance Explained, and Wilks'  $\lambda$  for Discriminant Function 1

| <b>Index</b>          | <b>DF 1</b> |
|-----------------------|-------------|
| p4L                   | 0.892       |
| m1L                   | 0.395       |
| Eigenvalue            | 0.206       |
| % variance explained  | 100         |
| Canonical correlation | 0.413       |
| Wilks' $\lambda$      | 0.829       |
| <i>p</i> -value       | < 0.001     |

Table 37. *Mustela* sp. Genus Analysis Classification Matrix

|                        |                             | Predicted genus |                |                |       |
|------------------------|-----------------------------|-----------------|----------------|----------------|-------|
|                        |                             | % Correct       | <i>Mustela</i> | <i>Neogale</i> | Total |
| <b>Original</b>        | <i>Mustela</i>              | 93.3            | 168            | 12             | 180   |
|                        | <i>Neogale</i>              | 25.4            | 44             | 15             | 59    |
|                        | <i>Mustela</i> sp. (#7559)  | -               | 1              | -              | 1     |
|                        | <i>Mustela</i> sp. (#12861) | -               | 1              | -              | 1     |
| <b>Cross-validated</b> | <i>Mustela</i>              | 93.3            | 168            | 12             | 180   |
|                        | <i>Neogale</i>              | 25.4            | 44             | 15             | 59    |

### *Species Classification*

A total of five of the seven indices are included in the stepwise discriminant model (Table 38). The DFA separated each species fairly well and was significant (Wilks'  $\lambda = 0.018$ ,  $P < 0.001$ ). #7559 was classified as *N. frenata* and #12861 was classified as *M. subpalmata*. The second-highest predicted species for #7559 was *M. rexroadensis* and for #12861 the second-highest species was *N. frenata*. The analysis yielded two discriminant functions with eigenvalues  $>1$  and accounted for 87.1% of the variance in the data set. DF1 accounted for 74.1% of the variance, was positively correlated with m1L, p4L, m1W, and p4W, and negatively correlated with m1L/W. #7559 had a slightly negative score and #12861 had a moderately negative score for DF1. DF2 accounted for 13% of the variance, was positively correlated with p4L, m1W, and p4W, and negatively correlated with m1L and m1L/W. #7559 had a slightly negative score and #12861 had a moderately positive score for DF2 (Figure 19).

Table 38. *Mustela* sp. Species Analysis Structure Matrix, Eigenvalue, Percent Variance Explained, and Wilks'  $\lambda$  for Discriminant Functions 1 and 2

| <b>Index</b>          | <b>DF 1</b> | <b>DF 2</b> |
|-----------------------|-------------|-------------|
| m1L                   | 0.812       | -0.292      |
| p4L                   | 0.666       | 0.382       |
| m1W                   | 0.659       | 0.468       |
| p4W                   | 0.550       | 0.430       |
| m1L/W                 | -0.256      | -0.792      |
| Eigenvalue            | 7.518       | 1.320       |
| % variance explained  | 74.1        | 13          |
| Canonical correlation | 0.939       | 0.754       |
| Wilks' $\lambda$      | 0.018       | 0.151       |
| <i>p</i> -value       | < 0.001     | < 0.001     |

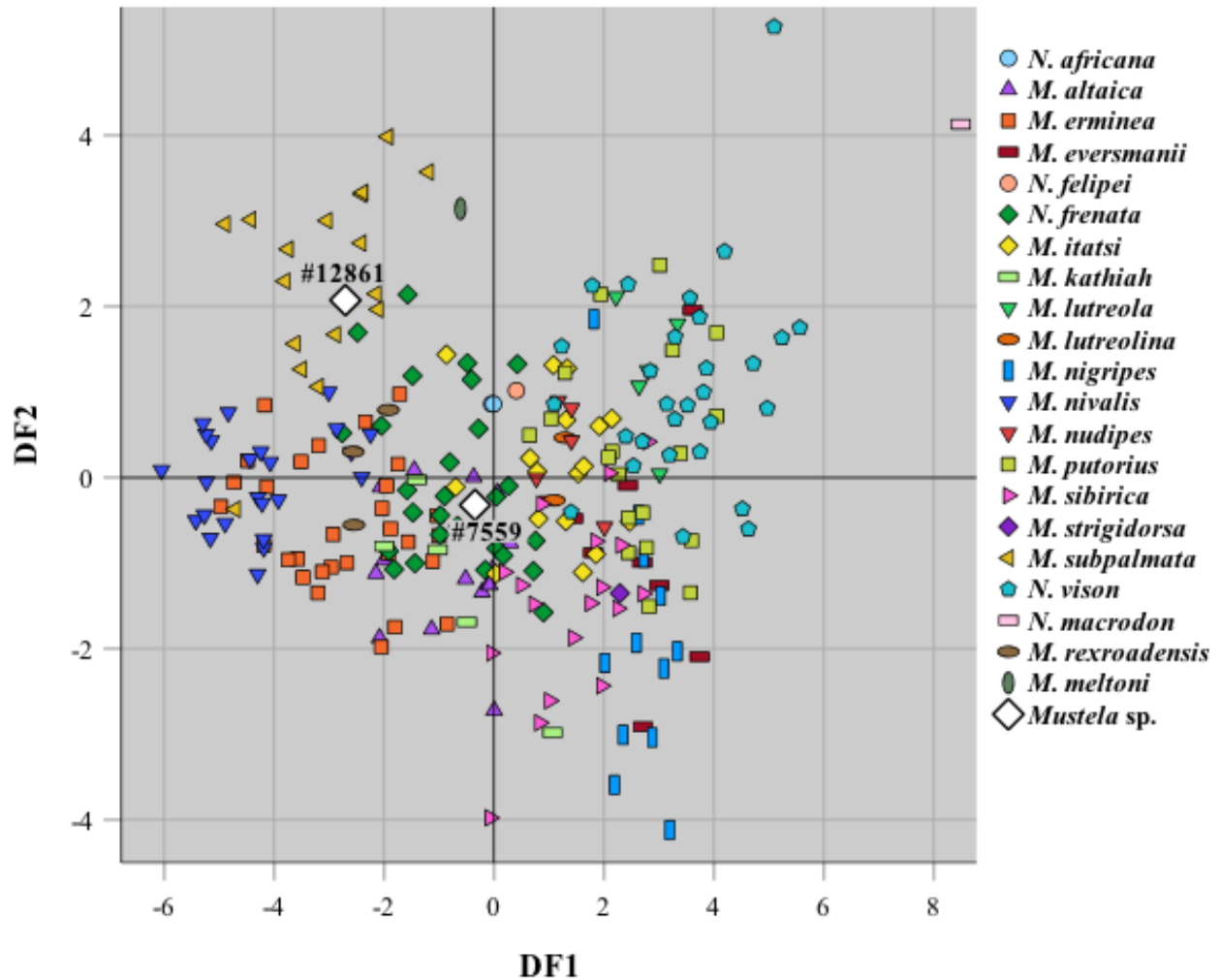


Figure 19. *Mustela sp.* species analysis scatterplot comparing DF1 vs. DF2

### Clade Classification

A total of three of the seven indices are included in the stepwise discriminant model (Table 39). The DFA did not separate most clades well; however, Clades #1, #5, and #9 were separated fairly well (Wilks'  $\lambda = 0.214$ ,  $P < 0.001$ ). The classification showed #7559 being assigned to Clade #1 and #12861 being assigned to Clade #5 (Table 40). The analysis yielded one discriminant function with an eigenvalue  $>1$  and accounted for 82.6% of the variance in the data set. DF1 was positively correlated with all indices (m1L, p4L, and p4W). DF2 had an

eigenvalue of 0.254, accounted for 9.9% of the variance, was positively correlated with p4L and p4W, and negatively correlated with m1L. #7559 had a slightly negative score for both DF1 and a moderately positive score for DF2. #12861 had a moderately negative score for DF1 and a highly positive score for DF2 (Figure 20).

Table 39. *Mustela* sp. Clade Analysis Structure Matrix, Eigenvalue, Percent Variance Explained, and Wilks'  $\lambda$  for Discriminant Functions 1 and 2

| <b>Index</b>          | <b>DF 1</b> | <b>DF2</b> |
|-----------------------|-------------|------------|
| m1L                   | 0.925       | -0.373     |
| p4L                   | 0.784       | 0.590      |
| p4W                   | 0.673       | 0.047      |
| Eigenvalue            | 2.125       | 0.254      |
| % variance explained  | 82.6        | 9.9        |
| Canonical correlation | 0.825       | 0.450      |
| Wilks' $\lambda$      | 0.214       | 0.667      |
| <i>p</i> -value       | < 0.001     | < 0.001    |

Table 40. *Mustela* sp. Clade Analysis Classification Matrix

| Clade  | % Correct | Predicted Clade |   |   |   |    |   |   |   |    | Total |
|--|-----------|-----------------|---|---|---|----|---|---|---|----|-------|
|  |           | 1               | 2 | 3 | 4 | 5  | 6 | 7 | 8 | 9  |       |
| <i>Mustela</i> sp. (#7559)   | -         | 1               | - | - | - | -  | - | - | - | -  | 1     |
| <i>Mustela</i> sp. (#12861)  | -         | -               | - | - | - | 1  | - | - | - | -  | 1     |
| 1 ( <i>N. africana</i> , <i>N. felipei</i> , <i>N. frenata</i> , <i>N. vison</i> ) | 62.7      | 37              | - | - | - | 12 | - | - | 8 | 9  | 59    |
| 2 ( <i>M. nudipes</i> , <i>M. strigidorsa</i> )                                    | 0         | 6               | - | - | - | -  | - | - | - | -  | 6     |
| 3 ( <i>M. kathiah</i> )  | 0         | 1               | - | - | - | 3  | - | 1 | - | -  | 5     |
| 4 ( <i>M. erminea</i> )  | 13.3      | 1               | - | - | 4 | 24 | - | 1 | - | -  | 30    |
| 5 ( <i>M. altaica</i> , <i>M. nivalis</i> , <i>M. subpalmata</i> )                 | 77.2      | 5               | - | - | 3 | 44 | - | 5 | - | -  | 57    |
| 6 ( <i>M. itatsi</i> )   | 0         | 12              | - | - | - | -  | - | 9 | - | 1  | 17    |
| 7 ( <i>M. lutreolina</i> , <i>M. sibirica</i> )                                    | 45        | 10              | - | - | - | -  | - | 9 | - | 1  | 20    |
| 8 ( <i>M. lutreola</i> )   | 0         | 5               | - | - | - | -  | - | - | - | -  | 5     |
| 9 ( <i>M. eversmanii</i> , <i>M. nigripes</i> , <i>M. putorius</i> )               | 60        | 13              | - | - | - | -  | - | 3 | - | 24 | 40    |

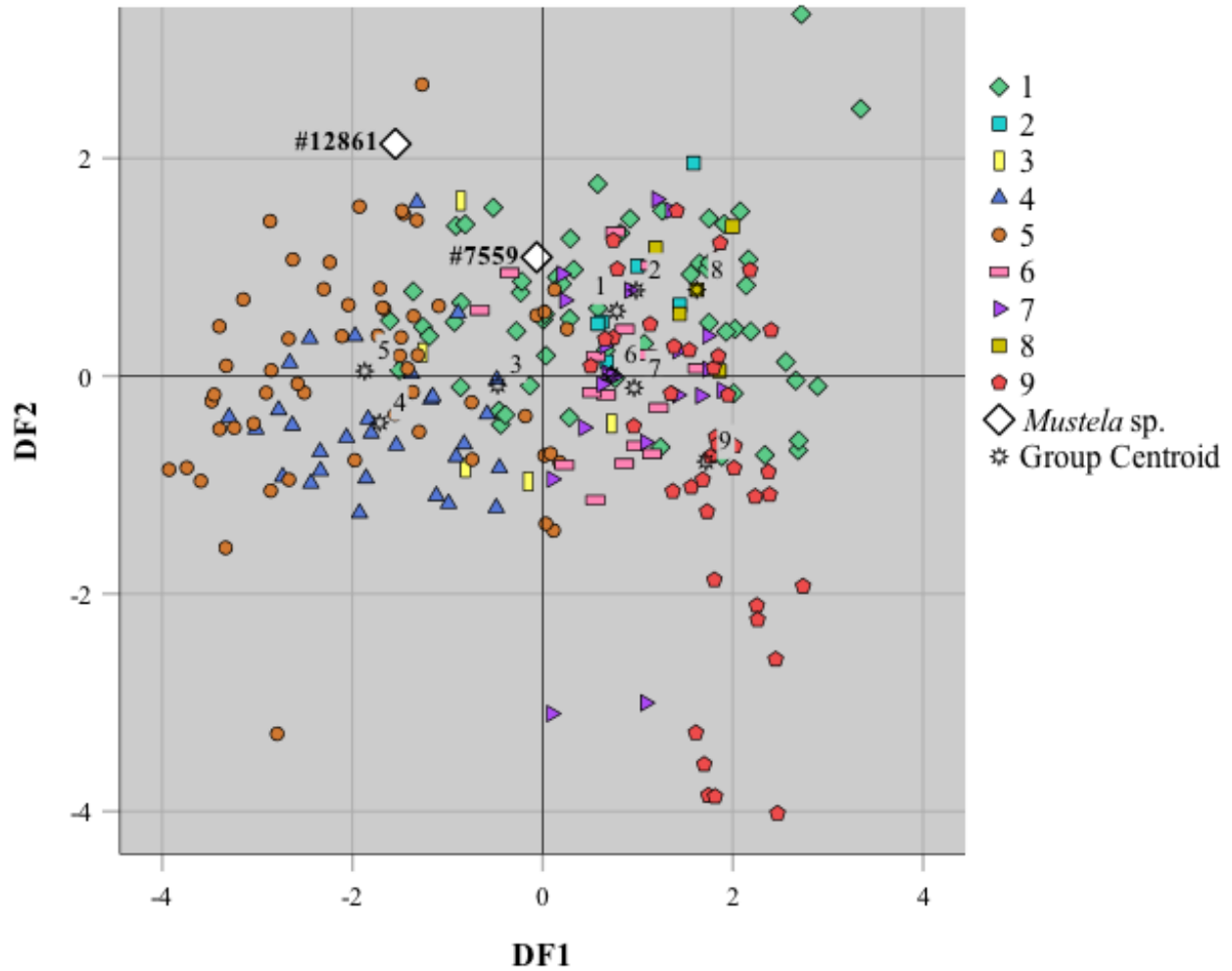


Figure 20. *Mustela* sp. clade analysis scatterplot comparing DF1 vs. DF2. Clade 1 = *N. africana*, *N. felipei*, *N. frenata*, *N. vison*; Clade 2 = *M. nudipes*, *M. strigidorsa*; Clade 3 = *M. kathiah*; Clade 4 = *M. erminea*; Clade 5 = *M. altaica*, *M. nivalis*, *M. subpalmata*; Clade 6 = *M. itatsi*; Clade 7 = *M. lutreolina*, *M. sibirica*; Clade 8 = *M. lutreola*; and Clade 9 = *M. eversmanii*, *M. nigripes*, *M. putorius*.



## CHAPTER 8. DISCUSSION

### *Character State Analysis*

The results of the character state analysis revealed a total of six characters that may assist in potentially distinguishing *Mustela* from *Neogale* (#27, #30, #34, #35, #39, #40), although significant overlap between genera was observed (Tables 5 and 6). While no single trait can easily distinguish genera, a combination of traits can allow diagnosis of genera. Most traits useful in diagnosis are seen in the P4, M1, and m1, which are commonly found in fossil specimens.

For #27 (p2 occurrence), 100% of *Mustela* showed *a* (present) and 97% of *Neogale* showed *a* with *N. africana* being the only member of *Neogale* to show *b* (absent). *N. africana* is the only musteline known to exhibit absence of the p2 (Ramirez-Chavez et al. 2014) which indicates that character #27 is only reliable in distinguishing *N. africana* and not the remaining members of *Neogale*.

For #30 (P4 protocone), 87% of *Mustela* specimens showed *a* (no prominent cusp, but a raised ridge or cuspule present, smaller in width than the parastyle) and 57% of *Neogale* showed *b* (small cusp, larger in width than the parastyle); however, *N. vison* was the only member of *Neogale* to have a majority of specimens showing *b*. This indicates that character #30 is only significantly reliable in distinguishing *N. vison* from the remaining mustelines.

For #34, both genera exhibited *b* (M1 subequal in size to P4) and *c* (M1 clearly smaller than P4); however, the majority of *Mustela* (70%) showed *c* while the majority of *Neogale* (62%) showed *b*. The only member of *Neogale* that did not have a majority of specimens showing *b* was *N. frenata*. *M. erminea* had 93% of specimens showing *b*; and since *N. frenata* and *M.*

*erminea* are known to often exhibit significant morphological overlap (King and Powell 2007), character #34 may assist in potentially distinguishing the two species.

For #35, both genera exhibited *c* (lingual half of M1 crown subequal in length to buccal half, both halves separated from each other by anteroposterior constriction) and *d* (lingual half of M1 crown longer than buccal half, both halves separated from each other by anteroposterior constriction). The majority of *Mustela* (55%) showed *c* while the majority of *Neogale* (63%) showed *d*; however, *N. vison* was the only member of *Neogale* with a majority of specimens showing *d* (86%). This indicates that M1 morphology is significant in distinguishing *N. vison* from the remaining musteline taxa. Furthermore, 100% of *N. macrodon* showed *c*, thus suggesting the two species of mink could potentially be distinguished from each other based on relation of anteroposterior length of the lingual half to that of the buccal half of the M1.

For #39, 100% of *Mustela* and 51% of *Neogale* showed *c* (absent). *N. vison* and *N. macrodon* were the only mustelines to show *c* (much smaller than the other trigonid cusps and often positioned posteriorly) with 100% of specimens of each species exhibiting this character state. This indicates that the presence or absence of the m1 metaconid is crucial when distinguishing the two mink species from the remaining mustelines.

Character #40 (relation of m1 trigonid to talonid) showed both genera favoring *a* (trigonid less than three times as long as talonid) (84% of *Mustela* and 100% of *Neogale*). The 16% of *Mustela* specimens that showed *b* (trigonid three times as long as talonid) include *M. altaica*, *M. erminea*, *M. eversmanni*, *M. nivalis*, *M. putorius*, and *M. subpalmata*. Of these species, *M. subpalmata* was the only one to have a majority of the sample showing *b* (53%). And because only 12% of *M. nivalis* showed *b*, character #40 could assist in further distinguishing *M. subpalmata* as a separate species from *M. nivalis* as originally postulated by van Zyll de Jong

(1992) and later supported by Reig (1997). van Zyll de Jong (1992) conducted an analysis of cranial variation in *M. nivalis* and found that of all the subspecific groups used in the study, *M. n. subpalmata* was the only group that did not form part of the *M. nivalis* morphological continuum, thus supporting the distinction of *M. subpalmata* as a separate species. The study revealed that *M. subpalmata* differs from *M. nivalis* in basal skull width, interorbital width, and greatest width of P4 (van Zyll de Jong 1992). Additionally, Reig (1997) examined geographic variation in the skulls of *M. nivalis* and also concluded *M. subpalmata* to be a distinct taxon deserving of species status.

#### *Extant Taxa Analysis*

The results of the DFA revealed significant separation of genus, species, and clade which indicates the measurements and ratios used in the analysis are reliable when distinguishing the extant taxa.

#### *Genus Classification*

Members of *Mustela* generally had positive DF1 scores while the majority of *Neogale* scores were negative. Size of the P4 parastyle relative to the protocone, condylobasal skull length, and m1 trigonid length relative to talonid length are most useful when distinguishing between genera. Bivariate scatterplots indicate that members of *Mustela* overall have a greater P4PastW/ProW, CBL, and m1TriL/TalL compared to *Neogale* (Figure 8). This indicates that, in *Neogale*, the P4 protocone is more often larger in width than the parastyle. Additionally, the ratio of m1 trigonid to talonid is generally slightly smaller in *Neogale*, thus indicating that the m1 talonid is relatively larger in *Neogale* compared to *Mustela*. The upper grinding surface area, the size of the P4 parastyle relative to the protocone, and the size of the M1 lingual and buccal lobes are most significant when distinguishing *N. vison* from all other mustelines. *N. vison* generally

has a larger upper grinding area, a wider P4 protocone relative to the parastyle, and a longer M1 lingual lobe than those of *Mustela*. Park and Nowosielski-Slepowron (1980) examined tooth morphology of *N. vison* and noted that the P4 paracone was larger than the parastyle and the M1 lingual lobe was more expanded than the buccal lobe, thus supporting the results of this analysis. Butler (1946) showed that in mustelines the upper premolars are specialized for shearing and the M1 for crushing. Although *N. vison* is considered an opportunistic feeder and its diet will ultimately reflect the local prey base (Ben-David et al. 1997), it is often associated with aquatic environments with a diet typically comprised mostly of fish, amphibians, crustaceans, muskrats, and small mammals (Larivière 1999).

### *Species Classification*

The upper and lower grinding surface areas, measurements of the upper and lower carnassials, and condylobasal skull length relative to maximum cranial width are most useful when separating species. Only seven of the 18 extant musteline species were not 100% correctly classified in the analysis. Although at least some overlap was expected, scatter plots comparing DF1 vs. DF2 and DF1 vs. DF3 clearly demonstrate a clustering for each species, thus supporting the ability of the DFA to accurately separate each taxon at the species-level. When comparing DF1 vs. DF2 in Figure #, notable overlap among *M. lutreola*, and *M. putorius*, *M. strigidorsa*, and *N. vison* occurred. Additionally, *M. eversmannii*, *M. itatsi*, *M. lutreolina*, *M. nigripes*, and *M. nudipes* showed some overlap. Of the seven species not 100% correctly classified, *M. erminea*, *M. nivalis*, and *N. frenata* exhibited the most variation, with these species showing more overlap with each other than any other given grouping of species (Table 11). Several authors have recognized the striking degree of variation in size and sexual dimorphism of *M. erminea*, *N. frenata*, and *M. nivalis* throughout their respective ranges (Hall 1951; King 1980; Ralls and

Harvey 1985). The results of this study not only support these observations, but also indicate that all 18 species of extant mustelines can in fact reliably be distinguished from one another using the aforementioned measurements within a large sample size.

#### *Clade Classification*

Measurements and ratios involving condylobasal skull length, maximum cranial width, M1, and upper and lower carnassials are most useful when separating musteline clades. Of the nine clades used in the analysis, only two (clades 2 and 4) had <75% correct classification (Table #). Clade 2 (*M. nudipes*, *M. strigidorsa*) showed the lowest correct classification (50%); however, only six total specimens were available for this analysis. *M. nudipes* and *M. strigidorsa* are two of the rarest and least-recorded mustelids in the world, therefore very little is known about their morphology (Duckworth et al. 2006; Abramov et al. 2008). A larger sample size may eventually provide more reliable results when examining potential distinguishing morphological features of this poorly known musteline clade. Clade 4 (*M. erminea*) had the second-lowest correct classification (59.3%) and expectedly showed a considerable degree of overlap with clade 5 (*M. altaica*, *M. nivalis*, *M. subpalmata*) (Figure #). Additionally, clades 6 (*M. itatsi*) and 7 (*M. lutreolina*, *M. sibirica*) showed slight overlap, as did clade 8 (*M. lutreola*) with clades 1 (*N. africana*, *N. felipei*, *N. frenata*, *N. vison*) and 9 (*M. eversmannii*, *M. nigripes*, *M. putorius*). Despite this overlap, the scatter plots revealed group clustering, thus supporting the ability of the DFA to reliably separate each clade based on skull and tooth morphology.

#### *Extant Pleistocene Taxa Classification*

Regarding the extant North American Pleistocene specimens, all were correctly predicted at the genus-level. *M. nigripes* and *N. vison* were the only specimens to be correctly classified at the species-level; however, *M. nivalis* was correctly classified during the 2<sup>nd</sup> most likely species

prediction. *N. frenata* was the only specimen not correctly classified during the 1<sup>st</sup> and 2<sup>nd</sup> most likely species predictions. All specimens, except for *N. frenata*, were correctly classified to clade; however, *N. frenata* was correctly classified to clade during the 2<sup>nd</sup> most likely clade prediction. Nevertheless, Figure # shows the Pleistocene *N. frenata* specimen clearly occupying the same cluster as Holocene *M. frenata*. Overall, the clade analysis showed better correct classification compared to species classification. This suggests when attempting to identify an unknown Pleistocene specimen, classifying it to clade may yield more reliable results than attempting to classify species. The results indicate not only that the Pleistocene specimens can reliably be classified to genus, species, and clade, but also that Pleistocene North American mustelines are likely relatively indistinguishable morphologically when compared to their Holocene counterparts.

#### *'Neovison' macrodon Analysis*

*'Neovison' macrodon*, known as the sea mink, was first described by Prentiss (1903) who noted a significant morphological resemblance between the skull and that of *N. vison*; however, he pointed out that the teeth are decidedly larger and the carnassials are situated at a more acute angle with the long axis of the skull (Manville 1966). In contrast, Manville (1966) examined the type cranial material of *N. macrodon* and concluded there to be no substantial morphological differences when compared to *N. vison*, thus suggesting it to be a subspecies of *N. vison*. Still, *N. macrodon* remained inadequately described until Mead et al. (2000) compared measurements from a large archaeological sample of *N. macrodon* specimens to five subspecies of *N. vison*. They discovered *N. macrodon* to be morphologically distinct from all subspecies of *N. vison*, thus suggesting its designation as a separate species. They noted that the P4 exhibits a relatively longer paracone and the junction of the anterior margin of the zygomatic with the cranium is

over the P4 on *N. macrodon* (versus between the P3 and P4 in *N. vison*) (Mead et al. 2000). Similarly, Sealfon (2007) quantitatively examined dental measurements of *N. macrodon* and also concluded it to be sufficiently distinct from *N. vison*, further supporting recognition as a separate species. She observed *N. macrodon* as having a relative reduction in length of the upper carnassial blade and a relative increase in width of the upper carnassial and suggested an adaptation for consuming aquatic prey that are harder-bodied than those consumed by *N. vison* (Sealfon 2007). Both Mead et al. (2000) and Sealfon (2007) agree that diet likely played a major role in the divergence of *N. macrodon* and *N. vison*.

The results of this analysis support the findings of Mead et al. (2000) and Sealfon (2007) that *N. macrodon* can be distinguished from *N. vison* using skull and tooth measurements from an adequate comparative sample size. The DFA showed *N. macrodon* having a higher DF1 score than any *N. vison* specimen. *N. macrodon* showed larger averages for both UGA and LGA (UGA=31.43 mm; LGA=19.05) compared to *N. vison* (UGA=18.79 mm; LGA=8.86) with no size overlap between species. Additionally, *N. macrodon* had an average M1LinL of 5.54 mm while *N. vison* had an average of 4.05 mm with no overlap between species, thus aligning with the results of the character state analysis which showed all *N. macrodon* specimens having the lingual half of the M1 crown subequal in length to the buccal half while all *N. vison* specimens showed a longer lingual half relative to the buccal half (character #36). This study also supports the observation by Mead et al. (2000) that the P4 of *N. macrodon* has a more lingually elongated paracone when compared to *N. vison*. *N. macrodon* had an average P4WPar of 4.1 mm while that of *N. vison* was just 2.9 mm (with only slight overlap), thus indicating the presence of a relatively larger P4 paracone for *N. macrodon*. Clade classification placed *N. macrodon* into Clade #1 which consists of the newly designated genus *Neogale*. And with all of the New World

musteline taxa (including *N. vison*) recently being placed into this genus (Patterson et al. 2021), it is recommended that *N. macrodon* deserves generic revision to this group.

#### *Mustela rexroadensis* Analysis

*Mustela rexroadensis*, often referred to as the Rexroad weasel, is known from a single Late/Upper Hemphillian locality of Nebraska (5.9 – 4.9 Ma) (Voorhies 1990) as well as Blancan localities of Kansas (4.9 – 2.6 Ma) (Hibbard 1950; 1952; 1954), Idaho (4 – 3.2 Ma) (Bjork 1970), Texas (4.9 – 2.6 Ma) (Dalquest 1978), and Washington (4.9 – 2.6 Ma) (Morgan and Morgan 1995). A medium-sized musteline, it was originally described by Hibbard (1950) who distinguished it from recent mustelines by an open lower carnassial notch, a low, compressed m1 paraconid, and a P4 paracone that does not extend as far anteriorly in relation to the anterior root. Bjork (1970) subsequently described topotype material from the Hagerman local fauna and distinguished it from *N. frenata* by a more compressed and acuminate p3 and p4 (Kurtén and Anderson 1980). Additionally, he mentioned that the distinctly open lower carnassial notch of the holotype specimen described by Hibbard (1950) is peculiar when compared to the topotype material from Hagerman. He suggested the discrepancy is in part due to a lower m1 paraconid in the holotype potentially caused by differential wear, further noting the presence of similar variations seen in *N. frenata* (Bjork 1970). Anderson (1989) commented that *N. frenata* likely descended from *M. rexroadensis*; however, *M. rexroadensis* continues to be inadequately understood as a result of its osteological description being restricted solely to the characters observed in the Fox Canyon and Hagerman specimens (Hibbard 1950; Bjork 1970).

The results of this analysis showed characters of the upper and lower carnassial, p4, and mandible being most useful when classifying *M. rexroadensis* to genus and clade (Table 19, 21). Although the descriptions made by Bjork (1970) suggest close affinity to *N. frenata*, clade



classification yielded *M. rexroadensis* being assigned to Clade #4 (*M. erminea*) with the 2<sup>nd</sup> most likely clade being #5 (*M. altaica*, *M. nivalis*, *M. subpalmata*), thus contradicting the hypothesis of a New World origin made by previous authors (Bjork 1970; Anderson 1989). This presents the possibility that the ancestry of *M. rexroadensis* is of Eurasian origin despite fossil distribution being restricted to North America (Kurtén and Anderson 1980).

Additionally, the clade analysis showed *M. rexroadensis* having a moderately positive score for DF1 and a moderately negative score for DF2 while *N. frenata* had slightly negative to slightly positive scores for both DF1 and DF2. This indicates that *M. rexroadensis* can potentially be distinguished from *N. frenata* by the P4, p4, and m1. The results of this analysis support the claim by Bjork (1970) that the p4 of *M. rexroadensis* is more compressed relative to *N. frenata*; however, it simultaneously contradicts his indication that the P4 of *M. rexroadensis* is very similar in appearance to that of *N. frenata*. As only one *M. rexroadensis* specimen containing a P4 was available for this analysis, a larger sample would be necessary in order to better understand distinguishing characters between the two species.

#### *Mustela meltoni* Analysis

Only one occurrence of *Mustela meltoni* (“Melton’s mink”), a left lower mandible from the Blancan-aged Fox Canyon local fauna of Kansas, has been recorded from the fossil record. Bjork (1973) described the holotype specimen as being a “mink-like mustelid” and noted it having a robust mandible, crowded premolars with well-developed posterior cingula on the p3 and p4, a metaconid crest on the m1, and a highly reduced m2. When compared to *N. vison*, the mandible is relatively deeper, the m1 is slightly broader, and the m2 is significantly more reduced yet still retains the small anteroposterior crest seen in *N. vison* (Bjork 1973). He hypothesized that *M. meltoni* was more derived and unlikely ancestral to *N. vison* due to the

significant reduction of the m2 (Bjork 1973). *M. meltoni* is the only known Pre-Pleistocene occurrence of a mink-like musteline in North America, with records of *N. vison* extending only as far back as the Irvingtonian (1.8 – 0.3 Ma) (Gidley and Gazin 1938; Paulson 1961; Hibbard 1963; Barnosky and Rasmussen 1988).

The results of this analysis predicted *M. meltoni* as a member of *Mustela*; however, only 45.9% of *Neogale* specimens were correctly classified to genus (Table #). The reason for the relatively lower eigenvalue of the *M. meltoni* genus analysis is primarily due to the fact that no upper tooth measurements were available for *M. meltoni*. The *N. vison* specimens were decidedly larger than *M. meltoni*, with minimal overlap in range sizes. The lower grinding surface area (LGA) of *M. meltoni* is especially smaller when compared to *N. vison*, supporting the m2 comparisons by Bjork (1973). However, neither mandibular depth (MD) nor m1 width for *M. meltoni* was larger compared to *N. vison*, thus conflicting with the descriptions of Bjork (1973).

Clade classification yielded *M. meltoni* being assigned to Clade #1 (*N. africana*, *N. felipei*, *N. frenata*, and *N. vison*). And since all members of Clade #1 comprise the New World genus *Neogale*, it is possible that *M. meltoni* may potentially deserve generic reassignment to *Neogale*. Nevertheless, a larger sample size containing additional measurements is ultimately necessary in order to more adequately understand *M. meltoni*. It is possible that, with more sample data, future studies may support classification within *Neogale*.

#### *GFS Musteline Analysis*

A left P4 and M1 consistent with the morphological characteristics of Mustelinae were recently recovered from the early Pliocene age (4.9 – 4.5 Ma) Gray Fossil Site (GFS) in northeastern Tennessee and is first documented here. This find represents the first reported pre-Pleistocene occurrence of a musteline in the eastern United States. The specimen appears distinct

from the well-known Miocene ischyriictine mustelid *Plionictis* but falls within the size range of *Mustela* and *Neogale*. The P4 is missing both the parastyle and protocone, with significant wear visible on the occlusal surface. The M1 is noticeably larger than that of *N. frenata* and has three roots. Moreover, the parastyle is pronounced, the metacone is small, and the talon is relatively deep (compared to *N. frenata*). Compared to *N. vison*, the M1 shows similar morphology; however, the anteroposterior constriction extends further lingually, and the parastyle appears slightly more pronounced with a more distinct cingulum.

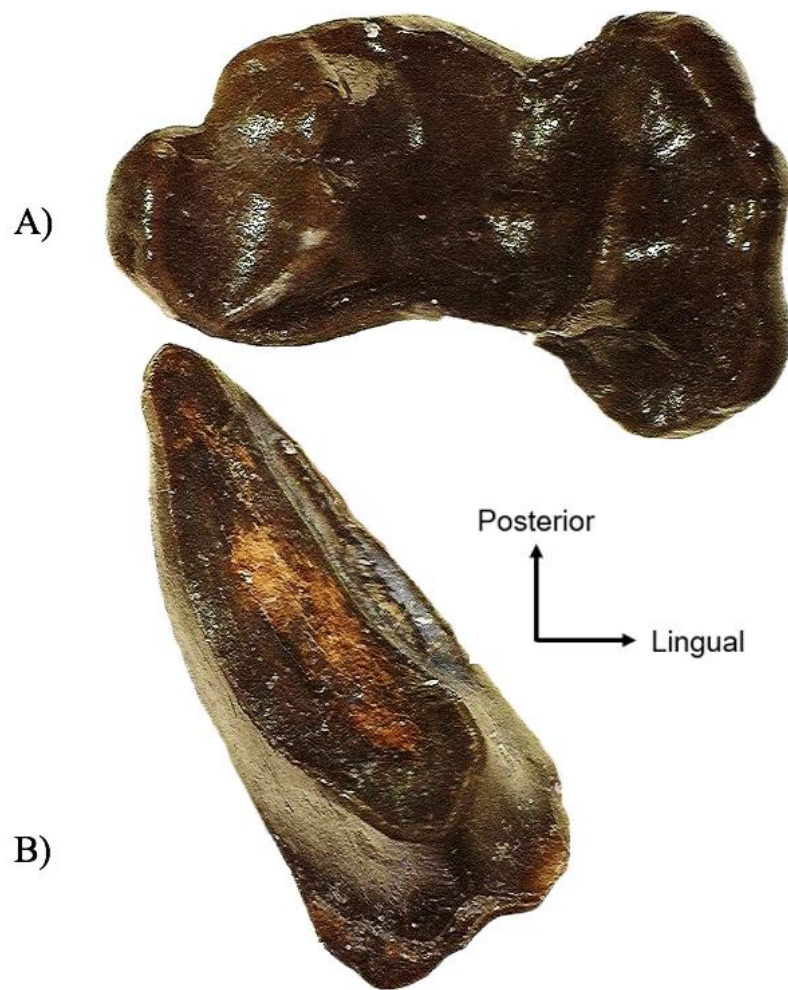


Figure 21. GFS musteline left M1 (ETMNH 22420) (A) and left P4 (ETMNH 22419) (B) in occlusal view.

These characteristics allow the hypothesis that this individual may have been more semi-aquatic in ecology similar to *N. vison*. This hypothesis is consistent with the paleoenvironment surrounding GFS during the Early Pliocene. Both fauna (e.g., *Pristinailurus*, *Tapirus*) and flora (e.g., *Caryra*, *Pinus*, *Quercus*) at GFS are characteristic of densely forested climates (Wallace and Wang 2004; Hulbert et al. 2009; Samuels et al. 2018). In addition, the occurrence of *Taxodium* and *Nyssa* leaves and pollen, as well as fauna indicative of aquatic environments (e.g., *Alligator*, *Ambystoma*, *Sternotherus*, *Trachemys*), suggest the presence of a perennial body of water (Wallace and Wang 2004; Boardman and Schubert 2011; Brandon 2013; Worobiec et al. 2013; Samuels et al. 2018). The absence of grassland-adapted taxa and the predominance of forest-adapted taxa suggest that GFS likely contrasts greatly with most of the continent where there was expansion of grassland environments through the late Miocene-early Pliocene (Wallace and Wang 2004; DeSantis and Wallace 2008).

Both DFA analyses for the GFS musteline support indication of a mink-like morphology. The genus analysis (eigenvalue = 0.404) classified the specimen as *Neogale*, with 53.2% of *Neogale* specimens being correctly classified. The clade analysis predicted the GFS musteline to most likely belong to Clade #4 (*M. erminea*) and predicted Clade #1 (*N. africana*, *N. felipei*, *N. frenata*, and *N. vison*) for the 2<sup>nd</sup> most likely clade. With Clade #4 likely originating from Eurasia, combined with the knowledge of fauna from GFS representing a unique combination of North American and Eurasian taxa, it is certainly possible that the GFS musteline descended from a Eurasian ancestor (Wallace and Wang 2004; Law et al. 2017). Although, it is worth noting that Clade #4 showed only 46.4% correct classification while Clade #1 showed 72.1% correct classification. A larger comparative sample is necessary in order to better understand the origin of the GFS musteline.

### *Extinct Pleistocene Taxa Analysis*

Two poorly known extinct Pleistocene musteline taxa, *M. gazini* and *M. jacksoni*, were included in the analysis for genus, species, and clade classification. The findings of this analysis raise the question of whether these are valid taxa or simply samples of extant species. Only two specimens of *M. gazini* have been described by Hibbard (1958) and Eshelman (1975) from Early Pleistocene sites of Idaho and Kansas respectively. The holotype, a left dentary bearing the p3 – m2, was distinguished from *N. frenata* by having a lesser transverse width of the heel of the p3 and p4, and a more centrally located principal cusp of the p3 and p4 (Hibbard 1958). The anterior portion of the p3 and p4 is also not as reduced as in recent mustelines (Hibbard 1958). In addition, Hibbard (1958) distinguished *M. gazini* from *M. rexroadensis* by its larger size, a more developed anterior base of the p3 and p4, and a more tightly closed m1 carnassial notch. However, Bjork (1970) noted that the discrepancy of the m1 carnassial notch between the *M. gazini* and *M. rexroadensis* holotypes is due to differential wear of the m1 of *M. rexroadensis*, thus resulting in the carnassial notch to appear more distinctly open. He subsequently noted that the *M. gazini* holotype is actually more typical of *M. rexroadensis* topotype material, thus leading it to be considered synonymous under *M. rexroadensis* (Bjork 1970; Eshelman 1975).

The results of this analysis seem to support the original descriptions by Hibbard (1958) of *M. gazini* being distinguishable from *M. rexroadensis*. The DF1 vs. DF2 species analysis scatterplot (Figure 17) shows *M. gazini* being clearly separated from *M. rexroadensis*. *M. gazini* showed highly positive scores for both DF1 and DF2 while *M. rexroadensis* exhibited slightly negative scores for both. This indicates that *M. gazini* can possibly be distinguished from *M. rexroadensis* based on measurements and ratios of the p4 and m1. The results suggest that *M.*

*gazini* does seem to have a relatively more robust dentary with a longer and wider p4 and m1, as noted by Hibbard (1958).

Only two specimens of *M. jacksoni*, a left dentary with the p3 – m1 and a right dentary with the p2 – m1, have been described from Fort Selkirk local fauna (Early Pleistocene, 1.55 – 1.6 Ma) of Yukon Territory, Canada (Storer 2004). Storer (2004) described *M. jacksoni* as being a small musteline similar to *M. nivalis*, but slightly larger in size. The most apparent features distinguishing it from *M. nivalis* are the premolars, which are more robust, higher-crowned, and more expanded and broader posteriorly (Storer 2004). The m1 is similar to that of *M. nivalis*, although the talonid is broader buccolingually with a better developed lingual basin and a more rounded posterior margin on the heel (Storer 2004). Storer (2004) suggested that *M. jacksoni* is likely not directly ancestral to *M. nivalis* due to the specialization in the degree of expansion of the lower premolars.

The results of this analysis show *M. jacksoni* exhibiting considerable overlap with *M. nivalis* (Figure 17), thus suggesting close affinity between the two species. *M. jacksoni* does appear to be larger than most specimens of *M. nivalis* used in this study; however, it did not fall outside of the size range of *M. nivalis*, contrary to the results of Storer (2004). Clade classification assigned *M. jacksoni* to #5 (most likely clade) and #4 (2<sup>nd</sup> most likely clade), suggesting that it is likely very closely related to *M. nivalis*, if not simply a larger-than-average specimen of *M. nivalis*. It may also be possible that *M. jacksoni* actually belongs to *M. praenivalis*, an ancestor of *M. nivalis* known from Early – Middle Pleistocene sites of Eurasia (Kurtén 1968). There seems to be a slight decrease in overall size and robustness throughout the gradual yet continuous succession of the *M. nivalis* lineage from the Early Pliocene to present day (Stach 1959; Kurtén 1968). Among the characters distinguishing *M. praenivalis* from *M.*

*nivalis*, Kormos (1934) described *M. praenivalis* as having a more robust mandible with larger, wider, and higher-crowned premolars and m1. The measurements for *M. jacksoni* fall within the size range of *M. praenivalis* measurements taken by Kormos (1934).

#### *Mustela* sp. Analysis

Two specimens classified as *Mustela* sp. aff. *rexroadensis* (IMNH 7559 and IMNH 12861) by Hearst (1999) from the Blancan-aged Birch Creek local fauna of Idaho were included in the analysis to examine the reliability of classification for specimens not previously given a complete taxonomic status. IMNH 7559 includes a right dentary with the p2 – m2 and IMNH 12861 includes a right dentary with the p4 – m2. The dentaries are described as being morphologically similar to *M. rexroadensis* with IMNH 7559 being approximately 28% larger than IMNH 12861 (Hearst 1999). IMNH 7559 appears to be very similar in size compared to *M. rexroadensis*, although IMNH 12861 was noted to be slightly smaller than the mandible of *M. rexroadensis* (Hibbard 1950; Bjork 1970; Hearst 1999).

The results of this analysis showed both specimens of *Mustela* sp., especially IMNH #7559, having close affinity to *M. rexroadensis* (Figure #). IMNH #12861 was likely not assigned to *M. rexroadensis* for neither 1<sup>st</sup> nor 2<sup>nd</sup> most likely species due its slightly smaller size compared to the *M. rexroadensis* specimens available. Despite this, the 2<sup>nd</sup> most likely species for IMNH #12861 was *N. frenata*, which has been observed to share significant morphological similarities with *M. rexroadensis* (Bjork 1970). Overall, the analysis indicated that the unclassified fossil *Mustela* sp aff. *rexroadensis* specimens can fairly reliably be assigned to genus, species, and clade, even with fragmentary remains and a small sample size of *M. rexroadensis*.

## CHAPTER 9. CONCLUSIONS

*Mustela* and *Neogale* can be difficult to distinguish osteologically due to similarities in skull and tooth morphology (Abramov 2000), with morphological synapomorphies between the two genera remaining unresolved. High degrees of sexual dimorphism and geographic variation within Mustelinae (King and Powell 2007) introduce additional obstacles for distinguishing among taxa. Several studies have examined phylogenetic and morphological relationships among mustelines (e.g., Anderson 1989; Abramov 2000; Heptner et al. 2001; Marmi et al. 2004; Sato et al. 2003; Harding and Smith 2009; Law et al. 2018); however, no study has aimed to distinguish all 18 extant taxa at genus-, species-, and clade-level using a combination of qualitative and quantitative analyses. Furthermore, no study has used such a large dataset that also includes extinct fossil musteline taxa for classification.

For this study, a combination of qualitative and quantitative analyses was conducted to maximize the potential for distinguishing *Mustela* and *Neogale* using skull and tooth characters. A primary goal was to examine for potential classification from not only a research setting with a large dataset, but especially from a paleontological setting where scarce and/or fragmentary fossil remains may limit the amount of collectable data. Both the character state analysis and DFA proved reliable in distinguishing *Mustela* from *Neogale* based on skull and tooth morphology. Additionally, the DFA further demonstrated reliable separation of species and clade. When utilized, measurements and ratios involving the P4, M1, and m1 contributed most to distinction. Overall, 91.3% of all extant specimens were correctly classified to genus, 89.9% were correctly classified to species, and 81.9% were correctly classified to clade.



This study indicates that *Mustela* and *Neogale* can fairly accurately be distinguished based on skull and tooth morphology, although a larger sample size of all *Neogale* species is necessary to more accurately identify potential morphological synapomorphies for the genus. On the other hand, clade analyses suggest that certain phylogenetic groups of species contained within *Mustela* are also in themselves morphologically distinct, thus raising the question of whether or not those groups deserve separate generic status. A larger sample size of poorly known taxa (e.g., *M. strigidorsa*) is necessary to aid in better understanding the morphological distinctions within *Mustela*. Additionally, greater consideration and assessment of geographic variation and sexual dimorphism in species, as well as what morphological differences among taxa may mean regarding their ecology, are important next steps to take when addressing future work surrounding this topic.

Since all extant musteline taxa can be distinguished morphologically, it is possible to reliably propose genus, species, and clade classification of fossil mustelines, even if the available material is scarce and/or fragmentary. It is important to understand, however, what the responsible level is to which fragmentary musteline remains should be identified. Based on results of the analyses of fossil taxa, identification to species-level from a paleontological perspective will likely yield the least informative results when compared to identification to genus or clade. And as previously mentioned, since the phylogenetic groups within *Mustela* are indeed morphologically distinct themselves, identification to clade may actually serve more useful than identification to genus when attempting to better understand the fossil remains of extinct mustelines.

## REFERENCES

- Abramov AV. A taxonomic review of the genus *Mustela* (Mammalia, Carnivora). *Zoosyst Ross.* 2000;8(2):357-364.
- Abramov AV, Baryshnikov GF. Geographic variation and intraspecific taxonomy of weasel *Mustela nivalis* (Carnivora, Mustelidae). *Zoosyst Ross.* 2000;8(2):365-402.
- Abramov AV, Tumanov, IL. Sexual dimorphism in the skull of the European mink *Mustela lutreola* from NW part of Russia. *Acta Theriol.* 2003;48(2):239-246.
- Abramov AV, Duckworth JW, Wang YX, Robertson SI. The stripe-backed weasel *Mustela strigidorsa*: Taxonomy, ecology, distribution and status. *Mamm Rev.* 2008;38(4):247-266.
- Abramov AV, Puzachenko AY. Spatial variation of sexual dimorphism in the Siberian weasel *Mustela sibirica* (Mustelidae, Carnivora). *Russ J Theriol.* 2009;8(1):17-28.
- Abramov AV, Puzachenko AY. Species co-existence and morphological divergence in west Siberian mustelids (Carnivora, Mustelidae). *Mamm Stud.* 2012;37: 255-259.
- Abramov AV, Meschersky IG, Aniskin VM, Rozhnov VV. The mountain weasel *Mustela kathiah* (Carnivora: Mustelidae): Molecular and karyological data. *Biol Bull.* 2013;40:52-60.
- Abramov AV, Puzachenko AY, Tumanov, IL. Morphological differentiation of the skull in two closely-related Mustelid species (Carnivora: Mustelidae). *Zool Stud.* 2016;55(1).
- Abramov AV, Puzachenko AY, Masuda R. Cranial variation in the Siberian weasel *Mustela sibirica* (Carnivora, Mustelidae) and its possible taxonomic implications. *Zool Stud.* 2018;57(14).
- Anderson E. Ferret of the Pleistocene of central Alaska. *J Mammal.* 1973;54(3):778-779.

- Anderson E. Pleistocene Mustelidae (Mammalia, Carnivora) from Fairbanks, Alaska. *Bull Mus Comp Zool.* 1977;148(1).
- Anderson E. The phylogeny of Mustelids and the systematics of ferrets. In: Seal US, editor. *Conservation biology and the black-footed ferret.* New Haven: Yale University Press; 1989. p. 10-20.
- Anderson E, Forrest SC, Clark TW, Richardson L. Paleobiology, biogeography, and systematics of the black-footed ferret, *Mustela nigripes* (Audubon and Bachman), 1851. *Great Basin Nat Mem.* 1986;8.
- Aulerich RJ, Swindler DR. The dentition of the mink (*Mustela vison*). *J Mammal.* 1968;49(3):488-494.
- Barnosky AD, Rasmussen DL. Middle Pleistocene arvicoline rodents and environmental change at 2900-meters elevation, Porcupine Cave, South Park, Colorado. *Ann Carnegie Mus.* 1988;57(12):267-292.
- Baryshnikov GF, Abramov AV. Structure of baculum (os penis) in Mustelidae (Mammalia, Carnivora), communication 1. *Russ J Zool.* 1997;76(12):1399-1410.
- Baryshnikov GF, Abramov AV, Bininda-Emonds ORP. Morphological variability and evolution of the baculum (os penis) in Mustelidae (Carnivora). *J Mammal.* 2003;84(2):673-690.
- Baryshnikov GF, Alekseeva EV. Late Pleistocene and Holocene *Mustela* remains (Carnivora Mustelidae) from Bliznets Cave in the Russian far east. *Russ J Theriol.* 2017;16(1):1-14.
- Baskin JA. Mustelidae. In: Janis CM, Scott KM, Jacobs LL, editors. *Evolution of tertiary mammals of North America.* Cambridge: Cambridge University Press; 1998. p. 152-173.
- Ben-David M. Seasonal diets of mink and marten: Effects of spatial and temporal changes in resource abundance [dissertation]. Fairbanks (AK): University of Alaska; 1996.

- Bjork PR. The Carnivora of the Hagerman local fauna (Late Pliocene) of Southwestern Idaho. Trans Am Philos Soc. 1970;60(7):3-54.
- Bjork PR. Additional Carnivores from the Rexroad Formation (Upper Pliocene) of Southwestern Kansas. Trans Kans Acad Sci. 1973;76(1):24-38.
- Boardman GS, Schubert BW. First Mio-Pliocene salamander fossil assemblage from the southern Appalachians. Palaeontol Electron. 2011;14(2).
- Brandon S. Discovery of bald cypress fossil leaves at the Gray Fossil Site, Tennessee and their ecological significance [thesis]. Johnson City (TN): East Tennessee State University; 2013.
- Brown JH, Lasiewski RC. Metabolism of weasels: The cost of being long and thin. Ecology. 1972;53(5):939-943.
- Bryant HN, Russell AP, Fitch WD. Phylogenetic relationships within the extant Mustelidae (Carnivora): Appraisal of the cladistic status of the Simpsonian subfamilies. Zool J Linn Soc. 1993;108:301-334.
- Butler PM. The evolution of carnassial dentition in the Mammalia. Proc Zool Soc Lond. 1946;116:198-220.
- Cserkés Z, Kiss C, Barkaszi Z, Görfö T, Zagorodniuk I, Sramkó G, Csorba G. Intra- and interspecific morphological variation in sympatric and allopatric populations of *Mustela putorius* and *M. eversmannii* (Carnivora: Mustelidae) and detection of potential hybrids. Mammal Res. 2020.
- Dalquest WW. Early Blancan mammals of the Beck Ranch local fauna of Texas. J Mammal. 1978;59(2):269-298.
- Davison A, Griffiths HI, Brookes RC, Maran T, Macdonald DW, Sidorovich VE, Kitchener AC,

- Irizar I, Villate I, González-Esteban, J, et al. Mitochondrial DNA and palaeontological evidence for the origins of endangered European mink, *Mustela lutreola*. *Anim Conserv.* 2000;4:345-355.
- Dayan T, Simberloff D, Tchernov E, Yom-Tov Y. Inter- and intraspecific character displacement in Mustelids. *Ecology.* 1989;70(5):1526-1539.
- Dayan T, Simberloff D. Character displacement, sexual dimorphism, and morphological variation among British and Irish Mustelids. *Ecology.* 1994;75(4):1063-1073.
- DeMarinis AM. Craniometric variability of polecat *Mustela putorius* L. 1758 from North-Central Italy. *Hystrix.* 1995;7(1-2):57-68.
- DeSantis LRG, Wallace SC. Ancient ecology and climate of the Gray Fossil Site. In: Schubert BW, Mead JI, editors. *Gray Fossil Site: 10 years of research.* Johnson City: Don Sundquist Center of Excellence in Paleontology, East Tennessee State University; 2011.
- Duckworth JW, Lee BPY-H, Meijaard E, Meiri S. The Malay Weasel *Mustela nudipes*: Distribution, natural history and a global conservation status review. *Small Carniv Conserv.* 2006;35:2–21.
- Eger JL. Patterns of geographic variation in the skull of the Nearctic Ermine (*Mustela erminea*). *Can J Zool.* 1990;68:1241-1249.
- Ellerman JR, Morrison-Scott TCS. *Checklist of Palaearctic and Indian Mammals (1758 to 1946).* London: British Museum (Natural History); 1951.
- Erlinge S. Feeding habits of the weasel *Mustela nivalis* in relation to prey abundance. *Oikos.* 1975;26(3):378-384.
- Erlinge S. Adaptive significance of sexual dimorphism in weasels. *Oikos.* 1979;33(2):233-245.
- Eshelman RE. Geology and paleontology of the early Pleistocene (late Blancan) White Rock

- fauna from north-central Kansas. *Papers Paleontol.* 1975;13:1-60.
- Fairley JS. A north-south cline in the size of the Irish stoat. *Proc R Ir Acad.* 1981;81:5-10.
- Finarelli JA. A total evidence phylogeny of the Arctoidea (Carnivora: Mammalia): Relationships among basal taxa. *J Mammal Evol.* 2008;15:231-259. doi: 10.1007/s10914-008-9074-x.
- Fox NS. Analysis of Snake Creek Burial Cave *Mustela* fossils using linear & landmark-based morphometrics: Implications for weasel classification & black-footed ferret conservation [thesis]. Johnson City (TN): East Tennessee State University; 2014.
- Fox NS, Wallace SC, Mead JI. Fossil *Mustela nigripes* from Snake Creek Burial Cave, Nevada, and implications for black-footed ferret paleoecology. *West N Am Nat.* 2017;77(2):137-151.
- Friscia AR, Van Valkenburgh B, Biknevicius AR. An ecomorphological analysis of extant small carnivorans. *J Zool.* 2007;272:82-100.
- Gazin CL. Upper Pliocene Mustelids from the Snake River Basin of Idaho. *J Mammal.* 1934;15(2):137-149.
- Getz LL. Middle Pleistocene carnivores from Southwestern Kansas. *J Mammal.* 1960;41(3):361-365.
- Gidley JW, Gazin CL. The Pleistocene vertebrate fauna from Cumberland Cave, Maryland. *United States Natl Mus.* 1938;171.
- Gittleman JL, editor. *Carnivore behavior, ecology, and evolution.* Ithaca: Cornell University Press; 1989.
- Gliwicz J. Sexual dimorphism in small Mustelids: Body diameter limitation. *Oikos.* 1988;53(3):411-414.
- Graham RW. Comment on "Skeleton of extinct North American Sea Mink (*Mustela macrodon*)"

- by Mead et al. *Quat Res.* 2001;56:419-421.
- Grassman Jr LI, Kreetiyutanont K, Tewes ME. The back-striped weasel *Mustela strigidorsa* gray, 1853 in northeastern Thailand. *Small Carniv Conserv.* 2002;26.
- Guilday JE. The Clark's Cave bone deposit and the late Pleistocene paleoecology of the central Appalachian Mountains of Virginia. *Bull Carnegie Mus Nat Hist.* 1977.
- Hall ER. Three new genera of Mustelidae from the Later Tertiary of North America. *J Mammal.* 1930;11(2):146-155.
- Hall ER. Mustelid mammals from the Pleistocene of North America, with systemic notes on some recent members of the genera *Mustela*, *Taxidea*, and *Mephitis*. *Carnegie Inst Wash.* 1936;473:41-119.
- Hall ER. *American weasels.* Lawrence: University of Kansas Publications; 1951.
- Hall ER. *The mammals of North America.* New York: Wiley; 1981.
- Harding LE, Smith FA. *Mustela* or *Vison*? Evidence for the taxonomic status of the American mink and a distinct biogeographic radiation of American weasels. *Mol Phylogenet Evol.* 2009;52.
- Harris AH. A Late-Pleistocene occurrence of ermine (*Mustela erminea*) in Southeastern New Mexico. *Southwest Nat.* 1993a;38(3):279-280.
- Harris AH. Quaternary vertebrates of New Mexico. *Vertebr Paleontol New Mex, New Mex Mus Nat Hist.* 1993b;2:179-197.
- Hassanin A, Veron G, Ropiquet A, Jansen van Vuuren B, Lécuyer A, Goodman SM, Haider J, Nguyen TT. Evolutionary history of Carnivora (Mammalia, Laurasiatheria) inferred from mitochondrial genomes. *PLoS ONE*, 2021;16(2). doi: 10.1371/journal.pone.0240770.
- Hearst JM. The mammalian paleontology and depositional environments of the Birch Creek

- Local Fauna (Pliocene: Blancan), Owyhee County, Idaho [dissertation]. Lawrence (KS): University of Kansas; 1999.
- Heptner VG, Naumov NP, Yurgenson PB, Sludskii AA, Chirkova AF, Bannikov AG. Mammals of the Soviet Union: Carnivora (weasels; additional species). Janpath: Amerind Publishing Co. Pvt. Ltd.; 2002. Vols. 2-1b.
- Hibbard CW. Mammals of the Rexroad Formation from Fox Canyon, Kansas. *Mus Paleontol, Univers Mich.* 1950;8(6):113-192.
- Hibbard CW. A contribution to the Rexroad fauna. *Trans Kans Acad Sci.* 1952;55(2):196-208.
- Hibbard CW. Second contribution to the Rexroad fauna. *Trans Kans Acad Sci.* 1954;57(2):221-237.
- Hibbard CW. A new weasel from the Lower Pleistocene of Idaho. *J Mammal.* 1958;39(2):245-246.
- Hibbard CW. A late Illinoian fauna from Kansas and its climatic significance. *Papers Mich Acad Sci Art Let.* 1963;48:187-221.
- Hillman CN, Clark TW. *Mustela nigripes*. *Mamm Species.* 1980;126:1-3.
- Hollister N. A synopsis of the American minks. *United States Natl Mus.* 1955;44:471-480.
- Holmes T. Sexual dimorphism in North American weasels with a phylogeny of the Mustelidae [dissertation]. Lawrence, KS: University of Kansas; 1988.
- Hosoda T, Suzuki H, Harada M, Tsuchiya K, Han SH, Zhang Y, Kryukov AP, Lin LK. Evolutionary trends of the mitochondrial lineage differentiation in species of genera *Martes* and *Mustela*. *Genes Genet Syst.* 2000;15(5):259-267. doi: 10.1266/ggs.75.259.
- Hulbert RC, Wallace SC, Klippel WE, Parmalee PW. Cranial morphology and systematics of an extraordinary sample of the late Neogene dwarf tapir, *Tapirus Polkensis* (Olsen). *J*



- Paleont. 2009;83(2), 238-262.
- Humphrey SR, Setzer HW. Geographic variation and taxonomic revision of mink (*Mustela vison*) in Florida. J Mammal. 1989;70(2):241-252.
- Hutchinson GE. Homage to Santa Rosalia or why are there so many kinds of animals? Am Nat. 1959;93(870):145-159.
- Izor RJ, de la Torre L. A new species of weasel (*Mustela*) from the Highlands of Colombia, with comments on the evolution and distribution of South American weasels. J Mammal. 1978;59(1):92-102.
- Izor RJ, Peterson NE. Notes on South American weasels. J Mammal. 1985;66(4):788-790.
- Jiangzuo Q, Gimranov D, Liu J, Liu S, Jin C, Liu J. A new fossil marten from Jinyuan Cave, northeastern China reveals the origin of the Holarctic marten group. Quat Int. 2020.
- Jung TS, Rivest G, Blakeburn DA, Hamm E R, van Eyk A, Kukka PM, Robitaille J. Dental anomalies suggest an evolutionary trend in the dentition of wolverine (*Gulo gulo*). Mamm Res. 2016;61:361-366.
- King CM, editor. Biology of Mustelids: Some Soviet Research. New Zealand: Department of Scientific and Industrial Research; 1980. Vol. 2.
- King CM. *Mustela erminea*. Mamm Species. 1983;195:1-8.
- King CM. The advantages and disadvantages of small size to weasels, *Mustela* species. In: Gittleman J, editor. Carnivore behavior, ecology & evolution. Ithaca: Cornell University Press; 1989. p. 302-334.
- King CM, Powell RA. The Natural history of weasels and stoats: Ecology, behavior, and management. 2nd ed. New York: Oxford University Press; 2007.
- Koepfli K, Wayne RK. Phylogenetic relationships of otters (Carnivora Mustelidae) based on

- mitochondrial cytochrome *b* sequences. *J Zool.* 1998;246(4):401-416.
- Koepfli K, Wayne RK. Type-I STS markers are more informative than cytochrome *b* in phylogenetic reconstruction of the Mustelidae (Mammalia: Carnivora). *Syst Biol.* 2003;52(5):571-593.
- Koepfli, K, Deere KA, Slater GJ, Begg C, Bett K, Grassman L, Lucherini M, Veron G, Wayne RK. Multigene phylogeny of the Mustelidae: Resolving relationships tempo and biogeographic history of a mammalian adaptive radiation. *BMC Biol.* 2008;6(10).
- Korablev MP, Korablev NP, Korablev PN. Population aspects of sexual dimorphism in Mustelidae from the example of four species (*Mustela lutreola*, *Neovison vison*, *Mustela putorius*, and *Martes martes*). *Biol Bull.* 2013;40(1):61-69.
- Kormos T. Neue und wenig bekannte Musteliden aus dem ungarischen Oberpliozan. *Folia Hydrobiol.* 1934;5:129-158.
- Korpimäki E, Norrdahl K, Rinta-Jaskari T. Responses of stoats and least weasels to fluctuating food abundances: Is the low phase of the vole cycle due to Mustelid predation? *Oecologia.* 1991;88(4):552-561.
- Kurose, N., Abramov, A. V., & Masuda, R. (2008). Molecular phylogeny and taxonomy of the genus *Mustela* (Mustelidae, Carnivora), inferred from mitochondrial DNA sequences: New perspectives on phylogenetic status of the back-striped weasel and American mink. *Mamm Stud.* 2008;33:25-33.
- Kurtén B. Pleistocene Mammals of Europe. London: Weidenfeld & Nicolson; 1968.
- Kurtén B, Anderson E. Pleistocene mammals of North America. New York: Columbia University Press; 1980.
- Larivière S. *Mustela vison*. *Mamm Species.* 1999;608:1-9.

- Law CJ. *Mustela sibirica* (Carnivora: Mustelidae). *Mamm Species*. 2018;50(966):109-118.
- Law CJ, Slater GJ, Mehta RS. Lineage diversity and size disparity in Musteloidea: Testing patterns of adaptive radiation using molecular and fossil-based methods. *Syst Biol*. 2018;1-18.
- Law CJ, Duran E, Hung N, Richards E, Santillan I, Mehta RS. Effects of diet on cranial morphology and biting ability in musteloid mammals. *J Evol Biol*. 2018.
- Lee S, Mill PJ. Cranial variation in British Mustelids. *J Morphol*. 2004;260:57-64.
- Linn I, Birks JDS. Mink (Mammalia; Carnivora; Mustelidae): Correction of a widely quoted error. *Mamm Rev*. 1989;19(4):175-179.
- Lunde DP, Musser GG. A recently discovered specimen of Indonesian Mountain Weasel (*Mustela lutreolina* Robinson & Thomas 1917) from Sumatra. *Small Carniv Conserv*. 2003;28:23-25.
- Macdonald DW, Newman C, Harrington LA. *Biology and conservation of Musteloids*. Oxford: Oxford University Press; 2018. doi:10.1093/oso/9780198759805.001.0001.
- MacPherson AH. The origin of diversity in mammals of the Canadian Arctic Tundra. *Syst Zool*. 1965;14(3):153-173.
- Madar SI, Rose MD, Kelley J, MacLatchy L, Pilbeam D. New *Sivapithecus* postcranial specimens from the Siwaliks of Pakistan. *J Hum Evol*. 2002;42:705-752.
- Manville RH. The extinct sea mink with taxonomic notes. *Proc Unites States Natl Mus*. 1966;122(3584).
- Maran T, Kruuk H, Macdonald DW, Polma M. Diet of two species of mink in Estonia: Displacement of *Mustela lutreola* by *M. vison*. *J Zool Lond*. 1998;245:218-222.
- Marciszak A, Socha P. Stoat *Mustela erminea* Linnaeus, 1758 and weasel *Mustela nivalis*

- Linnaeus, 1766 in palaeoecological analysis: A case study of Bišnik Cave. *Quat Int.* 2014;258-265.
- Marmi J, López-Giráldez JF, Domingo-Roura X. Phylogeny, evolutionary history and taxonomy of Mustelidae based on sequences of the cytochrome *b* gene and a complex repetitive flanking region. *Zool Scr*, 2004;33(6):481-499.
- Martin RA. Description of a new genus of weasel from the Pleistocene of South Dakota. *J Mammal.* 1973;54(4):924-929.
- McDonald RA, Webbon C, Harris S. The diet of stoats (*Mustela erminea*) and weasels (*Mustela nivalis*) in Great Britain. *J Zool Lond.* 2000;252:363-371.
- McNab BK. On the ecological significance of Bergmann's Rule. *Ecology*, 1971;52(5):845-854.
- Mead EM, Mead JI. Snake Creek Burial Cave and a review of the Quaternary mustelids of the Great Basin. *Great Basin Nat.* 1989;49(2):143-154.
- Mead JI, Spiess AE, Sobolik KD. Skeleton of extinct North American sea mink (*Mustela macrodon*). *Quat Res.* 2000;53:247-262.
- Mead JI, Spiess AE. Reply to Russell Graham about *Mustela macrodon*. *Quat Res.* 2001;56:422-423.
- Meiri S, Duckworth JW, Meijaard E. Biogeography of Indonesian mountain weasel *Mustela lutreolina* and a newly discovered specimen. *Small Carniv Conserv.* 2007;37.
- Merriam CH. North American fauna: Synopsis of the weasels of North America. 11th ed. Washington, DC: U. S. Department of Agriculture; 1896.
- Moors PJ. Sexual dimorphism in the body size of Mustelids (Carnivora): The roles of food habits and breeding systems. *Oikos*, 1980;34(2):147-158.
- Morgan, J. K., & Morgan, N. H. (1995). A new species of *Capromeryx* (Mammalia:

- Artiodactyla) from the Taunton Local Fauna of Washington, and the correlation with other Blancan faunas of Washington and Idaho. *J Vertebr Paleontol.* 1995;15(1):160-170.
- Nowak RM. *Walker's Carnivores of the World*. Baltimore: John Hopkins University Press; 2005.
- Oliveira do Nascimento F. On the correct name for some subfamilies of Mustelidae (Mammalia, Carnivora). *Pap Avulsos Zool.* 2014;54(21):307-313.
- Owen PR, Bell CJ, Mead EM. Fossils, diet, and conservation of black-footed ferrets (*Mustela nigripes*). *J Mammal.* 2000;81(2):422-433.
- Park AW, Nowosielski-Slepowron JA. Aspects of skull and dentition morphology of the mink (*Mustela vison*). *Acta Morphol Neerl Scand.* 1980;18(1):47-65.
- Paterson R, Samuels JX, Rybczynski N, Ryan MJ, Maddin HC. The earliest mustelid in North America. *Zool J Linn Soc.* 2020;188:1318-1339.
- Patterson BD, Ramírez Chavez HE, Vilela JF, Soares AER, Grewe F. On the nomenclature of the American clade of weasels (Carnivora: Mustelidae). *J Anim Divers.* 2021;3(2).
- Paulson, G. R. (1961). The mammals of the Cudahy Fauna. *Papers Mich Acad Sci Art Let.* 1961;46:127-153.
- Pavlinov IY, Borisenko AV, Kruskop SV, Yakhontov EL. Mlekopitayushchie Evrazii. II. Non Rodentia: sistematiko-geograficheskii spravochnik [Mammals of Eurasia. II. Non-Rodentia: systematic and geographic reference book]. *Arch Zool Mus Mosc St Univers.* 1995;33.
- Powell RA. Mustelid spacing patterns: Variations on a theme by *Mustela*. *Z Tierpsychol.* 1976;50(2):153-165.
- Powell RA, King CM. Variation in body size, sexual dimorphism and age-specific survival in stoats, *Mustela erminea* (Mammalia: Carnivora), with fluctuating food supplies. *Biol J*

- Linn Soc. 1997;62:165-194.
- Prentiss DW. Description of an extinct mink from the shell-heaps of the Maine Coast. United States Natl Mus. 1903;26(1336):887-888.
- Puzachenko AY, Masuda R, Abramov AV. Sexual dimorphism of craniological characters in the Altai weasel *Mustela altaica* (Carnivora, Mustelidae). Russ J Theriol. 2019;18(1):12-19.
- Ralls K, Harvey PH. Geographic variation in size and sexual dimorphism of North American weasels. Biol J Linn Soc. 1985;25:119-167.
- Ramírez-Chaves HE, Patterson BD. *Mustela felipei* (Carnivora: Mustelidae). Mamm Species. 2014;46(906), 11-15.
- Ramírez-Chaves HE, Arango-Guerra HL, Patterson BD. *Mustela africana* (Carnivora: Mustelidae). Mamm Species. 2014;46(917):110-115.
- Randinsky LB. Evolution of skull shape in carnivores. 3. The origin and early radiation of the modern carnivore families. Paleobiology. 1982;8(3):177-195.
- Rasband WS. ImageJ. Bethesda (MD): U. S. National Institutes of Health; 1997-2018.  
<https://imagej.nih.gov/ij/>.
- Reig S. Geographic variation in Pine Marten (*Martes martes*) and Beech Marten (*M. foina*) in Europe. J Mammal. 1992;73(4):744-769.
- Reig S. Biogeographic and evolutionary implications of size variation in North American least weasels (*Mustela nivalis*). Can J Zool. 1997;75:2036-2049.
- Retallack GJ. Cenozoic paleoclimate on land in North America. J Geol. 2007;115:271-294.
- Robinson HC, Thomas O. A new mink-like *Mustela* from Java. Ann Mag Nat Hist. 1917;20(117):261-262.
- Robles JM, Alba DM, Moyà-Solà S. The morphology of the upper fourth premolar in

- Trocharion albanense* Major, 1903 (Mustelidae: Leptarctinae) and the independent loss of the carnassial notch in leparctines and other mustelids. *Paleolusitana*. 2009;1:403-409.
- Rosenzweig ML. Community structure in sympatric Carnivora. *J Mammal*. 1966;47(4):602-612.
- Rosenzweig ML. The strategy of body size in Mammalian Carnivores. *Am Midl Nat*. 1968;80(2):299-315.
- Reumer JWF. Een bruikbaar onderscheid tussen deschedels van de wezel (*Mustela nivalis*) in de hermelijn (*Mustela erminea*). *Dieren*. 1988;5:106-108.
- Ruiz-Olmo J, Palazon S. Occurrence of the European mink (*Mustela lutreola*) in Catalonia. *Misc Zool*. 1990;14:249-253.
- Samuels JX, Hopkins Samantha SB. The impacts of Cenozoic climate and habitat changes on small mammal diversity in North America. *Glob Planet Change*. 2017;149:36-52. doi: 10.1016/j.gloplacha.2016.12.014.
- Samuels JX, Bredehoeft KE, Wallace SC. A new species of *Gulo* from the Early Pliocene Gray Fossil Site (Eastern United States); Rethinking the evolution of wolverines. *PeerJ*. 2018. doi: 10.7717/peerj.4648.
- Sandell M. Ecological energetics, optimal body size and sexual size dimorphism: A model applied to the stoat, *Mustela erminea* L. *Funct Ecol*. 1989;3(3):315-324.
- Sato JJ, Hosoda T, Wolsan M, Tsuchiya K, Yamamoto M, Suzuki H. Phylogenetic relationships and divergence times among Mustelids (Mammalia: Carnivora) based on nucleotide sequences of the nuclear interphotoreceptor retinoid binding protein and mitochondrial cytochrome *b* genes. *Zool Sci*. 2003;20:243-264.
- Sato JJ, Wolsan M, Minami S, Hosoda T, Sinaga MH, Hiyama K, Yamaguchi Y, Suzuki H. Deciphering and dating the red panda's ancestry and early adaptive radiation of

- Musteloidea. Mol Phylogenet Evol. 2009;53(3):907-922.
- Sato JJ, Wolsan M, Prevosti FJ, D'Elia G, Begg C, Begg K, Hosoda T, Campbell KL, Suzuki H. Evolutionary and biogeographic history of weasel-like carnivorans (Musteloidea). Mol Phylogenet Evol. 2012;63:745-757.
- Schmidt K. Skull variability of *Mustela nivalis* Linnaeus, 1766 in Poland. Acta Theriol. 1992;37(1-2):141-162.
- Sealfon RA. Dental divergence supports species status of the extinct sea mink (Carnivora: Mustelidae: *Neovison macrodon*). J Mammal. 2007;88(2):371-383.
- Sheffield SR, King CM. *Mustela nivalis*. Mamm Species. 1994;454:1-10.
- Sheffield SR, Thomas HH. *Mustela frenata*. Mamm Species. 1997;570:1-9.
- Simpson, GG. The principles of classification and a classification of mammals. Bull Am Mus Nat Hist. 1945;85:1-350.
- St-Pierre C, Ouellet J, Dufresne F, Chaput-Bardy A, Hubert F. Morphological and molecular discrimination of *Mustela erminea* (Ermines) and *M. frenata* (Long-tailed Weasels) in Eastern Canada. Northeast Nat. 2006;13(2):143-152.
- Stach J. On some Mustelinae from the Pliocene bone Breccia of Węże. Acta Palaeontol Pol. 1959;4(2):101-120.
- Stevens RT, Kennedy ML. Spatial patterns of sexual dimorphism in minks (*Mustela vison*). Am Midl Nat. 2005;142:207-216.
- Storer JE. A new species of *Mustela* (Mammalia; Carnivora; Mustelidae) from the Fort Selkirk fauna (Early Pleistocene) of Yukon Territory, Canada. Paludicola. 2004;4(4):151-155.
- Strömberg CAE. Evolution of grasses and grassland ecosystems. Annu Rev Earth Planet Sci. 2011;39:517-544.



- Suzuki S, Abe M, Motokawa M. Allometric comparison of skulls from two closely related weasels, *Mustela itatsi* and *M. sibirica*. *Zool Sci.* 2011;28:676-688.
- Suzuki S, Abe M, Motokawa M. Integrative study on static skull variation in the Japanese weasel (Carnivora: Mustelidae). *J Zool.* 2012. doi:10.1111/j.1469-7998.2012.00924.x.
- Suzuki S, Matsumoto M. Geographic skull variation of the Japanese weasel, *Mustela itatsi* in islands adjacent to southern Kyushu. *Mamm Stud.* 2020;45(1):27-39.
- Tedford RH, Albright III LB, Barnosky AD, Ferrusquia-Villafranca I, Hunt Jr RM, Storer JE, Swisher III CC, Voorhies MR, Webb SD, Whistler DP. Mammalian biochronology of the Arikarean through Hemphillian interval (late Oligocene through early Pliocene epochs). In: Woodburne MO, editor. *Late Cretaceous and Cenozoic mammals of North America: Biostratigraphy and geochronology.* New York: Columbia University Press; 1987.
- The NOW Community. *New and Old Worlds Database of Fossil Mammals (NOW)*. Licensed under CC BY 4.0. 2021. doi: 10.5281/zenodo.4268068.
- Thom MD, Harrington LA, Macdonald DW. Why are American mink sexually dimorphic? A role for niche separation. *Oikos.* 2004;105:235-252.
- van Bree PH, Boeadi MS. Notes on the Indonesian mountain weasel, *Mustela lutreolina* Robinson and Thomas, 1917. *Z. Säugetierkd.* 1978;43:166-171.
- van Zyll de Jong CG. A morphometric analysis of cranial variation in Holarctic weasels (*Mustela nivalis*). *Z. Säugetierkd.* 1932;57:77-93.
- Voorhies MR. Vertebrate biostratigraphy of the Ogallala Group in Nebraska. In: Gustavson TC, editor. *Geologic Framework and Regional Hydrology: Upper Cenozoic Blackwater Draw and Ogallala Formations, Great Plains.* Austin: The University of Texas at Austin, Bureau of Economic Geology; 1990.

- Wallace SC, Wang X. Two new carnivores from an unusual late Tertiary forest biota in eastern North America. *Nature*. 2004;431:556-559.
- Waters JH, Ray CE. Former range of the sea mink. *J Mammal*. 1961;42(3):380-383.
- Waters JH, Mack CW. Second find of sea mink in Southeastern Massachusetts. *J Mammal*. 1962;43(3):429-430.
- Williamson M. The analysis of biological populations. London: Edward Arnold; 1972.
- Wolsan M. Ancestral characters in the dentition of the weasel *Mustela nivalis* L. (Carnivora, Mustelidae). *Ann Zool Fennici*. 1983;20:47-51.
- Wolsan M. Phylogeny and classification of early European *Mustelida* (Mammalia: Carnivora). *Acta Theriol*. 1993;38(4):345-384.
- Worobiec E, Liu Y, Zavada MS. Palaeoenvironment of late Neogene lacustrine sediments at the Gray Fossil Site, Tennessee, USA. *Ann Soc Geol Pol*. 2013;83:51-63.
- Wozencraft WC. Carnivora. In: Wilson DE, Reeder DM, editors. *Mammal species of the world: A taxonomic and geographic reference*. Baltimore: John Hopkins University Press; 2005.
- Youngman PM. Distribution and systematics of the European mink *Mustela lutreola* Linnaeus 1791. *Acta Zool Fenn*. 1982;166:1-48.
- Youngman PM. *Mustela lutreola*. *Mamm Species*. 1990;362:1-3.
- Zub K, Sonnichsen L, Szafranska PA. Habitat requirements of weasels *Mustela nivalis* constrain their impact on prey populations in complex ecosystems of the temperate zone. *Oecologia*, 2008;175:571-582.

APPENDIX: Examined Specimens of *Mustela* and *Neogale* Utilized in the Analyses

| <b>Museum</b> | <b>Catalog #</b> | <b>Species</b>            | <b>Sex</b> | <b>Location</b>       |
|---------------|------------------|---------------------------|------------|-----------------------|
| USNM          | 255119           | <i>Neogale africana</i>   | M          | Peru                  |
| AMNH          | 37475            | <i>Neogale africana</i>   | M          | Brazil                |
| USNM          | 62110            | <i>Mustela altaica</i>    | M          | China                 |
| USNM          | 270534           | <i>Mustela altaica</i>    | M          | China                 |
| USNM          | 270608           | <i>Mustela altaica</i>    | F          | China                 |
| USNM          | 198473           | <i>Mustela altaica</i>    | F          | India                 |
| USNM          | 84059            | <i>Mustela altaica</i>    | F          | India                 |
| USNM          | 84058            | <i>Mustela altaica</i>    | F          | India                 |
| USNM          | 198476           | <i>Mustela altaica</i>    | M          | India                 |
| USNM          | 198475           | <i>Mustela altaica</i>    | M          | India                 |
| USNM          | 198477           | <i>Mustela altaica</i>    | M          | India                 |
| USNM          | 198478           | <i>Mustela altaica</i>    | M          | India                 |
| USNM          | 198479           | <i>Mustela altaica</i>    | M          | India                 |
| USNM          | 176034           | <i>Mustela altaica</i>    | F          | Pakistan              |
| USNM          | 176035           | <i>Mustela altaica</i>    | F          | Pakistan              |
| USNM          | 176037           | <i>Mustela altaica</i>    | M          | Pakistan              |
| USNM          | 354421           | <i>Mustela altaica</i>    | M          | Pakistan              |
| USNM          | 354422           | <i>Mustela altaica</i>    | M          | Pakistan              |
| ZIN           | 37923            | <i>Mustela altaica</i>    |            | Bliznets Cave, Russia |
| USNM          | 155161           | <i>Mustela eversmanii</i> | M          | China                 |
| USNM          | 240710           | <i>Mustela eversmanii</i> | M          | China                 |
| USNM          | 240709           | <i>Mustela eversmanii</i> | F          | China                 |
| USNM          | A22192           | <i>Mustela eversmanii</i> |            | Russia                |
| USNM          | 259792           | <i>Mustela eversmanii</i> |            |                       |
| USNM          | 188448           | <i>Mustela eversmanii</i> | F          | Russia                |
| USNM          | 188449           | <i>Mustela eversmanii</i> | M          | Russia                |
| USNM          | 269134           | <i>Mustela eversmanii</i> |            |                       |
| USNM          | 001452/A38365    | <i>Mustela eversmanii</i> |            | Russia                |
| ZIN           | 37928-11         | <i>Mustela eversmanii</i> |            | Bliznets Cave, Russia |
| ZIN           | 37928-30         | <i>Mustela eversmanii</i> |            | Bliznets Cave, Russia |
| USNM          | 188444           | <i>Mustela kathiah</i>    |            | India                 |
| USNM          | 254587           | <i>Mustela kathiah</i>    | F          | China                 |
| USNM          | 258180           | <i>Mustela kathiah</i>    | M          | China                 |

|      |               |                           |   |           |
|------|---------------|---------------------------|---|-----------|
| USNM | 254411        | <i>Mustela kathiah</i>    |   | China     |
| UMMZ | 112553        | <i>Mustela kathiah</i>    | M | India     |
| USNM | 007772/A38466 | <i>Mustela lutreola</i>   |   | Russia    |
| NMC  | 27534         | <i>Mustela lutreola</i>   | M | Russia    |
| SZM  | 6878          | <i>Mustela lutreola</i>   | M | Russia    |
|      | 89060001      | <i>Mustela lutreola</i>   |   | Spain     |
| BZM  | 1.9.36        | <i>Mustela lutreolina</i> | M | Indonesia |
| RMNH |               | <i>Mustela lutreolina</i> |   | Indonesia |
| USNM | 301102        | <i>Mustela nudipes</i>    |   | Malaysia  |
| USNM | 489386        | <i>Mustela nudipes</i>    | M | Malaysia  |
| USNM | 489385        | <i>Mustela nudipes</i>    | M | Malaysia  |
| USNM | 267386        | <i>Mustela nudipes</i>    | M | Indonesia |
| USNM | 151878        | <i>Mustela nudipes</i>    | M | Indonesia |
| USNM | 277283        | <i>Mustela subpalmata</i> | M | Egypt     |
| USNM | 277262        | <i>Mustela subpalmata</i> | F | Egypt     |
| USNM | 277284        | <i>Mustela subpalmata</i> | F | Egypt     |
| USNM | 283266        | <i>Mustela subpalmata</i> | F | Egypt     |
| USNM | 283267        | <i>Mustela subpalmata</i> | F | Egypt     |
| USNM | 283268        | <i>Mustela subpalmata</i> | F | Egypt     |
| USNM | 317100        | <i>Mustela subpalmata</i> | M | Egypt     |
| USNM | 317099        | <i>Mustela subpalmata</i> | M | Egypt     |
| USNM | 317098        | <i>Mustela subpalmata</i> | M | Egypt     |
| USNM | 317097        | <i>Mustela subpalmata</i> | M | Egypt     |
| USNM | 317095        | <i>Mustela subpalmata</i> | F | Egypt     |
| USNM | 317096        | <i>Mustela subpalmata</i> | M | Egypt     |
| USNM | 300294        | <i>Mustela subpalmata</i> |   | Egypt     |
| USNM | 300293        | <i>Mustela subpalmata</i> |   | Egypt     |
| USNM | 317101        | <i>Mustela subpalmata</i> | M | Egypt     |
| USNM | 317102        | <i>Mustela subpalmata</i> | M | Egypt     |
| USNM | 317103        | <i>Mustela subpalmata</i> | M | Egypt     |
| USNM | 317106        | <i>Mustela subpalmata</i> | F | Egypt     |
| USNM | 350094        | <i>Mustela subpalmata</i> | M | Egypt     |
| USNM | 140895        | <i>Mustela itatsi</i>     | M | Japan     |
| USNM | 140892        | <i>Mustela itatsi</i>     | M | Japan     |
| USNM | 01384/A20942  | <i>Mustela itatsi</i>     | M | Japan     |
| USNM | 140890        | <i>Mustela itatsi</i>     | M | Japan     |
| USNM | 140893        | <i>Mustela itatsi</i>     | M | Japan     |

|      |               |                            |   |                       |
|------|---------------|----------------------------|---|-----------------------|
| USNM | 140894        | <i>Mustela itatsi</i>      | F | Japan                 |
| USNM | 140897        | <i>Mustela itatsi</i>      | M | Japan                 |
| USNM | 140896        | <i>Mustela itatsi</i>      | M | Japan                 |
| USNM | 140898        | <i>Mustela itatsi</i>      | M | Japan                 |
| USNM | 140899        | <i>Mustela itatsi</i>      | M | Japan                 |
| USNM | 140900        | <i>Mustela itatsi</i>      | M | Japan                 |
| USNM | 140902        | <i>Mustela itatsi</i>      | F | Japan                 |
| USNM | 140911        | <i>Mustela itatsi</i>      | M | Japan                 |
| USNM | 140904        | <i>Mustela itatsi</i>      | M | Japan                 |
| USNM | 140908        | <i>Mustela itatsi</i>      | M | Japan                 |
| USNM | 140905        | <i>Mustela itatsi</i>      | M | Japan                 |
| USNM | 140906        | <i>Mustela itatsi</i>      | M | Japan                 |
| USNM | 155114        | <i>Mustela sibirica</i>    | M | China                 |
| USNM | 155113        | <i>Mustela sibirica</i>    | M | China                 |
| USNM | 172537        | <i>Mustela sibirica</i>    | F | China                 |
| USNM | 172536        | <i>Mustela sibirica</i>    | F | China                 |
| USNM | 173320        | <i>Mustela sibirica</i>    | M | India                 |
| USNM | 173319        | <i>Mustela sibirica</i>    | F | India                 |
| USNM | 020400/A37532 | <i>Mustela sibirica</i>    | M | India                 |
| USNM | 173322        | <i>Mustela sibirica</i>    | M | India                 |
| USNM | 173318        | <i>Mustela sibirica</i>    | M | India                 |
| USNM | 00145/A37848  | <i>Mustela sibirica</i>    |   | Russia                |
| USNM | 270532        | <i>Mustela sibirica</i>    | M | China                 |
| USNM | 270533        | <i>Mustela sibirica</i>    | M | China                 |
| USNM | 270607        | <i>Mustela sibirica</i>    | F | China                 |
| USNM | 298999        | <i>Mustela sibirica</i>    | F | Korea                 |
| USNM | 333165        | <i>Mustela sibirica</i>    | M | Taiwan                |
| USNM | 333164        | <i>Mustela sibirica</i>    | M | Taiwan                |
| USNM | 333163        | <i>Mustela sibirica</i>    | F | Taiwan                |
| ZIN  | 38049         | <i>Mustela sibirica</i>    |   | Bliznets Cave, Russia |
| ZIN  | 37924-3       | <i>Mustela sibirica</i>    |   | Bliznets Cave, Russia |
| ZIN  | 37924-7       | <i>Mustela sibirica</i>    |   | Bliznets Cave, Russia |
| ZIN  | 37924-2       | <i>Mustela sibirica</i>    |   | Bliznets Cave, Russia |
| ZIN  | 37928-13      | <i>Mustela sibirica</i>    |   | Bliznets Cave, Russia |
| KIZ  | 760256        | <i>Mustela strigidorsa</i> |   | China                 |
| USNM | 548396        | <i>Neogale felipei</i>     | M | Ecuador               |
| USNM | 545050        | <i>Neogale felipei</i>     |   | Ecuador               |

|      |               |                         |   |                  |
|------|---------------|-------------------------|---|------------------|
| USNM | 319222        | <i>Mustela putorius</i> | M | Italy            |
| USNM | 152675        | <i>Mustela putorius</i> | M | Italy            |
| USNM | 348113        | <i>Mustela putorius</i> | M | Netherlands      |
| USNM | 115213        | <i>Mustela putorius</i> | M | Switzerland      |
| USNM | 152668        | <i>Mustela putorius</i> | M | Germany          |
| USNM | 188447        | <i>Mustela putorius</i> | F | Germany          |
| USNM | 152676        | <i>Mustela putorius</i> | F | Spain            |
| USNM | 115214        | <i>Mustela putorius</i> | F | Switzerland      |
| USNM | 319223        | <i>Mustela putorius</i> | F | Italy            |
| USNM | 123629        | <i>Mustela putorius</i> | F | Switzerland      |
| USNM | 021959/A36838 | <i>Mustela putorius</i> | F |                  |
| USNM | 260373        | <i>Mustela putorius</i> | F |                  |
| USNM | 152669        | <i>Mustela putorius</i> | F | Germany          |
| USNM | 123629        | <i>Mustela putorius</i> | F | Switzerland      |
| USNM | 154158        | <i>Mustela putorius</i> | F | Spain            |
| USNM | 174958        | <i>Mustela putorius</i> | M |                  |
| USNM | 188446        | <i>Mustela putorius</i> | M | Germany          |
| USNM | 257966        | <i>Mustela putorius</i> | M |                  |
| USNM | 267593        | <i>Mustela putorius</i> |   | France           |
| USNM | 56973         | <i>Neogale vison</i>    | M | British Columbia |
| USNM | 56975         | <i>Neogale vison</i>    | F | British Columbia |
| USNM | 80292         | <i>Neogale vison</i>    | M | Yukon            |
| USNM | 135112        | <i>Neogale vison</i>    | F | Yukon            |
| USNM | 75626         | <i>Neogale vison</i>    | M | Alberta          |
| USNM | 235963        | <i>Neogale vison</i>    | F | Alberta          |
| USNM | 136339        | <i>Neogale vison</i>    | M | Alaska           |
| USNM | 136342        | <i>Neogale vison</i>    | F | Alaska           |
| USNM | A49324        | <i>Neogale vison</i>    | M | California       |
| USNM | 50966         | <i>Neogale vison</i>    | F | California       |
| USNM | 025268/A32678 | <i>Neogale vison</i>    | M | Kansas           |
| USNM | 172896        | <i>Neogale vison</i>    | M | Maine            |
| USNM | 188351        | <i>Neogale vison</i>    | M | Connecticut      |
| USNM | 035909/A48218 | <i>Neogale vison</i>    | M | Colorado         |
| USNM | 136276        | <i>Neogale vison</i>    | M | New Mexico       |
| USNM | 215866        | <i>Neogale vison</i>    | M | Illinois         |
| USNM | 77136         | <i>Neogale vison</i>    | M | Oregon           |
| USNM | 180801        | <i>Neogale vison</i>    | M | Alabama          |

|      |               |                        |   |                           |
|------|---------------|------------------------|---|---------------------------|
| USNM | 234380        | <i>Neogale vison</i>   | M | Florida                   |
| USNM | 188340        | <i>Neogale vison</i>   | F | Wyoming                   |
| USNM | 76598         | <i>Neogale vison</i>   | F | Maryland                  |
| USNM | 210966        | <i>Neogale vison</i>   | F | Alabama                   |
| USNM | 188357        | <i>Neogale vison</i>   | F | South Carolina            |
| USNM | 64437         | <i>Neogale vison</i>   | F | Indiana                   |
| USNM | 264616        | <i>Neogale vison</i>   | F | North Dakota              |
| USNM | 66231         | <i>Neogale vison</i>   | F | Washington                |
| USNM | 035912/A48221 | <i>Neogale vison</i>   | F | Colorado                  |
| USNM | 170141        | <i>Neogale vison</i>   | F | Montana                   |
| F:AM | 30821         | <i>Neogale vison</i>   |   | Alaska                    |
| USNM | 8156          | <i>Neogale vison</i>   | M | Cumberland Cave, Maryland |
| UMMP | 38341         | <i>Neogale vison</i>   |   | Kansas                    |
| USNM | 119831        | <i>Mustela erminea</i> | M | Alaska                    |
| USNM | 119751        | <i>Mustela erminea</i> | F | Alaska                    |
| USNM | 92240         | <i>Mustela erminea</i> | F | Oregon                    |
| USNM | 266451        | <i>Mustela erminea</i> | M | South Dakota              |
| USNM | 526670        | <i>Mustela erminea</i> | F | South Dakota              |
| USNM | 118301        | <i>Mustela erminea</i> | M | Maine                     |
| USNM | 64686         | <i>Mustela erminea</i> | M | Massachusetts             |
| USNM | 242638        | <i>Mustela erminea</i> | F | Massachusetts             |
| USNM | 96947         | <i>Mustela erminea</i> | M | Massachusetts             |
| USNM | 240712        | <i>Mustela erminea</i> | M | China                     |
| USNM | 152654        | <i>Mustela erminea</i> | M | Germany                   |
| USNM | 152655        | <i>Mustela erminea</i> | M | Germany                   |
| USNM | 152650        | <i>Mustela erminea</i> | M | Ireland                   |
| USNM | 152649        | <i>Mustela erminea</i> | F | Ireland                   |
| USNM | 99735         | <i>Mustela erminea</i> | M | British Columbia          |
| USNM | 75373         | <i>Mustela erminea</i> | F | British Columbia          |
| USNM | 314859        | <i>Mustela erminea</i> | M | Northwest Territories     |
| USNM | 264360        | <i>Mustela erminea</i> | F | Northwest Territories     |
| USNM | 000382/A37421 | <i>Mustela erminea</i> | M | Sweden                    |
| USNM | 188442        | <i>Mustela erminea</i> | M | Sweden                    |
| USNM | 174068        | <i>Mustela erminea</i> | F | India                     |
| USNM | 174067        | <i>Mustela erminea</i> | M | India                     |
| USNM | 354423        | <i>Mustela erminea</i> | M | Pakistan                  |
| USNM | 354424        | <i>Mustela erminea</i> | F | Pakistan                  |

|      |               |                        |   |                       |
|------|---------------|------------------------|---|-----------------------|
| USNM | 200699        | <i>Mustela erminea</i> | M | Russia                |
| USNM | 200700        | <i>Mustela erminea</i> | M | Russia                |
| USNM | 133431        | <i>Mustela erminea</i> | M | New Mexico            |
| USNM | 554484        | <i>Mustela erminea</i> | F | New Mexico            |
| ZIN  | 37925         | <i>Mustela erminea</i> |   | Bliznets Cave, Russia |
| ZIN  | 37922         | <i>Mustela erminea</i> |   | Bliznets Cave, Russia |
| F:AM | 49340         | <i>Mustela erminea</i> |   | Alaska                |
| UMMP | 38339         | <i>Mustela erminea</i> |   | Kansas                |
| UMMP | 38340         | <i>Mustela erminea</i> |   | Kansas                |
| UMMP | 38338         | <i>Mustela erminea</i> |   | Kansas                |
| UTEP | 12-240        | <i>Mustela erminea</i> | F | Dry Cave, New Mexico  |
| USNM | 251910        | <i>Neogale frenata</i> | M | Columbia              |
| USNM | 000601/A01724 | <i>Neogale frenata</i> | M | Mexico                |
| USNM | 363345        | <i>Neogale frenata</i> | M | Panama                |
| USNM | 392237        | <i>Neogale frenata</i> | F | Mexico                |
| USNM | 137513        | <i>Neogale frenata</i> | M | Peru                  |
| USNM | 565508        | <i>Neogale frenata</i> | F | Honduras              |
| USNM | 143812        | <i>Neogale frenata</i> | M | Venezuela             |
| USNM | 137515        | <i>Neogale frenata</i> | F | Venezuela             |
| USNM | 194329        | <i>Neogale frenata</i> | F | Peru                  |
| USNM | 188373        | <i>Neogale frenata</i> | M | California            |
| USNM | 188374        | <i>Neogale frenata</i> | F | California            |
| USNM | 72767         | <i>Neogale frenata</i> | M | Montana               |
| USNM | 261845        | <i>Neogale frenata</i> | M | Montana               |
| USNM | 169978        | <i>Neogale frenata</i> | F | Montana               |
| USNM | 209410        | <i>Neogale frenata</i> | F | Montana               |
| USNM | 021778/A36483 | <i>Neogale frenata</i> | M | Texas                 |
| USNM | 017319/A24240 | <i>Neogale frenata</i> | F | Texas                 |
| USNM | 024679/A32071 | <i>Neogale frenata</i> | M | Arizona               |
| USNM | 177679        | <i>Neogale frenata</i> | M | Connecticut           |
| USNM | 64344         | <i>Neogale frenata</i> | F | Connecticut           |
| USNM | 253922        | <i>Neogale frenata</i> | M | New York              |
| USNM | 253920        | <i>Neogale frenata</i> | F | New York              |
| USNM | 147375        | <i>Neogale frenata</i> | M | Nebraska              |
| USNM | 171559        | <i>Neogale frenata</i> | F | Alabama               |
| USNM | 147762        | <i>Neogale frenata</i> | F | Nebraska              |
| USNM | 261655        | <i>Neogale frenata</i> | M | Georgia               |



|      |               |                         |   |                              |
|------|---------------|-------------------------|---|------------------------------|
| USNM | 261658        | <i>Neogale frenata</i>  | F | Georgia                      |
| UTEP | 120-191       | <i>Neogale frenata</i>  |   | Big Manhole Cave, New Mexico |
| UTEP | 120-169       | <i>Neogale frenata</i>  | F | Big Manhole Cave, New Mexico |
| USNM | 319221        | <i>Mustela nivalis</i>  | M | Italy                        |
| USNM | 197780        | <i>Mustela nivalis</i>  | M | China                        |
| USNM | 299250        | <i>Mustela nivalis</i>  | M | Korea                        |
| USNM | 476026        | <i>Mustela nivalis</i>  | M | Morocco                      |
| USNM | 476025        | <i>Mustela nivalis</i>  | F | Morocco                      |
| USNM | 152632        | <i>Mustela nivalis</i>  | F | Italy                        |
| USNM | 363980        | <i>Mustela nivalis</i>  | M | North Carolina               |
| USNM | 245843        | <i>Mustela nivalis</i>  | F | North Carolina               |
| USNM | 332422        | <i>Mustela nivalis</i>  | M | Tennessee                    |
| USNM | 545049        | <i>Mustela nivalis</i>  | F | Tennessee                    |
| USNM | 554486        | <i>Mustela nivalis</i>  | M | Missouri                     |
| USNM | 554489        | <i>Mustela nivalis</i>  | F | Missouri                     |
| USNM | 271829        | <i>Mustela nivalis</i>  | M | Alaska                       |
| USNM | 225628        | <i>Mustela nivalis</i>  | F | Alaska                       |
| USNM | 288573        | <i>Mustela nivalis</i>  | M | North Dakota                 |
| USNM | 288574        | <i>Mustela nivalis</i>  | F | North Dakota                 |
| USNM | 200767        | <i>Mustela nivalis</i>  | M | Russia                       |
| USNM | 200760        | <i>Mustela nivalis</i>  | M | Russia                       |
| USNM | 327731        | <i>Mustela nivalis</i>  | M | Turkey                       |
| USNM | 327730        | <i>Mustela nivalis</i>  | F | Turkey                       |
| USNM | 265614        | <i>Mustela nivalis</i>  | M | Montana                      |
| USNM | 152631        | <i>Mustela nivalis</i>  | M | United Kingdom               |
| USNM | 232787        | <i>Mustela nivalis</i>  | F | United Kingdom               |
| USNM | 000385/A37787 | <i>Mustela nivalis</i>  | M | Sweden                       |
| ZIN  | 37927-3       | <i>Mustela nivalis</i>  |   | Bliznets Cave, Russia        |
| ZIN  | 37929-5       | <i>Mustela nivalis</i>  |   | Bliznets Cave, Russia        |
| ZIN  | 37929-3       | <i>Mustela nivalis</i>  |   | Bliznets Cave, Russia        |
| USNM | 247073        | <i>Mustela nigripes</i> | F | Colorado                     |
| USNM | 234972        | <i>Mustela nigripes</i> | F | Montana                      |
| USNM | 228233        | <i>Mustela nigripes</i> | M | Arizona                      |
| USNM | 188458        | <i>Mustela nigripes</i> | M | Kansas                       |
| ETVP | 10028         | <i>Mustela nigripes</i> | F | Wyoming                      |
| ETVP | 3887          | <i>Mustela nigripes</i> |   |                              |
| NVPL | 7072          | <i>Mustela nigripes</i> | M | Wyoming                      |

|        |           |                             |   |                                 |
|--------|-----------|-----------------------------|---|---------------------------------|
| NVPL   | 7009      | <i>Mustela nigripes</i>     | M | Wyoming                         |
| ETVP   | 18215     | <i>Mustela nigripes</i>     | M | Colorado                        |
| UMMZ   | 103451    | <i>Mustela nigripes</i>     | M | North Dakota                    |
| DMNH   | 2248      | <i>Mustela nigripes</i>     | M | Colorado                        |
| UTEP   | 46-16     | <i>Mustela nigripes</i>     |   | Isleta Cave, New Mexico         |
| UTEP   | 120-98    | <i>Mustela nigripes</i>     |   | Big Manhole Cave, New Mexico    |
| NAUQSP | 8711/116B | <i>Mustela nigripes</i>     |   | Snake Creek Burial Cave, Nevada |
| NAUQSP | 8711/195B | <i>Mustela nigripes</i>     |   | Snake Creek Burial Cave, Nevada |
| NAUQSP | 8711/197B | <i>Mustela nigripes</i>     |   | Snake Creek Burial Cave, Nevada |
| NAUQSP | 11140     | <i>Mustela nigripes</i>     |   | Cathedral Cave, Nevada          |
| USNM   | 395193    | <i>Neovison macrodon</i>    |   | Maine                           |
| USNM   | 395194    | <i>Neovison macrodon</i>    |   | Maine                           |
| USNM   | 395195    | <i>Neovison macrodon</i>    |   | Maine                           |
| USNM   | 395196    | <i>Neovison macrodon</i>    |   | Maine                           |
| USNM   | 395197    | <i>Neovison macrodon</i>    |   | Maine                           |
| USNM   | 359199    | <i>Neovison macrodon</i>    |   | Maine                           |
| USNM   | 395187    | <i>Neovison macrodon</i>    |   | Maine                           |
| USNM   | 395200    | <i>Neovison macrodon</i>    |   | Maine                           |
| USNM   | 395202    | <i>Neovison macrodon</i>    |   | Maine                           |
| USNM   | 395203    | <i>Neovison macrodon</i>    |   | Maine                           |
| USNM   | 395206    | <i>Neovison macrodon</i>    |   | Maine                           |
| USNM   | 395207    | <i>Neovison macrodon</i>    |   | Maine                           |
| USNM   | 395184    | <i>Neovison macrodon</i>    |   | Maine                           |
| USNM   | 395185    | <i>Neovison macrodon</i>    |   | Maine                           |
| USNM   | 395188    | <i>Neovison macrodon</i>    |   | Maine                           |
| USNM   | 395189    | <i>Neovison macrodon</i>    |   | Maine                           |
| USNM   | 395190    | <i>Neovison macrodon</i>    |   | Maine                           |
| USNM   | 395208    | <i>Neovison macrodon</i>    |   | Maine                           |
| USNM   | 395209    | <i>Neovison macrodon</i>    |   | Maine                           |
| USNM   | 395210    | <i>Neovison macrodon</i>    |   | Maine                           |
| USNM   | 395211    | <i>Neovison macrodon</i>    |   | Maine                           |
| USNM   | 395213    | <i>Neovison macrodon</i>    |   | Maine                           |
| USNM   | 395227    | <i>Neovison macrodon</i>    |   | Maine                           |
| USNM   | 395228    | <i>Neovison macrodon</i>    |   | Maine                           |
| USNM   | 395235    | <i>Neovison macrodon</i>    |   | Maine                           |
| USNM   | 395230    | <i>Neovison macrodon</i>    |   | Maine                           |
| UMMP   | 25767     | <i>Mustela rexroadensis</i> |   | Kansas                          |

|        |             |                             |  |                             |
|--------|-------------|-----------------------------|--|-----------------------------|
| UMMP   | 25768       | <i>Mustela rexroadensis</i> |  | Kansas                      |
| UMMP   | 28432       | <i>Mustela rexroadensis</i> |  | Kansas                      |
| UM-Ida | V55950      | <i>Mustela rexroadensis</i> |  | Idaho                       |
| UM-Ida | V50089      | <i>Mustela rexroadensis</i> |  | Idaho                       |
| UMMP   | 30243       | <i>Mustela rexroadensis</i> |  |                             |
| UMMP   | V45457      | <i>Mustela meltoni</i>      |  | Wendell Fox Pasture, Kansas |
| USNM   | 21824       | <i>Mustela gazini</i>       |  | Idaho                       |
| YG     | 95.4        | <i>Mustela jacksoni</i>     |  | Yukon Territory, Canada     |
| IMNH   | 7559        | <i>Mustela</i> sp.          |  | Owyhee Co., Idaho           |
| IMNH   | 12861       | <i>Mustela</i> sp.          |  | Owyhee Co., Idaho           |
| IMNH   | 124355      | <i>Mustela</i> sp.          |  | Owyhee Co., Idaho           |
| IMNH   | 124354      | <i>Mustela</i> sp.          |  | Owyhee Co., Idaho           |
| KUMVP  | 5750        | <i>Mustela</i> sp.          |  | Meade Co., Kansas           |
| ETMNH  | 22419/22420 | GFS musteline               |  | Gray Fossil Site, Tennessee |

VITA

RONALD W. PEERY

- Education: M.S. Geosciences, East Tennessee State University, Johnson  
City, Tennessee, 2021
- B.S. Geosciences, East Tennessee State University, Johnson  
City, Tennessee, 2016
- Public Schools, Jonesborough, Tennessee, 2011
- Professional Experience: Paleontological Field Technician, Applied Earthworks, Inc.;  
Fresno, California, 2021-
- Graduate Teaching Assistant, East Tennessee State University,  
College of Arts and Sciences; Johnson City, Tennessee,  
2019-2020
- Graduate Research Assistant, East Tennessee State University,  
College of Arts and Sciences; Johnson City, Tennessee,  
2018-2019
- Field Crew, Gray Fossil Site; Gray, Tennessee, 2016-2018
- Honors and Awards: ETSU Featured Student of the Month (September), East Tennessee  
State University, 2016
- Paleontology Student of the Year, East Tennessee State University,  
2015-2016